


Spring 2024

A Party of Particles: Constructing a Cyclotron to Accelerate Protons

Luke Christopher Ingraham
Bard College

Follow this and additional works at: https://digitalcommons.bard.edu/senproj_s2024

 Part of the [Atomic, Molecular and Optical Physics Commons](#), [Electrical and Electronics Commons](#), [Electromagnetics and Photonics Commons](#), [Elementary Particles and Fields and String Theory Commons](#), and the [Engineering Physics Commons](#)



This work is licensed under a [Creative Commons Attribution-Noncommercial-No Derivative Works 4.0 License](#).

Recommended Citation

Ingraham, Luke Christopher, "A Party of Particles: Constructing a Cyclotron to Accelerate Protons" (2024). *Senior Projects Spring 2024*. 134.

https://digitalcommons.bard.edu/senproj_s2024/134

This Open Access is brought to you for free and open access by the Bard Undergraduate Senior Projects at Bard Digital Commons. It has been accepted for inclusion in Senior Projects Spring 2024 by an authorized administrator of Bard Digital Commons. For more information, please contact digitalcommons@bard.edu.

**A Party of Particles: Constructing a Cyclotron to
Accelerate Protons**

**A Senior Project submitted to The Division of Science,
Mathematics, and Computing of Bard College**

by
Luke Ingraham

Annandale-on-Hudson, New York

May, 2024

Abstract

The first particle accelerators were developed by Ernest Lawrence at University of California, Berkeley nearly one hundred years ago. Lawrence's creation of the cyclotron has had an everlasting impact on physics and his experiments can be recreated today. A cyclotron is a charged particle accelerator that uses a magnetic field to confine particles to a spiral flight path in a vacuum chamber and an applied electrical field accelerates these particles to high energies. In this senior thesis, I embarked on a journey to build a fully functional cyclotron that is capable of accelerating protons to beyond 60keV. The complexity of the project is extensive because each component in the project needs to be manufactured. The components that need to be made are the electric field generator, magnetic field generator, vacuum chamber/pump, ionization source, and particle detector. I was able to construct the cyclotron from scratch and get to the point of testing. This cyclotron will be used for future senior projects and experimental demonstrations in numerous physics classes.

Dedications

I dedicate this project to those who hesitate to pursue their dreams when faced with daunting challenges. Even amidst uncertainty and occasional setbacks, remember to persevere, knowing that you have the strength to overcome any obstacle. Embrace the journey with joy and determination, for therein lies the true adventure.

Acknowledgements

I extend my heartfelt gratitude to all those that made this senior project a reality and to those who offered their unwavering support and assistance throughout this challenging journey.

I am deeply thankful to my parents and sisters for their never ending support and patience. A special thank you to my father for his caring nature and inspiring words of wisdom to follow my passion.

I would like to express my gratitude to Sasha Fraser for her endless kindness, love, and faith in my ability to complete this project. A sincere appreciation to her parents for their abundant generosity and encouragement.

My sincere thanks to all my friends and colleagues in the physics community for their invaluable ideas, support, and empathy, whether I shared moments of joy, confusion, or frustration. A heartfelt thank you goes out to Yashar Khan for his unwavering friendship and relentless dedication in assisting me with editing this document. I'm immensely grateful to Vera Topcik for her kindness, patience, and for keeping my imaginative ideas grounded. Special appreciation to Kace Colby for his exceptional efforts in the lab, aiding me in refining many of my concepts. To Josh Krienke, I extend my gratitude for his compassion and for being a supportive study companion. And to Sarah Seager for her years of unwavering friendship and support throughout the process. I'd like to extend my appreciation to Grace Sanger-Johnson for warmly welcoming me into the Bard Physics community. Without her support and kind gesture, this project would never have come to a reality.

I am particularly grateful to my project advisor, Professor Antonios Kontos, for his expertise and guidance throughout this ambitious endeavor. Working together on this project for the past year has been an absolute pleasure, and I would like to express my gratitude once more to him for joining me in taking on this ambitious task. Lastly, I want to express a very special thank you to my dear friend and collaborator, Kornelis Poort, for his dedicated work and unwavering support during countless hours of collaboration. Your dedication and kindness have been instrumental in making this journey possible.

To each of you, I extend my deepest appreciation for your contributions and support throughout this adventurous year. Without you all, completing this project would not have been possible.

Contents

1	Introduction and Theory	1
1.1	Cyclotrons	1
1.2	Why Protons?	3
1.3	The Vacuum Chamber	4
1.4	Magnetic and Electric Fields	6
1.5	Cyclotron Frequency	8
1.6	Thermionic Emission and Hydrogen Ionization	10
1.7	Particle Detectors	15
2	The Design and Construction Phase	17
2.1	Magnets	17
2.1.1	Electromagnets	17
2.1.2	Cooling The Coils	25
2.2	Generating the Electric Field	28
2.2.1	The Electric Plates	28
2.2.2	The Mounting System for the Plates	39
2.2.3	The Voltage Source	44
2.3	The Chamber and Generating a Vacuum	49
2.3.1	Chamber Design	49
2.3.2	Generating a Low Pressure Vacuum	57

2.3.3	Supplying Voltage into the Chamber	61
2.4	Ionizing Hydrogen	64
2.4.1	Providing Hydrogen	64
2.4.2	Safely Handling Hydrogen	67
2.4.3	Testing the Heating Filament	71
2.4.4	Securing the Filament and Gas Line	76
2.5	The Particle Detector	81
2.5.1	Making the FC	81
2.5.2	Current to Voltage Conversion and Detection	85
2.5.3	Mounting the Detector	87
2.5.4	Testing the Faraday Cup	88
3	Simulations Of the Protons Trajectory	97
3.1	Trajectory	97
3.2	Velocity Plots	102
4	Operating the Cyclotron	105
4.1	Operational Manual	105
4.2	Common Problems	107
5	Conclusions	111
5.1	Findings	111
5.2	Future Plans	112
A	Arduino Codes	117
A.1	Arduino Code for A Single Detector	117
B	Python Codes	125
B.1	Trajectory Calculation and Simulation	125
B.2	Plate Distance Estimate	137

,

Chapter 1

Introduction and Theory

1.1 Cyclotrons

The invention of the first cyclotron is credited to Ernest O. Lawrence in 1931 at the University of California, Berkeley Radiation Laboratory. Lawrence stated in his Nobel Prize lecture, “Although the cyclotron was, so to speak, invented early in 1929, actual experimental work on its development was begun in the spring of 1930”[20]. The cyclotron is a relatively simple particle accelerator which uses a combination of magnetic and electric fields to excite the particles in the vacuum chamber. The root of the word, 'cyclo-' means circular and the ending, '-tron' means an instrument[21]; together they mean a circular instrument. In reality the apparatus excites atomic and subatomic particles using an alternating electric field and a uniform magnetic field to accelerate the matter in a spiral pattern until it reaches its maximum velocity. In this case the maximum velocity is achieved when the particle collides with the walls of the vacuum chamber or the detector. The internal components housed inside the vacuum chamber make up the majority of the complexity of the project. The vacuum chamber is essential because it contains the excited particles and eliminates unwanted collisions with other particles. The magnetic field components are outside the chamber, while the system to create an alternating electric field is encased within the cham-

ber. The final major component of this cyclotron is the gas ionization system at the center of the chamber, which provides a sufficient supply of atomic material to accelerate.

The overall purpose of this device is to accelerate atomic material with the potential to be used in other experiments. For instance accelerated fundamental particles are required to create heavier particles. Most heavier particles like the Higgs Boson require a tremendous amount of energy to become a reality. To generate the energy necessary to create such heavy particles, lighter more fundamental particles are accelerated and smashed together. The goal of this senior thesis is to accelerate protons to the maximum kinetic energy possible with the designed apparatus. The approach to this endeavor is to properly research the methods and conduct calculations before the actual building process. This ensures that the project is feasible within the year and within a reasonable budget. By conducting the calculations first, it provides a deep understanding of the equipment that will be needed and the requirements from the physical setup. After conducting my initial research and calculations, I moved to the design and building phase, which was the longest phase of the project. The building phase is mapped out as followed:

1. Building or ordering electromagnets for the magnetic field,
2. Constructing the vacuum chamber,
3. Achieving the necessary pressure required,
4. Building the plates to create an electric field,
5. Ionizing hydrogen gas to get protons,
6. Buying or developing a detector for accelerated protons.

Throughout the process, each aspect was tested separately to ensure optimal functionality and safety. Then all the individual components will come together to hopefully create a working cyclotron for future uses in the department.

1.2 Why Protons?

Initially, the atomic material selected to accelerate was electrons, but upon further research, it was decided to excite protons because of the limited time frame and ultimate added complexity of using electrons. The first complexity is the mass of the electron because the mass is significantly smaller than any other atomic or subatomic particle that could potentially be accelerated in our apparatus. An electrons mass is $9.10938356 \times 10^{-31}kg$, while the mass of the proton is $1.67 \times 10^{-27} kg$ [15]. The proton is heavier than the electron by four orders of magnitude, which plays a significant role in the acceleration process. The electron is so light that any small force exerted will send it into a chaotic trajectory without the presence of immensely powerful magnets to correct its path. Powerful magnets are expensive and hard to acquire within the time frame of this project. Unlike the electron, the proton is heavy enough to be affected by much weaker magnets and easier to manipulate its trajectory. During the ionization process, electrons are generated, however, the electron will exit the process with a large velocity that could affect the trajectory. This can be shown by looking at equation 1.1:

$$KE = \frac{1}{2}mv^2 \quad (1.1)$$

In this equation, the kinetic energy is dependent on the mass and velocity of the object. For the case of an electron, the mass is very small, so the velocity must be immensely large to exit the ionization process with any kinetic energy. With such a large initial velocity after the ionization process, it makes the electrons hard to control over a spiral trajectory. With a large initial velocity, the electrons will experience a much greater push while in the electric field. To counteract this huge burst of energy, an extremely large magnetic field must be generated to correct the electrons path. The proton's mass is much greater, so the velocity exiting the ionization process will be much less than that of the electron.

The last and final reason why the electron is not a desirable choice of experimental medium for this experiment is the need for heavy shielding. When accelerating particles,

certain atomic materials emit radiation, electrons in particular will emit Bremsstrahlung Radiation[9]. The chamber would require strong protective shielding to dampen the radiation emitted during the process to protect both external equipment and myself. For these reasons, the proton is the optimal choice of material to accelerate. The process of generating electrons is much simpler compared to the proton, but the benefits of the protons outweigh the simplicity of the electron generation. Perhaps a future senior project could adapt the system to allow for the acceleration of other atomic material including electrons.

1.3 The Vacuum Chamber

The vacuum chamber houses all the internal components and contains the accelerated particles. It's important the bulk of the system is contained within a vacuum environment because the particle will be able to achieve their maximum velocity if there is very little material in its path. The minimum pressure must be deduced before building the chamber because it may affect the size of the chamber and the vacuum equipment required. Creating a vacuum environment minimizes the number of possible collision that can occur while the proton is being accelerated by the electric and magnetic fields. While maintaining an ultra-high vacuum pressure would significantly improve the outcome of the experiment, it is not required because the proton only needs a minimum pressure to achieve the desired mean free path (MFP). The mean free path is the average distance a particle travels before drastically changing direction or energy[35] due to a collision. The mean free path changes based on the pressure, so the vacuum pressure should be lowered to reduce the probability of unwanted collisions. As a result of a low pressure environment, the number of possible collisions is reduced which increases the chances of the protons reaching the detector. Use equation 1.2[35] to find the MFP.

$$MFP = \frac{K_B T}{\sqrt{2\pi} P r_{ave}^2} \quad (1.2)$$

Where K_B is the Boltzmann Constant, T is the temperature, r_{ave} is the average radius of the particles inside the chamber, and P is the vacuum pressure. The average radius and temperature remain constant throughout the calculation. The temperature is set $300K$ and the r_{ave} is calculated by taking an average radii of oxygen, nitrogen, and a proton, which results in approximately $9.00003 \times 10^{-11}m$ [12]. Figure 1.1 shows the mean free path as a function of pressure from $1 \times 10^{-3}torr$ to 1×10^3torr . This plot determines the ideal pressure for the total distance the proton will travel in the chamber without encountering an unexpected collision.

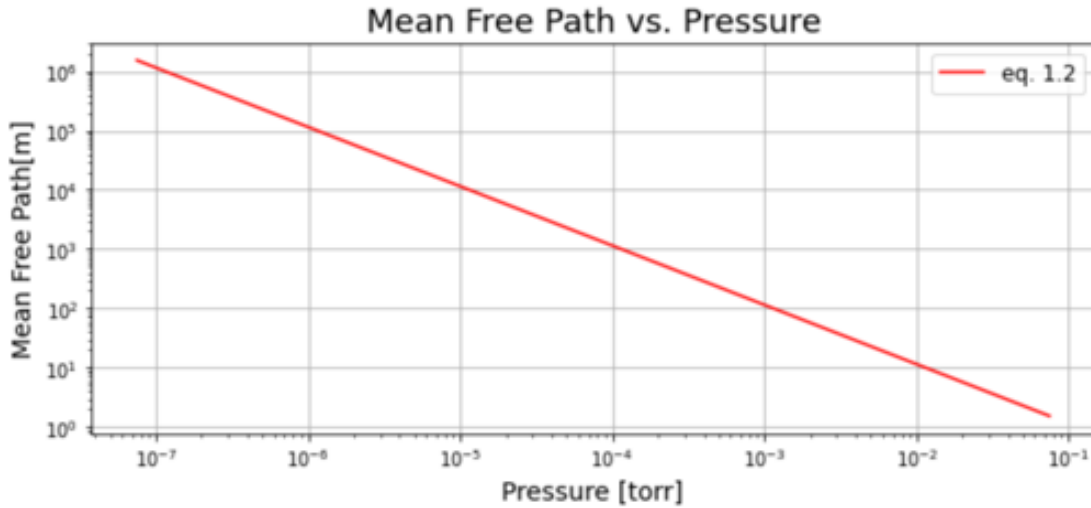


Figure 1.1: The mean free path of the proton vs. pressure of the chamber

To do this estimate, the expected length of the cyclotron trajectory of the particle must first be calculated using equation 1.3.

$$d = k_n 2\pi r_C \quad (1.3)$$

Where k_n is the number of kicks the proton will experience, in essence how many times the proton will enter the electric field. The number of kicks is found by using the kinetic energy KE and the voltage V between the plates. The Voltage must be multiplied by two to account for the proton going through the \vec{B} -field twice in a single orbit. q is the charge of

the accelerated material¹.

$$k_n = \frac{KE}{2Vq} \quad (1.4)$$

Using initial concept designs, the initial calculations determine the kinetic energy should be approximately $27keV$. The supplied voltage was set to be $50V$. Using equation 1.3, the expected displacement is approximately $140m$, which determines the pressure should be between $2 \times 10^{-3}torr$ and $1 \times 10^{-4}torr$. This pressure will be subject to change based on changes to the configuration, whether that be the magnetic or electric field strength or the maximum radius of the chamber. This calculation should be done regularly and specifically any time a significant change is made.

1.4 Magnetic and Electric Fields

The general principle of the cyclotron uses a magnetic field \vec{B} to change the direction and an electric field \vec{E} to speed up the atomic material. Particles in an electric field will travel parallel to the field, while particle in a magnetic field is will travel perpendicular to the field lines. That means a particle trapped in a uniform magnetic field will continuously travel in a circle until the field strength is changed or a supplementary force is applied. Increasing the \vec{B} -field increases the maximum velocity V_{max} because the particles are able to complete more circular orbits through the electric field. Each time the particle goes through the electric field, the particle receives a kick and increases the speed. Increasing the \vec{E} -field reduces the number of circular orbits, but increases the energy received per kick. The \vec{E} -field can be generated using two conductive plates connected to a voltage sources which is dependent upon the voltage supplied and the the distance separating the plates. Essentially the plates will behavior like a simple capacitor² and should be treated as such. The equation to describe

¹For proton, this is equivalent to 1.602×10^{-19} coulombs

²A capacitor is a device that stores electrical energy by accumulating electric charges on two closely spaced surfaces that are insulated from each other

the \vec{E} -field can be derived from a couple of equations. The first equation, equation 1.5, shows the force is determined by the charge and the electric field vector[18]. The \vec{E} -field carries the direction inherently, but the direction is subject to change depending on the charge Q .

$$F = Q \cdot E \quad (1.5)$$

The next equation is used to find the electric potential \vec{W} , which is the energy transferred to or from an object via the application of force along a specific displacement[18].

$$W = F \cdot d \quad (1.6)$$

This describes the direction of the energy transfer and how much is transferred along the distance d . The final equation required is a relation to voltage V from E . Voltage is defined as the potential energy per charge, which is the amount of energy each charge carries as it moves through a system.

$$V = \frac{W}{Q} = \frac{F \cdot d}{Q} \quad (1.7)$$

By rearrange the three equations and solving for V as a function of E and d , the following equation is derived.

$$E = \frac{F}{Q} = \frac{W}{Q \cdot d} = \frac{V}{d} \quad (1.8)$$

Using equation 1.8 to estimate the \vec{E} -field and the amount of energy the proton will gain every time it enters the field zone.

Now lets look to creating the magnetic field \vec{B} and how to estimate the field strength. A uniform magnetic field is required in a cyclotron because it ensures a perfect or mostly perfect path of flight. If the field isn't uniform, then the particle would be subject to variations at different locations along its path, resulting in a uneven spiral. An uneven spiral could cause the particle to completely jump out of the trajectory and miss the detector. There are two possible magnetic field sources available for this project to generate a uniform magnetic

field. The first possible source is a metal material that inherently gives off a magnetic field and the second is building an electromagnet. Natural magnets that give off magnetic fields naturally attract and repel ferromagnetic materials like iron and nickel[15]. To use this source, an array of smaller magnets would be necessary to create a uniform magnetic field. The electromagnet generates a magnetic field by running a current through a wire. When a current moves through a wire source, it generates a magnetic field that curls around the wire[15] and the field direction can be determined using the right-hand rule³. Coiling the wire in a circular spiral creates something called a solenoid. A solenoid creates a directed magnetic field through the center and extending around the coils in a circular fashion. Both sources are viable options, but the electromagnet allows for more flexibility down the road. Having the flexibility to change the magnetic field strength could be beneficial and may be required to accommodate other aspects of the experiment.

1.5 Cyclotron Frequency

The cyclotron frequency is the frequency of a charged particle moving perpendicular to a uniform magnetic field[36]. While an electric field will accelerate a charged particle moving parallel to the field, a charged particle will change direction in a magnetic field. While in the uniform magnetic field, charged particles will maintain a constant speed and will complete a full circle continuously. The motion of the particle is circular, so the forces affecting the particle are centripetal and Lorentz forces. Centripetal forces are a force that makes a body follow a curved path due to a force perpendicular to the direction of travel as seen in equation 1.9[18].

$$\vec{F} = \frac{mv^2}{r} \quad (1.9)$$

³Point your pointer finger in the direction the positive charge is moving, and then your middle finger in the direction of the magnetic field, your thumb points in the direction of the magnetic force pushing on the moving charge.

The Lorentz force is the combination of electric and magnetic forces on a point charge due to the affects of electromagnetic fields[15]. The Lorentz force can be described by equation 1.10.

$$\vec{F} = q(\vec{E} + \vec{v} \times \vec{B}) \quad (1.10)$$

The constant uniform magnetic field implies the cross product of \vec{v} and \vec{B} -field just becomes the multiplication of their magnitudes. The forces are not dependant upon any electric field, so the \vec{E} -field term goes away. While outside the electric plates, the particle only experiences the \vec{B} -field, so we ignore the effects of the \vec{E} -field force on the trajectory because the \vec{E} -field area is so short and the particle spends little time in this zone. The Lorentz force and the centripetal force balance each other out, causing the particle to move in a uniform circular trajectory. We can set these forces equal to one another and get the equation 1.11[36].

$$\frac{mv^2}{r} = qBv \quad (1.11)$$

Where q is the charge, m is the mass of the proton, r is the radius of our circular trajectory, v is the velocity, and B is the magnitude of the magnetic field. This equation can then be rearranged to describe the angular speed $\omega = \frac{v}{r}$. The angular speed has units of radians per second which then can be converted to describe frequency, $f = \frac{\omega}{2\pi}$. Thus this gives us equation 1.12 to describe the frequency of the charged particle.

$$f = \frac{qB}{2\pi m} \quad (1.12)$$

Knowing the cyclotron frequency is important because it describes the rate at which the electric field plates need to switch from a positive to a negative voltage. This frequency should be used as the frequency of our input AC voltage going to the plates. The voltage generating the electric field should switch because it changes the direction of acceleration while in the field. The charged particle needs to be accelerated in the same direction that it is currently traveling in the circle. This situation is demonstrated in figure 1.2.

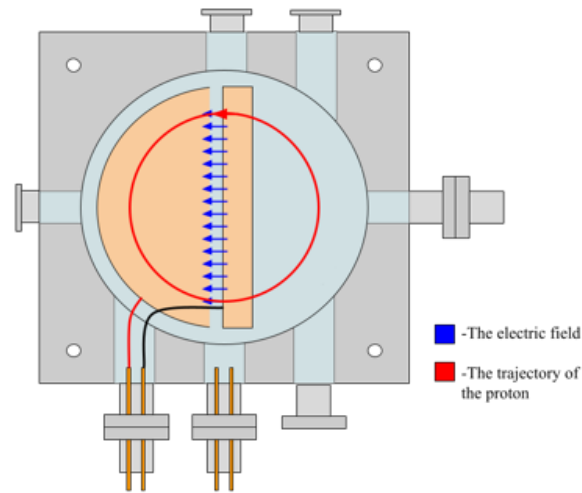


Figure 1.2: Electric Field Direction Alignment

The electric field arrows (blue lines) are pointing in the same direction the proton is traveling. When the proton travels 180° and is between the electric field plates, the voltage should switch and reverse the direction of the field lines. The magnitude of the field should stay the same, but the direction switches at the cyclotron frequency. This gives the proton the iconic spiral trajectory. If the plates were to switch at a frequency other than the cyclotron frequency, the trajectory may become unstable and hard to predict. If the field direction and the protons direction of travel don't match, then the protons will accelerate at different rates of time while in the electric field and could potentially slow down. With a mismatched frequency, the proton will eventually interact with the electric field in a negative way.

1.6 Thermionic Emission and Hydrogen Ionization

To accelerate protons, a constant supply of protons must be generated through a process called ionization. There are a number of other ways to ionize hydrogen gas, but there are many important factors to consider. There will be limited space within the vacuum chamber to house the components and the process must take place relatively close to the center of the

chamber. It is important the protons are generated near the center of the chamber because there is a possibility that multiple protons and unionized hydrogen gas will interact, thus reverting the protons back into their original state. It is also important to consider safety when working with hydrogen gas. Hydrogen becomes combustible when exposed to oxygen, so any potential spark could be disastrous. However, the vacuum environment should be void of oxygen, which would prevent any explosion. A possible method to ionize the hydrogen gas involves using radiation to heat the gas, increasing the kinetic energy of the atoms. This can be done using radio waves, similarly to the way a microwave works, transferring heat through radiation. The increase in kinetic energy allows atoms to scatter and break bonds, creating the ionized atom as a result. The frequency needed to start the ionization process is in the range of MHz to GHz which is well beyond the frequency capabilities of the equipment currently available[14]. Based on the size constraints of the chamber and surrounding materials, it may be difficult to generate radio waves into the center of the chamber. The next possible way to ionize hydrogen gas is to apply a high voltage to the gas. When the high voltage is applied, the gas starts to suffer from dielectric breakdown and begins to partially ionize. The voltage can continue to be applied and further ionize the remaining gas[11]. Applying a high voltage is not ideal because the breakdown of the gas environment increases the potential for a spark or arc to occur. Even though the vacuum chamber will be void of oxygen, there may still be a small percentage of oxygen remaining that could ignite. Not to mention that supplying the needed voltage would be challenging with the equipment accessible here. The final option to ionize the gas is to use a stream of electrons to bump off the valence electron of the hydrogen atom.

The process of ionizing hydrogen gas involves a steady source of electrons to strip the hydrogen of its electron. One method of producing a stream of electrons is known as thermionic emission, which involves using a heating filament⁴ at high temperatures. The heat is cre-

⁴A wire that is heated to a high temperature in order to produce a cloud of electrons. Often the filament is metallic and will glow red while heated.

ated by the current running through the wire as a function of I^2 using the power equation⁵, $P = RI^2$. The wire filament has almost no detectable resistance which means that the current must be high to produce a noticeable amount of heat. At sufficiently high temperatures, the electrons in the valence band are easily bumped off the metal because the thermal energy supplied overwhelms the force of attraction to the nucleus, thus splitting off the electron. Since emitted electrons must be derived, either directly or indirectly from the interior of the emitting body, it is important to look towards the filament material[31]. There are a number of different types of materials that emit electrons when heated to a sufficient temperature. It is also important that the temperature to emit electrons does not approach or go beyond the melting temperature of the material. Inherently many metals are strong candidates for thermionic emission because of the high melting point and their stellar conductive properties. A filaments ability to emit electrons can be described by Richard's equation of emitted current density J , as seen in equation 1.13[25]. The emitted current density provides information about the emitted current over an area for different metals.

$$J = AT^2 e^{-\frac{w}{kT}} \quad (1.13)$$

Where w is the work function of the material, determined through experimental observation and fitting. The work function is the minimum amount of energy necessary to start the emission of electrons from a metal's surface. For example, the work function of tungsten is approximately $4.50eV$ [8]. The constant A is defined as a material correction parameter determined by equation 1.14[38].

$$A = \lambda_R A_0 \quad (1.14)$$

λ_R is a material specific correction factor in the order of 0.5.⁶ A_0 is the universal constant

⁵Power is the rate at which work is done or energy transferred in a circuit.

⁶This correction value is unit less and changes slightly for each material. A general value for this correction factor is 0.5.

that can be determined by equation 1.15. This value is numerically calculated using equation 1.13 and assuming that the “surface heat” is proportional to the temperature during the emission process[17].

$$A_0 = \frac{4\pi m k^2 q_e}{h^3} = 1.20173 \times 10^6 \text{ A m}^{-2} \text{ K}^{-2} \quad (1.15)$$

The work functions listed below were selected as common metals from the Wikipedia page on thermionic emission[39]. The melting point was provided by a online website[26].

Material	Work Function (eV)	Melting Temperature(C)
Aluminum	4.06	660
Copper	5.10	1084
Iron	4.81	1538
Lithium	2.9	180
Titanium	3.84	1670
Tungsten	4.50	3672

Table 1.1: The Work Function for Different Metals

Using the work function for different metals, we can plot the expected number of electrons bumped off the filament as a function of temperature. This provides insight into electron generation of different metals and will be valuable when deciding the type of heating filament in the future. Figure 1.3 shows the number of electrons as a function time for multiple common metals that could be potential candidates.

While there are a number of metals that produce a steady supply of electrons at relatively low temperatures, there are very few that have a high melting point and high tensile strength⁷. While tungsten is an ideal material because it has a high melting point and high tensile strength, lithium produces a large number of electrons at a low temperature and has a very low melting point. The best candidates would be tungsten and titanium because of their high melting points and strength. Strength is essential because the filament might experience a lot of tension in the mounting process, so it must be strong and flexible.

Similarly to work function above, the energy required to remove an electron from the

⁷The maximum stress that a material can bear before breaking when it is allowed to be stretched or pulled

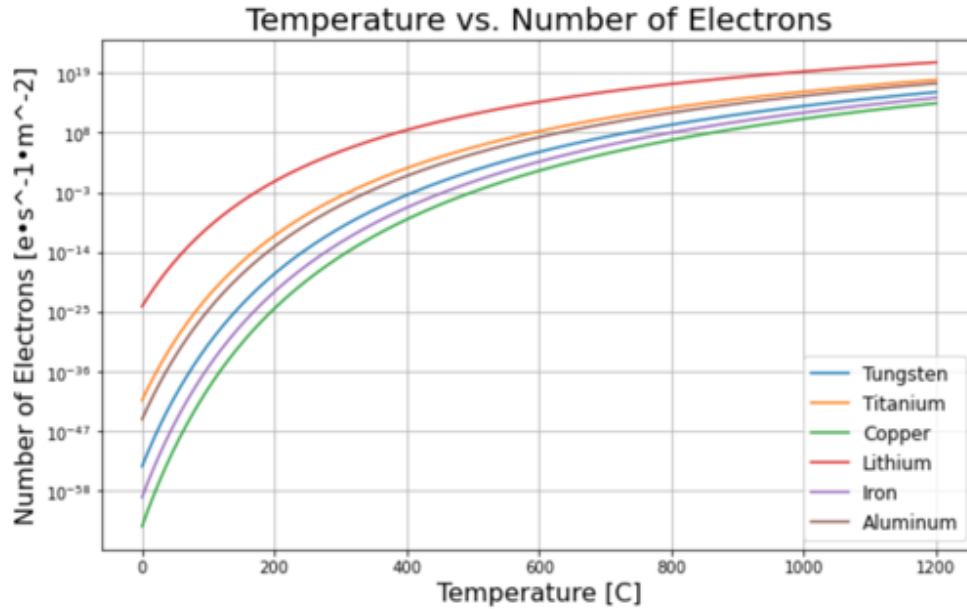


Figure 1.3: Temperature vs. Number of Electrons Generated for Different Metals

hydrogen atom is called the binding energy. The binding energy is the energy required to bump off the electron in the ground state⁸ to ionize the atom[16]. The equation that describes the allowed energies of an atom is known as the Bohr formula as seen in equation 1.16

$$E_n = - \left[\frac{m_e}{2\hbar^2} \left(\frac{e^2}{4\pi\epsilon_0} \right)^2 \right] \frac{1}{n^2} = \frac{E_1}{n^2}, \quad n = 1, 2, 3, \dots \quad (1.16)$$

Where m_e is the mass of an electron, \hbar is Plank's constant⁹, e is the charge of an electron¹⁰, and ϵ_0 is the permittivity of space¹¹. The binding energy of the hydrogen atom while in the ground state is equivalent to $-13.6eV$. This is the minimum energy that must be directed at the electron to separate is from the pull of the proton. This can be represented using equation 1.17 [4].

⁸The energy state of the lowest energy.

⁹Plank's constant, $\hbar = 1.05457 \times 10^{-34} Js$

¹⁰The charge of an electron, $-e = -1.60218 \times 10^{-19} C$

¹¹The permittivity of space is a constant that inhibits the ability of electrical fields to pass through a vacuum.[16], $\epsilon_0 = 8.85419 \times 10^{-12} C^2/Jm$



The binding energy determines the specific energy that is required to separate the electron from the hydrogen gas, so the electrons from the filament are required to have that minimum energy.

1.7 Particle Detectors

A particle detector is placed inside the chamber to track the existence of protons and highest energy achieved by the accelerated material. There is a wide variety of possible detectors that could be used to measure the output energy when the particles hit the detector. In principle, the protons will require a detector that is able to detect low level energies solely because of the electric and magnetic field limitations. Since the kinetic energy will be relatively low, the detector must be selected with the system limitations in mind. Using common materials and equipment while maintaining a budget will result in a low kinetic energy output in the range of $1 - 100keV$. The possible energy capabilities of the setup is discussed further in the simulations section of chapter 3. Due to the low kinetic energy yield, the ideal detector is a device called the Faraday Cup. A Faraday Cup (FC) is a simple device because it measures a current as the charged particles enter and hit the cup. As the charged particles hit the FC, the metallic components become slightly charged and the cup discharges by measuring the current. The current produced is proportional to the number of ions hitting the device[37]. The number of charged particles hitting the FC-assuming a continuous stream-can be determined using equation 1.18[37].

$$N = t \frac{I}{e} \quad (1.18)$$

Where e is the elementary charge, N is the number of ions observed in time t , and I is

the current measurement. This will give an approximation for the number of charged ions that hit the FC for an amount of time. The FC is a relatively simple design and can actually be manufactured here using the lathe. Hollowing out the center of a solid piece of brass using the lathe could make a simple particle catchers mitt as seen in figure 1.4.

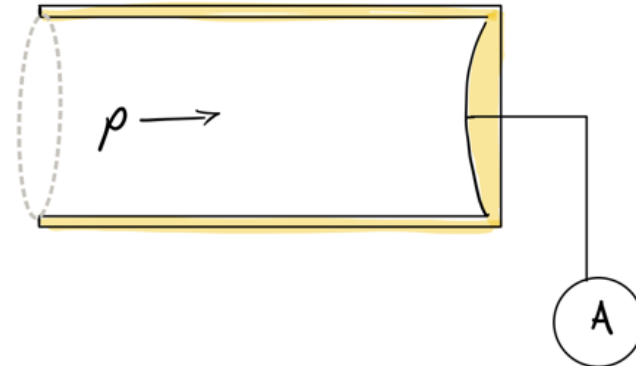


Figure 1.4: The Faraday Cup

To collect the charge and measure current, the cup should be connected in series¹² to a multi-meter¹³[3]. The ammeter¹⁴ needs to be extremely sensitive because the predicted current measurement will be in the range of a few μA to nA . This is incredibly small and a normal store-bought multi-meter won't have the sensitivity required. A voltage can also be applied to the FC to help attract the charged particles to the FC. The voltage applied should be the opposite charge of the charged particles.

¹²When building a circuit, there are two possible ways to connect electrical components: series and parallel. In series, the components are placed one after another. While in parallel, the electrical components are split down to paths and reconnected later.

¹³A device used when building circuits to measure voltage, current, resistance, and a number of other useful things.

¹⁴The specific setting of the multi-meter to measure current.

Chapter 2

The Design and Construction Phase

2.1 Magnets

2.1.1 Electromagnets

The initial idea involved constructing an array of smaller natural magnets to create a large uniform magnetic field, but this is a complicated process and would have required the magnets to be placed in specific places to ensure a uniform field. A very strong magnetic field is required to achieve as much kinetic energy as possible from the protons. The original goal for the magnetic field strength was roughly in the realm of $0.5T$. As a reference, a refrigerator magnet has a field strength of around $1 \times 10^{-3}T$ while the Earth's magnetic field is around $5 \times 10^{-5}T$. So the magnetic field that desired is much stronger and more dangerous to technology and potentially to humans. Strong electromagnetic fields can have adverse affects on the bodies neuromuscular systems and functions. It is recommended not to be exposed to magnetic fields of $5 \times 10^{-4}T$ for extended periods of time[19]. For this project, we were safe because the strongest point of the magnetic field was directed between to magnetic poles and we were not be between the poles while the field was active. There is a minor magnetic field outside the poles extending a few meters, but the intensity is small enough not to worry. Just to be safe, empty your pockets before turning on the field to

ensure your phone and credit cards aren't destroyed.

After exploring the bowels of the physics building, a set of large electromagnets were found from a previous experiment many years ago. If they worked, there would be the potential to generate a powerful uniform field and wouldn't require the construction of a complex array of smaller magnets or a mounting system. Figure 2.1 depicts the electromagnets and the steel frame that holds all the components in place.

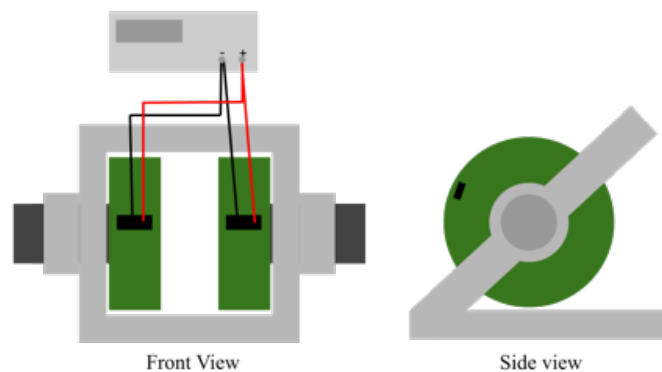


Figure 2.1: Electromagnets

The manual that came with the electromagnets had very minimal information for their specifications and operating procedures. The information that was provided suggests the coils are a 2-mil aluminum sheet laminated with 0.00025-mil Mylar Strip and the total length of the aluminum roll is estimated to be 2100 feet by 3-3/16 inches wide[13]. The total length of the roll is subject to debate and will be discussed further at the end of this section. Each coil has a set of connections on the exterior shell to connect the power supply, and have a substantial amount of current running through the leads. To protect myself and future users, protective covers were designed using Fusion360 and 3D printed in PLA filament. PLA filament is an insulator¹, which protects anyone from touching the leads and hurting themselves while maintaining the circuit. The basic idea of the protective cover was

¹A substance which prevents the passage of heat, sound, and electricity.

to completely eliminate the ability to bump or touch the terminals while the covers are on. It is also important to have easy access to the terminals when needed, so a simple latch mechanism was developed in Fusion360. Two latch connections were glued onto the coils and then the cover was fixed to the connections using a bolt and nut as seen in figure 2.2.

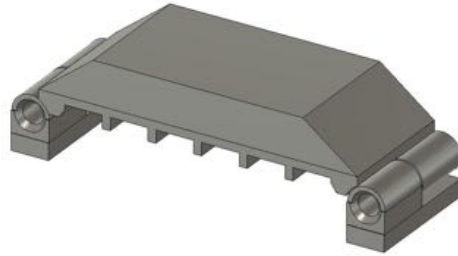


Figure 2.2: 3D printed covers to protect the terminals on the coils

The capabilities of the magnets were determined after numerous tests and the best power supply configuration was concluded to be connecting them in parallel. While in series or parallel, both configurations create advantages and drawbacks to the system. When connected in series, the current flowing through the coils is much higher, which increases the magnetic field generated, but it does draw a much higher voltage. While connected in parallel, the voltage demands was reduced greatly, but the current is split between the two coils, resulting in a less intense magnetic field. Measuring the current as a function of voltage and the \vec{B} -field as a function of current gave insight into the voltage and current requirements to produce a powerful uniform field. This also gave a maximum field estimate that is achievable with the apparatus. Due to the limitation of the power supply, the best available option was to connect the system in parallel to attain a high current while keeping the voltage low. It was important to connect to leads to the terminal directly on the power supply with high grade wires to reduce the risk of destroying the wires or starting a fire.

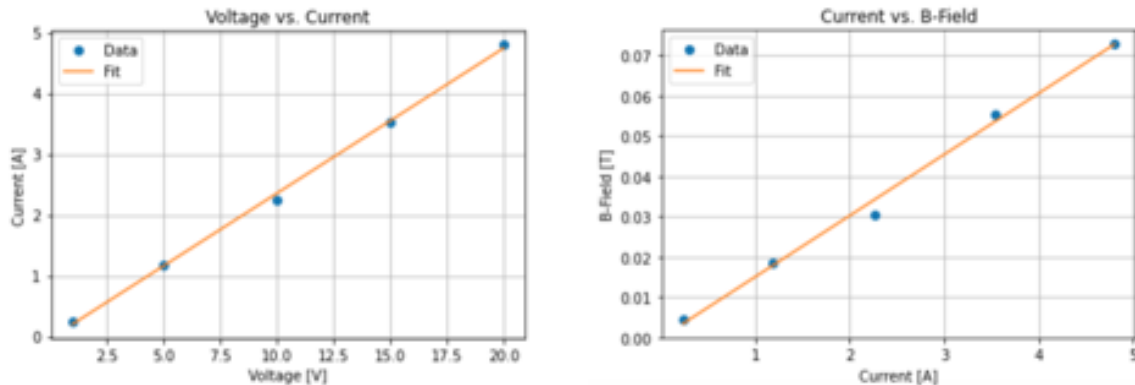


Figure 2.3: Plot for the Initial Electromagnet Strength(Left Coil Only)

Connection	Voltage(V)	Current(A)	Magnetic Field(T)
Left Coil Only	1.00	0.236	0.0044
	5.00	1.184	0.0185
	10.00	2.256	0.0305
	15.00	3.533	0.0555
	20.00	4.800	0.0728
Parallel	2.02	1.00	0.012
	4.04	2.00	0.023
	10.19	5.01	0.055
	14.05	7.01	0.077
	20.03	10.02	0.100
	23.93	12.02	0.129
	29.83	15.02	0.151
Series	8.47	1.00	0.022
	16.52	2.00	0.043
	24.89	3.00	0.065
	32.62	4.00	0.087
	40.36	5.01	0.109

Table 2.1: An initial test of the electromagnet strength

Another important aspect to measure and consider for the electromagnets was the uniformity of the field generated. It was important to create a map of the field and predict the field shape using a Gaussmeter² because it provides a reference for the possible capabilities of the magnets. These initial measurements showed the field was reasonably strong when directly between the magnets and the field strength increases as it goes outward until it reaches the

²A device that measures the magnetic field perpendicular to the surface of the probe.

pole faces. The distance between the magnetic pole faces for the initial measurement was 9cm .

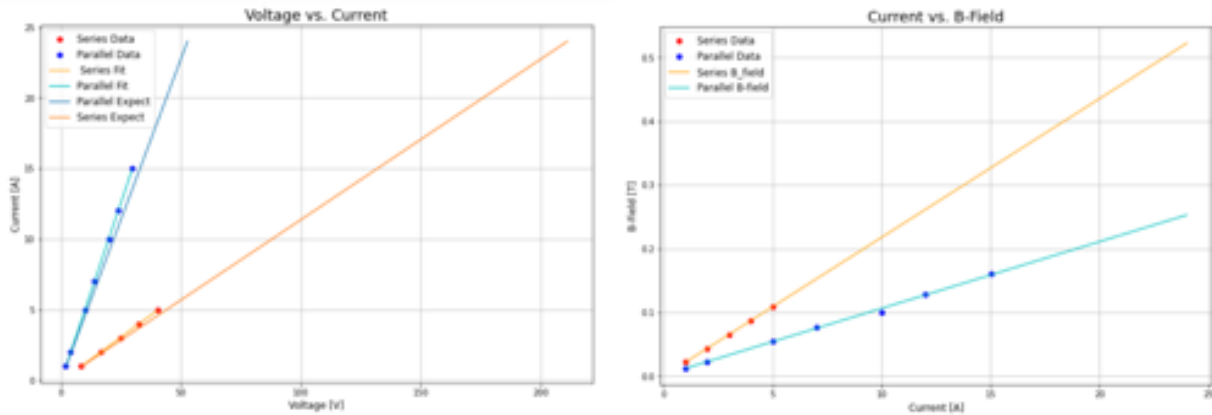


Figure 2.4: Plot for the electromagnet strength of both coils in series and parallel

To show that the electromagnets are behaving properly and haven't been damaged over years, a program was created to show the field intensity as a function of distance between the pole faces.

$$B(z) = \frac{\mu_0 I R^2}{2(R^2 + z^2)^{\frac{3}{2}}} \quad (2.1)$$

Equation 2.1 is the equation for the magnetic field of a single loop of current. In this circumstance, there isn't actually a single loop of current but this provides a decent estimate of the field. R is a fixed distance of the radius of the pole faces at the center of the coils and I is a constant current running through the current loop. R is approximately 6cm and I is set to 10.5A . z is the position between the two pole face starting at zero from the left coil going to the right coil at 9cm .

Comparing the predictions and measurements in figure 2.5, shows the prediction is accurate and the magnets are behaving as expected. This led to the conclusion that the magnets were operating within acceptable parameters and would be used for the experiment. When the chamber was implemented into the system, the gap distance was reduced. This reduction in the gap distance can be seen in figure 2.6. Carefully map data similar to that of figure 2.5 is not possible because of the space constraints inside the chamber.

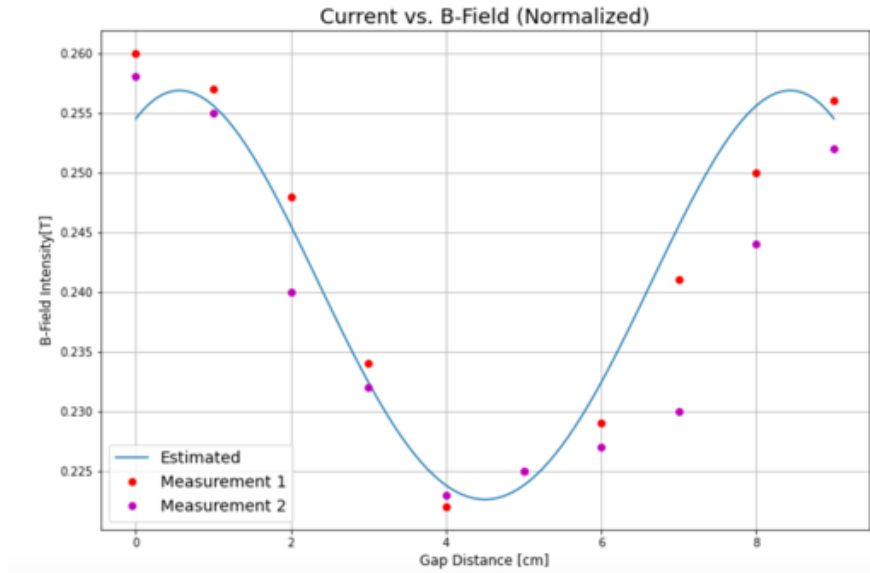


Figure 2.5: Estimate of the magnetic field intensity over the 9cm gap

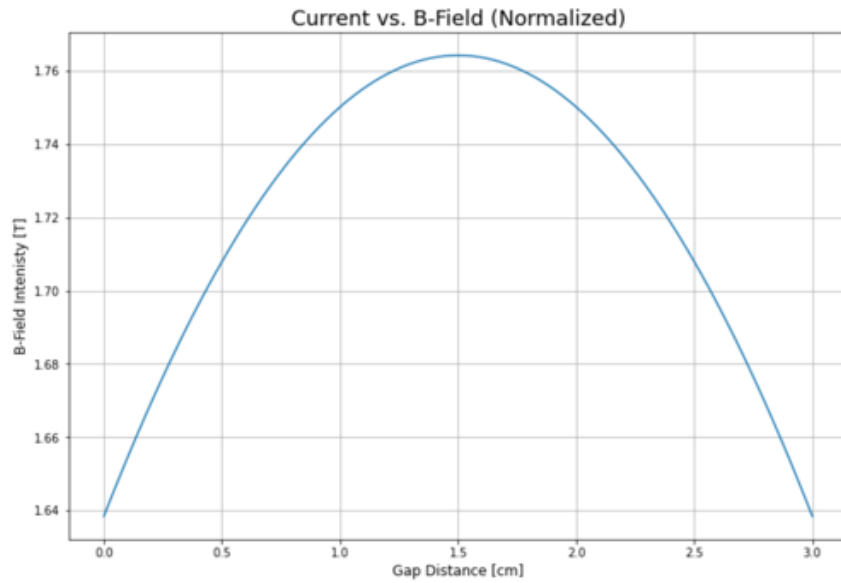


Figure 2.6: Estimate of the magnetic field intensity over the 3cm gap

To gain more knowledge about the magnets, the field could be estimated using the equation for magnetic induction using equation 2.2.

$$B = \frac{N_{turns}}{t} \cdot I \cdot \mu_0 \cdot \mu_{rel} \quad (2.2)$$

To do this calculation, the number of turns of each coil is needed, however, the manual doesn't specify the number of turns. So it must be calculated numerically using the information that was provided and any measured data. The method of calculating the number of turns was geometric in origin and used the provided inner and outer diameter of the coils. The circumference changes on each turn because the radius is increased by the thickness of the sheet upon each wrap. A Python code that utilizes a while-loop structure was made to complete this calculation. The while-loop continuously subtracts the circumference from the total length and the loop breaks once the length is equal to or less than zero. The number of turns calculated was 796. In addition, the relative permeability μ_0 of a material in respect to its magnetic properties is required. μ_0 should be in regards to the core centered in the coil because it amplifies and directs the magnetic field between the coils. However, the manual fails to mention the specific material of the core, so the value of μ_0 can not be so easily found. The value could have been estimated using magnetic field measurements and by simply guessing the material until a viable result was achieved. Using this method creates uncertainty and doubt about the accuracy of the measurements, so it was not a worthy pursuit.

During the first attempt to test the field at a reduced distance, the magnetic pole faces slipped the locking bolts and smashed together. The structure of the vacuum chamber is discussed in the next section, but the two main walls of the chamber are pole faces that connect to the coil cores. To connect them, the old pole faces were removed from the cores and replaced with the new ones specifically for the chamber. The cores have a large threaded one inch bolt that goes through the center and screws directly into the pole face. The pole

faces need to be secured while removing the bolts, otherwise they will fall and get damaged. The pole faces were heavy, weighing approximately five pounds each, so building a support structure would have been useful. Once the old pole faces were removed, the new faces were added by threading the bolt through the core and into the back of the new pole face. Since these pole faces are a component of the vacuum chamber, the distance between the faces must be reduced to approximately one inch. After attaching the poles, the distance that the cores protrude the coils must be adjusted. The fastening bolts on the frame were loosened and the cores adjusted to the desired distance. Without assembling the chamber, it was decided to attach the new pole faces with the reduced distance and measure the magnetic field strength in the gap. However, the fastening bolts holding the cores were not properly tightened because the cores slipped the bolts, smashing the delicate pole faces together. The poles smashed together in a fraction of a second at only 10A and the plan was to go to 24A. The reduced distance increased the magnetic field strength exponentially and was much stronger than the fastening bolts hold on the cores. To separate the poles, it was important to be very gentle not to scratch the surfaces even more. Removing the fastening bolts and the bolt securing the pole face to the core was not enough to unsandwich the poles. They were pushed together so tight that they couldn't be pushed, pulled, or hit in any direction. Ultimately, they were removed by building a small platform underneath the frame to catch the poles as they were hit downwards with a rubber mallet. After 45 minutes of struggle, the pole faces separated with minimal scratches to the surface. The next attempt to measure the field had the chamber between to ensure this didn't happen again. By minimally assembling the chamber and placing it into the magnetic field, a rough magnetic field strength measurement was taken. Table 2.2 and figure 2.7 depict the field strength from within the chamber at a reduced distance of 3cm. At a maximum current of 24A and voltage of 48V, the magnetic field reached approximately $0.7T$. The maximum \vec{B} -field prior to the reduced distance was $0.25T$, which is much weaker than the newest measurement. A stronger magnetic field would result in a increased kinetic energy because

the protons would be able to complete more orbits through the electric field.

Voltage(V)	Current(A)	Magnetic Field(T)
2.06	1.00	0.049
4.16	2.00	0.087
8.25	4.00	0.171
10.24	5.00	0.202
16.25	8.00	0.313
20.28	10.00	0.418
24.40	12.00	0.494
30.49	15.00	0.565
36.78	18.00	0.646
40.82	20.00	0.666
45.96	22.00	0.682
48.00	24.00	0.701

Table 2.2: Electromagnet strength connected in parallel inside the vacuum chamber

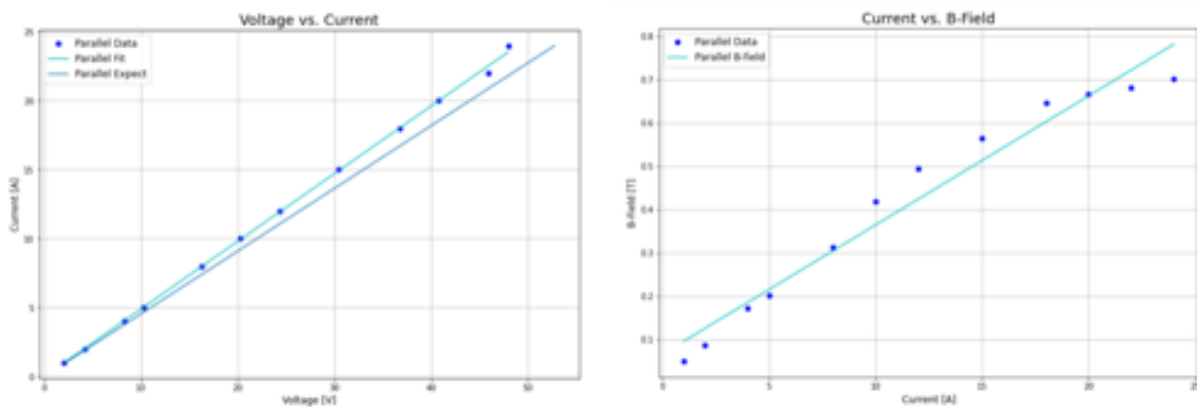


Figure 2.7: Plot for the electromagnet strength connected in parallel inside the vacuum chamber

2.1.2 Cooling The Coils

When running a current through a wire, the wires experience electrical resistance and release heat. The heat generated after a long period of time at a high current was substantial, so a cooling system was implemented. The coils need to be cooled with cold distilled water to prevent mineral buildup in the coil housing. Fortunately the coils come with built in water cooling intake and outtake copper tubes, so the implementation was simple. The heat given off by the wire was calculated as a function of time using equation 2.3, also known as Joules

Equation of Heat.

$$Q = I^2 \cdot R \cdot t \quad (2.3)$$

I is the current running through the wire and R is the resistance of wire. In this configuration, the coils were set in parallel, so the resistance was 2.2ohm and the maximum current provided to the coils was $24A$. The heat increased over time as seen in figure 2.8. This figure gave

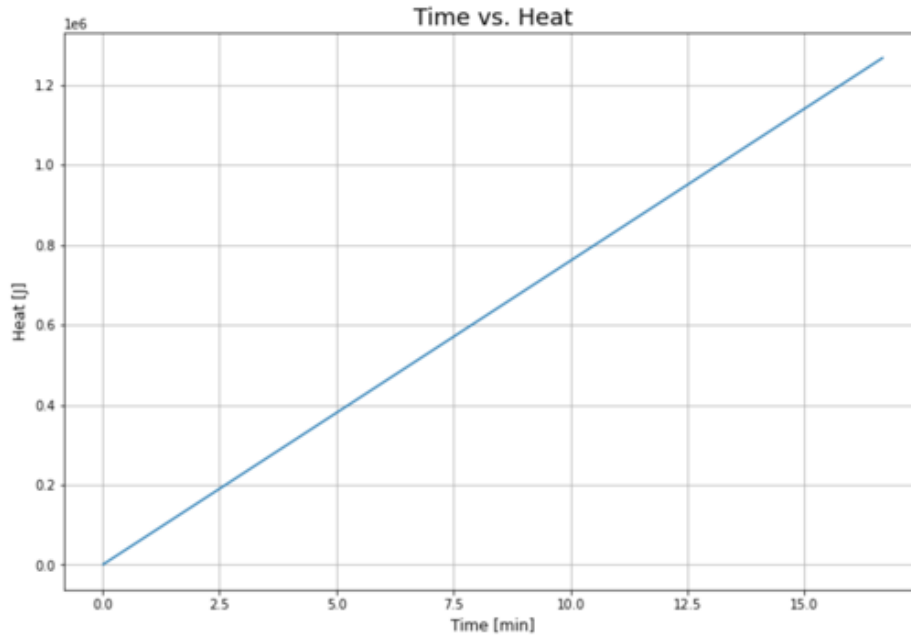


Figure 2.8: Heat as a function of time

a rough estimate for the amount of heat the coils gave off after continuous use without the water cooling. The user manual does suggest not to continuously run power through the coils for more than 30 minutes at a time to prevent permanent damage. To supply the water into the coils at a continuous flow, the cold water needed to be pumped from a cold reservoir into the coils and pumped back into the reservoir. A 3V submersible pump was bought to circulate the water through the coils. The pump came with some specifications, but also indicated that each model would vary slightly. Determining the proper amount of voltage required by the pump was important to maintain a constant flow of cool water. To test the water output as a function of voltage, water was pumped out of a container for a set amount of time and measured. This is important because the electromagnet manual

specifies the minimum water flow needed at maximum power is $1.5qt/min$ or $1420mL/min$. It is vital the pump is able to supply the coils with the necessary amount of water to keep from overheating. By varying the voltage, the amount of water pumped out changed after a span of 30 seconds.

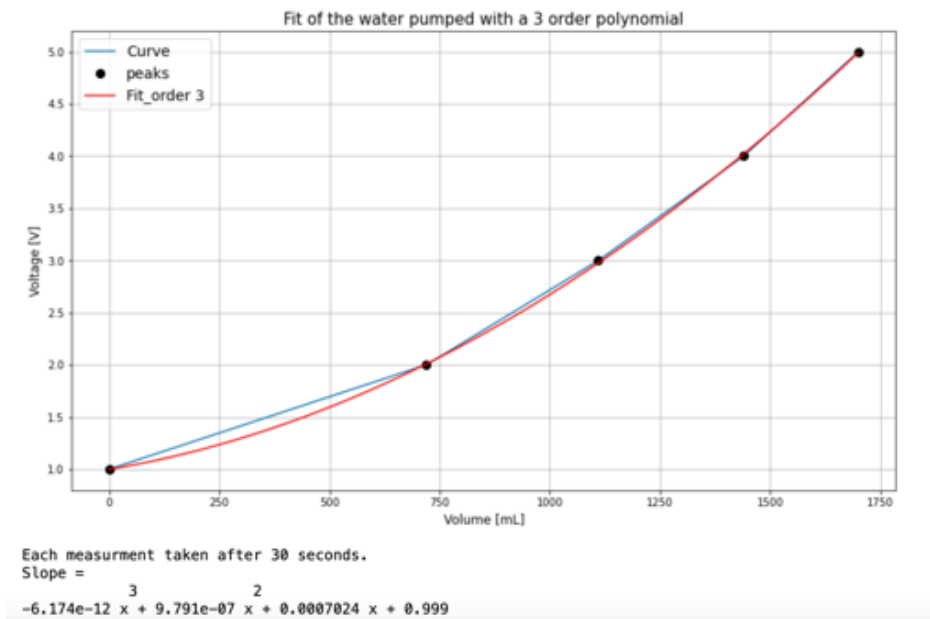


Figure 2.9: Plot of The water pumped over time

The voltage needed to satisfy the required flow rate was estimated using figure 2.9. The data was fit with a 3rd order polynomial and the slope was extracted. The pump needed to be supplied with approximately $4V$ to maintain the $1420mL/min$ flow rate. The electromagnets manual stated the internal coil temperature should not exceed $160^{\circ}F$. This was monitored using the thermal-couples attachments on the exterior screws and would determine when the power needed to be disconnected to prevent damaging the equipment. The power supply has a thermal-couple connection built-in which allows the temperature be to measure easily.

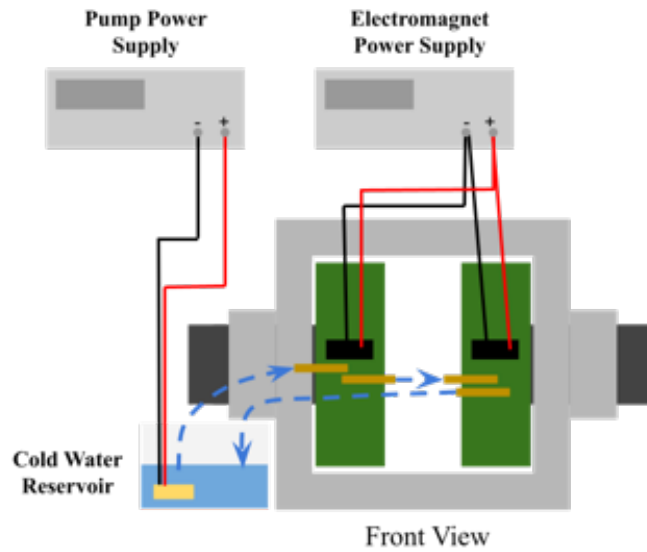


Figure 2.10: Cold water pump system

2.2 Generating the Electric Field

2.2.1 The Electric Plates

The electric field plates have a unique shape which pulled inspiration from a thesis paper[9]. The unique shape requires a hollow crescent moon and a rectangular frame as seen in figure 2.11 to provide a stable electric field space.

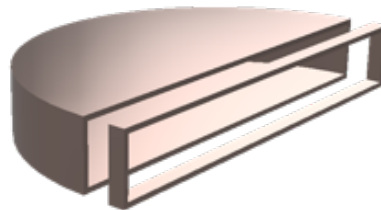


Figure 2.11: Electric field plates concept design

The hollow moon shape allowed for the protons to pass within the space without interfering with other components, while the rectangular frame acted as the other plate creating an electric potential. The rectangular frame minimized the surface area occupying the chamber and allowed for the maximization of space for wires, gas lines, and detectors. Since the plates have such a unique shape, the performance of the plate could be unpredictable and behave abnormally. To combat this uncertainty, it was important to simulate the electric field prior to constructing them in metal. Before simulating the electric field in COMSOL, a few calculations were made and the physical plates needed to be designed in Fusion360. Designing the plates in Fusion after estimating the approximate size of the maximum radius and plate thickness was a good starting point. To get an accurate simulation, the approximate distance between the plates, the material, and the voltage running into the plates needed to be determined. To determine the ideal distance between the plates, the simulation that predicts the trajectory of the protons within the chamber was run at different configurations and inspected for the best possible placement. Based on the shape of the spiral that was produced, it was concluded if the gap distance was too large or small.

In figure 2.12, the left image shows the proton trajectory when the gap distance was too small and the middle image shows the trajectory when the gap is too large. When the plates distance is too small, the proton gains all the energy almost instantaneously which over powers the strength of the magnetic field. Meaning that the magnetic field is not an adequate strength to change the direction of the proton fast enough before all the energy was transferred. While the plates were at a much larger distance, the proton spends far too much time in the electric field which means that energy given to the proton is spread out over a much longer time and not strong enough to match the turning power of the magnetic field.

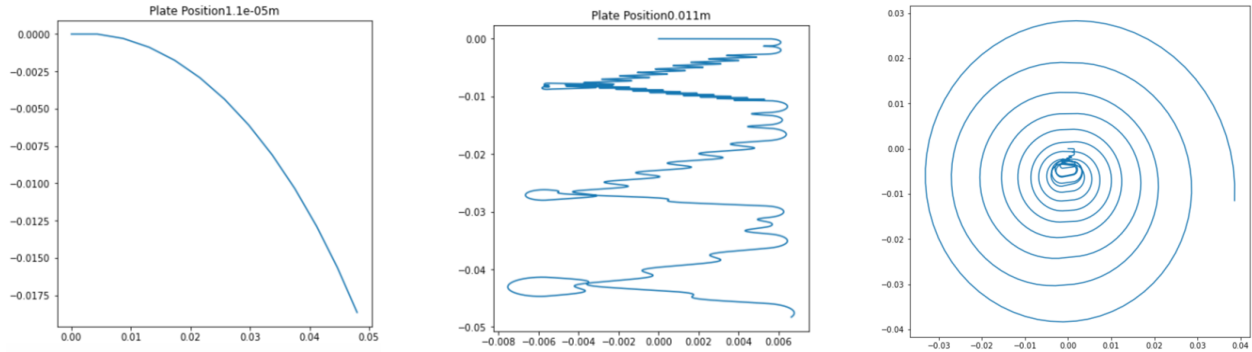


Figure 2.12: The proton trajectory based on different distances between the plates: left-very small gap, middle-very large gap, right-perfect size gap

A delicate balance of the electric and magnetic fields allow the proton to take the spiral trajectory seen in figure 2.12. To determine the ideal distance between the plates, the voltage was fixed at 50V and the plate distances were varied until a relatively uniform spiral trajectory was generated. A simple for-loop method was created to change the distance between the plates and return the results of each trial quickly. This process was not perfect because the best spiral was determined by merely looking at each spiral individually and selecting the one that looks the most uniform. A better method of determining the viability of a spiral would be developing a program to determine the uniformity of each spiral. Based on the first test at a fixed voltage of 50V, the ideal distance between the plates was $0.2mm$. This distance was very small and perhaps would be increased in the future, however this means that the voltage needed to be greatly increased to compensate for the change. For the design in Fusion360, the maximum diameter of the plates was estimated to be $105.2mm$ and the average thickness of a metal sheet was set to $1mm$. The thickness of the metal sheeting was estimated to be $1mm$ because the sheet needed to be thin enough to be easily workable, but still retain its rigidity while handling it. Similarly to the calculations regarding the vacuum chamber material, the material should not be magnetically shielding, so the ideal candidate would be aluminum, copper, or brass. The electric plates would generate an electric field, so the material needed to allow for the stable transfer of electricity. While all the possible material choices are conductive, copper is the most conductive, so it was the

ideal metal for this project. Now that all the missing data was collected, the simulations in COMSOL could be done. For this purpose, the electrics and electrostatics package provided with COMSOL was used. The geometry was uploaded to the simulation while maintaining the size and characteristics of the design. The hollow moon was assigned a voltage potential of 50V and the rectangular frame was set to ground. To simulate the electric field between the plates, a cub shaped vacuum environment was created around the plates. This allows the visualization of the electric field and electric potential. The electric field changes at different points in the vacuum environment, as seen in figure 2.13.

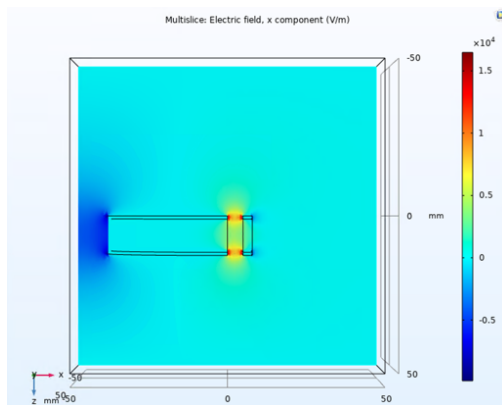


Figure 2.13: The electric field simulation in 2-dimensions, x-z plane

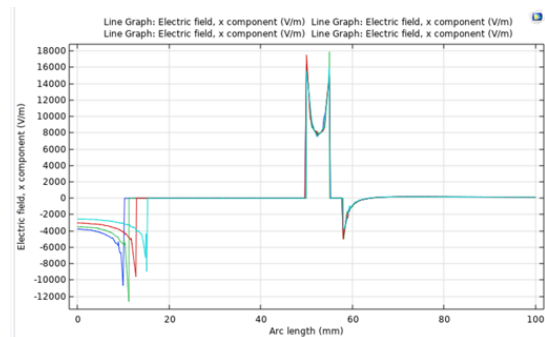


Figure 2.14: The electric field uniformity along the x-axis

Figure 2.13 shows the electric field inside and outside the plates along the z-x plane. There is a very strong positive electric field between the plates (the gap) and little to no electric field inside the plate gap. This means that the field inside the plates are canceling each other, while the area between the plates has a strong field. Allowing for the proton to only gain energy while between plate gap and no where else in the system. There is however a low level negative electric field outside the plates, but this won't affect the experiment. The strongest part of the electric field is located in the small area between the metal of each plate, seen in bright red in figure 2.13. This area does not matter as much because the proton will not be within this space, or at least should never be in that space. The important space is in the middle of the plates, so it was insightful to check the electric field's uniformity in this space. From this 2D plane, certain data was extracted to create 2D plots of the electric

field intensity as a function of position along one axis. Multiple data sets were taken along the x-axis and plotted as a function of electric field intensity. The lines have some variation between zero and twenty arc length, but this doesn't matter because the variation was as outside the plates along the curved portion of the hollow moon. After the fluctuation, the intensity flattens out inside the hollow moon uniformly and all the spikes at the same point around 50 arc length. The maximum intensity of each line is slightly different at the first and second peak, but the curve between the peak is relatively uniform. Each peak represents the face of the plate and the space of significance is this curve between the peaks. This area is mostly uniform, but experiences a drop of roughly $50000V/m$ from its min to max. The drop would be reduced by decreasing the distance between the plates and compressing the height of the plates. Initially, the height of the plates are set at a half an inch, but this was be reduced further after the simulations. It was originally set to a half an inch because it would allow the manufacturing process to be easier, as the parts would be larger. The distance between the plates was set to $1cm$ for the simulation, but the actual gap distance was be much smaller, so the uniformity will increase further.

It was also important to look at the simulation from another angle and examine the uniformity from that perspective. Looking at the x-y plane provides a completely different view of the simulation and its behaviors. Figure 2.15 shows the field directly through the middle of the plates along the longer side of the planes. This depicts how the field changes along the longest side of the plates.

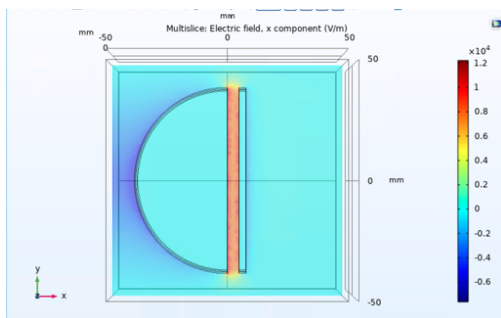


Figure 2.15: The electric field simulation in 2-dimensions, x-y plane

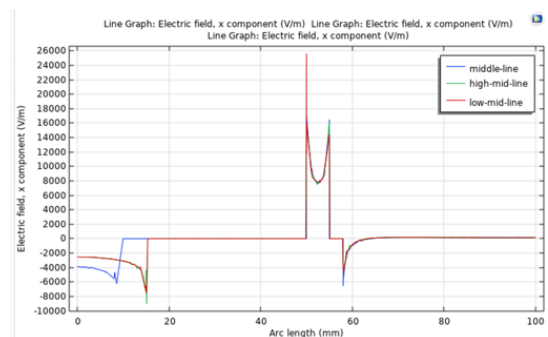


Figure 2.16: The electric field uniformity along the y-axis

From this plot, we can also look at the uniformity at different points along the y-axis. Figure 2.16 shows the field is mostly uniform within the curve between the peaks. The variability between the peaks and the minimum of the curve is rather quite large but this can also be reduced by decreasing the gap distance. From these simulations, it can be determined that the designs for the electric field plates were functional and operates as expected. Now that the plates should behave as expected, the ideal distance between the plate and the cyclotron frequency need to be considered. The cyclotron frequency is dependant on the desired atomic material and the strength of the magnetic field. The mass of the proton and the magnetic field strength were fixed, so the cyclotron frequency was a fixed value. This value was important to the electric field because this is the rate at which the electric field plates have to switch the direction of the field. The input signal needs be a square wave that allows for almost instantaneous switching from positive to negative voltage. This instantaneous switching was affected by the time constant of the system, which was determined by the capacitance of the plate. To determine the capacitance of the plates, equation 2.4 was used.

$$C = \frac{\epsilon_0 \cdot A}{d} \quad (2.4)$$

Where ϵ_0 is the vacuum permittivity constant, A is the area of the plates, and d is the distance between the plates. The time constant τ is equivalent to the cyclotron frequency and was calculated using the following equation.

$$\tau = R \cdot C \quad (2.5)$$

To accommodate the time constant, a resistor was added into the system. If the resistor needed is 500×10^{10} Ohm, then something was wrong and the distance was adjusted accordingly. The next step in the process was to build the plates from a sheet of copper. The quality of copper will affect the metals ability to conduct the AC signal, so it is necessary to have a pure copper sheet. A single sheet of 99% pure 1mm copper was order from Amazon

for reasonably cheap. A single sheet was large enough to make multiple prototypes of the plates. To maintain a constant steady uniform electric field, the plates needed to be smooth and symmetrical. The plates needed to be cut as cleanly as possible, so the first method devised was to use the laser cutter in the Art Department. The laser cutter is primarily used for wood and thin plastic, so the cutter should theoretically be able to cut a 1mm thin sheet of metal. However, copper is highly reflective and would fully reflect the IR laser. This could damage the laser and wouldn't cut the metal cleanly. The next method was to use a thin jewellery saw to cut the metal by hand, so a small coping saw was purchased from Lowes. To ensure a clean and symmetrical cut, a 2D blueprint was created in Fusion360 and glued to the metal sheet.

Cutting each face out separately and then soldering all the pieces together was the easiest method of constructing the plates without ordering out the manufacturing. The main concern about ordering parts was the amount of time to return the parts after sending the designs. However, it may be possible to use the TORMAC CNC machine in the metal shop to carve the plates out of a block of copper. At the moment, all the components were cut using the coping saw and then soldered together. By cutting the 2D geometry out and gluing it down to the face of the copper sheet, there was a simple outline to follow while cutting. The easiest parts to cut were the faces of the rectangular plate. As an initial test of concept and stability, the rectangular plate were cut out by hand first and then sanded down to provide a smooth bonding surface for soldering. To help create a better bond and make the process easier, soldering flux was applied on all the surfaces that will be connected together. By placing a layer of solder on all the connections it makes the final bond stronger and much simpler to connect. Starting with the bottom and the side walls, allowed for simple perpendicular connection to be made. Then the top face was added to the others. Copper is a great conductor, so the heat was easily transferred from the soldering iron to the plates. This makes the process harder because it can reheat the solder on the other corners and make the bonds come loose. To counteract this affect, the solder was applied quickly.

The first iteration of the rectangular plate went together well, but the one edge of the plate was slightly offset. The plates was offset as a result of the cutting process, one edge has a little extra material. To fix this problem, the next manufacturing process could use a mini-CNC machine. However, the mini-CNC machine was only a viable option for the straight pieces. The machine doesn't have the capability to make round cuts that that are required for the half-moon plates. The only possible way the mini-CNC machine could do the curved cuts, is by make a series a straight line cuts tangent to the curve³. Using this method may have worked to provide a smooth consistent curve, but it would be very time consuming and require dozens of separate cuts. The unpredictability of this method means it was more difficult than ordering the parts out.

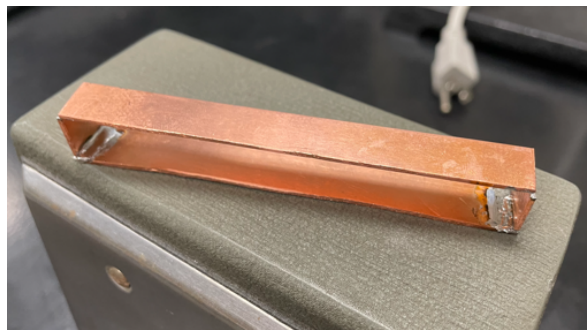


Figure 2.17: The first iteration of rectangular plates

After developing a first prototype of the rectangular plate by hand, there were concerns over the potential quality of the round half-moon plates. Cutting the copper with a coping saw for any straight line was relatively simple, but curved cuts will be very difficult and time consuming. It is important to maintain the symmetry of the curved plate due to the sensitivity of the field. If one side of the plate has more material, it could change the electric field and generate a force in a direction that would be detrimental to the desired trajectory. To ensure the best possible final product, an order to SendCutSend.com⁴ was placed for three sets of each plate structure. After uploading the individual plate faces to the company,

³The tangent to a curve at a given point is a straight line which “just touches” the curve at that point

⁴A company that takes designs and cuts them out of metal to be sent back with a short turn-around time. Normally, parts are cost effective, high quality, and fast shipping.

the desired thickness and material was selected. The manufacturer will only cut the desired geometry out of a $1mm$ thick sheet of 99% copper and the plates will be assembled here at Bard. By ordering multiple sets of the rectangular and half-moon plates, it provided the ability to test different methods of connecting the faces. The first method was similar to the first iteration of the plate, using solder and flux to essentially “weld” the parts together. The second method that might be worth investigating involves placing a long strand of solder on the surface of the plates and using a high heat torch to simultaneously make the bond. This method ensures that the solder is evenly applied to all surfaces and a stronger more uniform bond is made. This also reduces the possibility of warping the faces with uneven heat distribution.

Most faces simply needed to be connected with solder, but the back curved piece of the half-moon needed to be bent into the right geometry. To do this, a jig was developed in Fusion360 to be printed in PLA filament. The jig had a groove for the flat face to fit into as it was pushed down using a perfectly round handle. The handle had the correct size and curvature that was required for the curve of the half-moon while taking into account the thickness of the metal sheet. The jig and round handle can be seen in figure 2.18. The jig should create even pressure on the metal face while compressing it into the right shape in the jig. It provided a perfect surface to bend the metal around because of the guiding grooves and durability. To ensure that the bending process doesn’t break the jig, a stress test was conducted in Fusion360. By locking the position of all the surfaces and applying specific force to only the surfaces that make contact with the metal or the round handle, it showed how the jig deformed over time. Figure 2.19 shows how the jig deformed after a significant force was applied. The force was set to the average force of a human pushing on a surface, roughly $400N$. Figure 2.19 shows very little to no displacement of any section of the jig. The maximum displacement experienced was $9.0 \times 10^{-4}mm$, which is negligible in the long term. It is important to maintain the jigs shape when bending the metal. However, if the jig does break, another one could be printed quickly. One of the benefits of using 3D

parts is having easy access to make breakable parts quickly and cost effectively.



Figure 2.18: The jig used to curve the back face for the half-moon plate

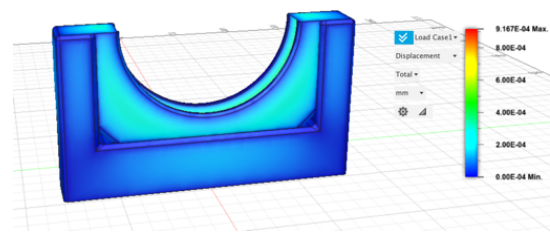


Figure 2.19: Stress testing the jig

When the manufactured parts from SendCutSend arrived, the next iteration of plates was built. Putting together another version of the rectangular plate gave an understanding of the metals qualities before building the half-moon plates. Specifically regarding the stiffness and temperature resistance of the metal used by the manufacturer. If the the manufacturer used a lower grade copper, the properties will differ from that of the 99% pure copper sheet used in the first iteration. Following the success of the first iteration, soldering the components together was easiest way of joining the metal. Throughout this iteration, an object with a perfect right angle was used to ensure all sides are perpendicular to one another. Since all the parts were machine cut and supposedly “perfectly” square, it was much easier to create right angles. Before soldering the joints, a layer of solder was applied to all possible edges/faces that could touch during the bonding process. This guaranteed a secure bond and made the process much simpler. The second iteration of the plate was a success and proved to be well worth ordering the parts from an outside manufacturer. The next step was to print the metal bending jig discussed above and craft the curved face of the half-moon plate. A hand-cut prototype from the original copper sheet was first used to test the capabilities and effectiveness of the jig. This prototype piece was not symmetrical, but it fit the dimensions of the jig and served as a good test. The component was placed on the top of the jig and then an even pressure was applied to copper rectangle, forcing it into the grooves of the jig to take it’s desired shape. This method overall worked and did curve the component to roughly the correct shape, but it was difficult to maintain the shape after

removing the bending handle. Specifically, the edges of the component would bend outward, making a parabolic shape. To counteract this affect, a slight amount of pressure was added to the edges, pushing them into the correct orientation to match the curvature of the flat half-moon sheets. The metal bending jig served as intended, but perhaps a future version could implement a bolt tightening system to maintain a steady pressure along all edges and have the ability to generate more bending force in specific areas.

The last component of the process was bent into shape and fused together with the half-moon sheets to create the half-moon electric field plate. Using the experience from the first and second iteration of the rectangular plate, the faces were joined using solder. After applying a thin layer of solder to all the edges and surfaces, the curved back face was placed on a single half-moon sheet. Having the initial layer of solder on the components made the process easier because the soldering iron could simply be dragged along the edge of the joint, remelting and pulling solder to fuse the parts together. The second half-moon plate was placed on the back face and the process was repeated. Fusing the first two parts was much easier because there was ample access to the seam from above, but adding the third part, reduces the access to the seam to only one side. The space between the plates is only 10mm , which was enough to allow the soldering iron to touch the back wall, but not directly touch the seams. The sections of the seam closest to the open face were easily sealed, but the section farthest away were the most difficult. It was impossible to close this section of the plate from the inside, so the plate was sealed from the outside edge. This worked and won't affect the overall capability of the plates. Figure 2.20 shows the first completed set of electric field plates made from SendCutSend parts.

The second iteration of the rectangular plate and the first iteration of the half-moon plate were completed and fitted into the mounting component. All the edges of the plates were filled down to provide a smooth and clean surface because it improves the quality and uniformity of the electric field. Upon testing the fit of the electric plates and the mounting system, a measuring error was revealed. The internal radius of the chamber was measured

to be 2mm too large and affected the fit of the whole system. A new set of plates were required to fit the components into the chamber. The rectangular plates were relatively easy to make by hand, but the half-moon plates was a concern. A new iteration of the plates was designed and 3D printed first to be fitted into the chamber to ensure a proper fit. The new designs were sent to SendCutSend and arrived a week later. Figure 2.21 depicts the snug fit of the 3D printed version in the chamber.



Figure 2.20: The first completed set of plates

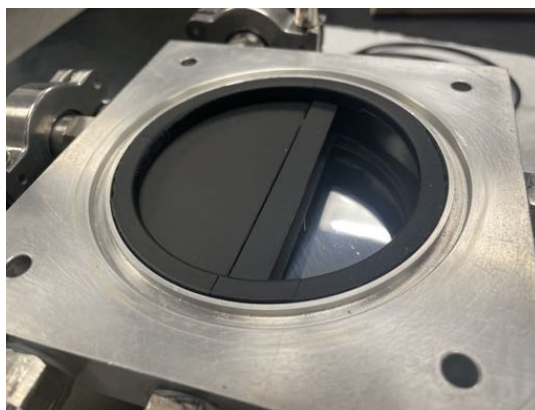


Figure 2.21: 3D version placed inside the chamber

2.2.2 The Mounting System for the Plates

The electric field plates are housed within the vacuum chamber and have a high voltage signal running through each plate. To prevent a short in the circuit, the plates must not touch any form of conductor within the chamber. The chamber itself is made of aluminum and the side walls of the chamber are iron, so all surrounding material is highly conductive. To isolate the plates, they must be held in position securely with a material that is strong, flexible, and non-conductive. The plate holder needed to be flexible because the chamber experiences some slight compression when the pump is activated. A perfect material for the holder was PLA or PETG⁵ filament because of its durability and the ability to reprint a new version when modification are required. The prints were precisely measured, but there

⁵Polyethylene Terephthalate Glycol (PETG) is a synthetic thermoplastic polyester used for 3D printing. It is a strong durable plastic filament, capable of handling high temperatures.

was still small defects in the printing process which affected the assembly process of the plates. Due to the limited space inside the chamber, the mounting system must fit within the empty space of the chamber and provide a number of access points for wires. The harness should be assembled in two parts because it would allow easy access to the plates and make modifications easier. If the two pieces need to be connected, a thin layer of tape can be applied on the joints to maintain a clean solid connection. Using glue would make the system fixed and using small magnets could affect the uniform magnetic field.

A positive and a negative wire are required to supply the voltage signal to the plate. A number of grooves, approximately the gauge⁶ of wire that will be needed for the high voltage source were carved into the sides of the mounting system. This means that no matter the location of the electrical feed through port, the wires would still have the ability to reach the plates. It was also important for the gas line to reach the center of the chamber without interfering with other components. This problem was a little trickery because the gas line is composed of a stainless steel tube which needs to feed directly to the center of the chamber. The gas line tube is not flexible and was essentially a fixed variable in the system, so all other components should be built around it. However, the gas line can only be set in place once the electric plates were built and placed into the mount. Another element that was consider in the design process was the ability to access the detector inside the chamber and allowing for ample space allocation. The exact dimension of the detector were unknown, so having a variable space for this the best option in the long term progress of the project.

The last component to include was the electrical lines to supply current to the heating filament. The electrical feed-through has four pins, so this was connected to the plate wires and the filament wires. All the wires started in the same place, but were directed into different parts of the chamber. The system to secure the filament wires, filament, and the gas line are discussed further in the hydrogen ionization section. Figure 2.22 depicts the first

⁶The size and voltage/current limits of a type of wire. The higher the gauge of wire, the more current and voltage the wire is able to handle without generating high amount of heat. This also creates the potential to destroy the plastic coating on the wire. It is important to use the proper gauge wire when dealing with high voltages/currents.

model which was modified further after building the detector.



Figure 2.22: The electric plate mounting system

To ensure the most freedom when mounting the plates and connecting the power supplies, many access spaces were integrated into the design. As mentioned previously, the mounting system was split into two parts. While one part was almost completely open, providing ample space and the other has structured walls. The half with the large rectangular opening holds the rectangular plate. This means that the plate won't block access to the back wall and all the wires, gas lines, and detectors will fit into this space with lots of flexibility. The other half has many more wall supports to provide structural security and ensure the other half maintains its shape under pressure. This half was allowed to have more walls without infringing on the space demands because it holds the half-moon plates. The half-moon plates will block access to that side anyways, so implementing extra support in this region is a practical use of space. The other major feature of the support mounts was their ability to create a precise fixed distance between the plates. As mentioned in the generating electric field section, the distance between the electric field plates is very delicate and requires the utmost thought. By creating a specific distance between the plates in the mounting system, it made the whole process much easier.

After once again fixing the Bambu X1-Carbon printer, the mounting plates were printed in PETG filament. The first two attempts to print the part failed due to failures in the support structure. The orientation of the parts in the first two trials were vertically, creating arches across the bed plate. This was done with the hope to minimize the amount of support

structure needed, but it turned out to be a remarkable adversary. The parts failed because the support structure had a “spaghetti”⁷ failure at the beginning of the printing process, resulting in a full restart of the print.

The next approach involved turning the model 90° to make each part print perpendicular to the curved section, as seen in figure 2.22. This method worked much better than the previous two trials and the print maintained all details from the model while remaining strong. The rigidity ensures the plates maintain their position throughout the entire process. The support material was easy to remove without causing any noticeable damage to the print, but upon further examination of the interior of the print, there was a series of layers that failed to stack properly. This most likely occurred because of the fillets⁸ that were added to the interior edges to hypothetically add more support in the printing process. Overhangs in the printing process are often neglected, which results in layer shifting. Fillets can be added to create a smooth transition and make a stronger edge of the model. However, when printing smaller components, the amount of layer used to create the fillet is fewer. This means that the distance the extruder shifts in the process is greater, increasing the chances the layer will not adhere properly. Layer shifting in the interior of the model should not affect the usability of the component, but it could be corrected by simply sanding down the surface with a low-grit⁹ sandpaper. This could also be remedied in the slicer program before printing by adjusting the speed and layer thickness. Slowing the speed and decreasing the layer thickness will force the printer to take a longer time moving along the fillets.

After finishing the complete set of electric plates, they were placed into the mounting structure. The initial design did not account for the thin layer of solder between the face

⁷This term is used to describe the filament building after failing to attach the intended edge of the build. The filament starts to form a bundle of tangled “spaghetti”. This ultimately means that the print is a failure and needs to be restarted. Even if the support structure is the failing component, it can interfere with the rest of the build later in the process. It can also clog the hotend extruder nozzle.

⁸The Fillet tool creates a set of tangent or curvature continuous faces that connect to the faces that meet the selected edges. This process creates a rounded edge around the selected faces or edges, resulting in a smoother transition between surfaces.

⁹The number of granular particle per square inch of the sheet of sandpaper. The high number of grit means that there are more grains of sand on the sheet as a whole. Low-grit sandpaper is used to remove more material, while high-grit sandpaper is used for smoothing and refining the surface.

and any other imperfection that would affect the size of the plates. To correct for these unexpected changes, the model was customized to this specific set of plates. Measuring and mapping the plates with electronic calipers determined the precise amount the tolerance for the plates on all sides. If another set of plates is manufactured in the future, then custom alteration will be required for that mount. The necessary alterations were made in Fusion360 and then the updated model was sent to the 3D printer. The plates fit securely into this version of the the print and appear to cover the same amount of space as the 3D model.



Figure 2.23: The electric plate in the mounting system

In figure 2.23, two iteration of the mounting system can be seen holding a 3D printed version of the electric field plates and the first complete set of plates. From the image, the plates were securely held in the harness with some wiggle room to allow for small adjustment for the electronics. This image also shows that this initial version of the metal plates matches the 3D printed template. This acts a visual representation of the similarities in concept between the printed and final product.

2.2.3 The Voltage Source

The available signal generators don't have the capability to supply a high frequency signal while maintaining a high voltage, so a signal amplification circuit was needed. A circuit needs to be designed to supply a high voltage square wave signal to the copper plates in order to generate the electric fields. The first design that could properly amplify an AC signal, was a non-inverting amplifier. The non-inverting amplifier uses a couple resistors and a operational amplifier (op-amp) integrated circuit. Figure 2.24 depicts a simple example of the circuit[33].

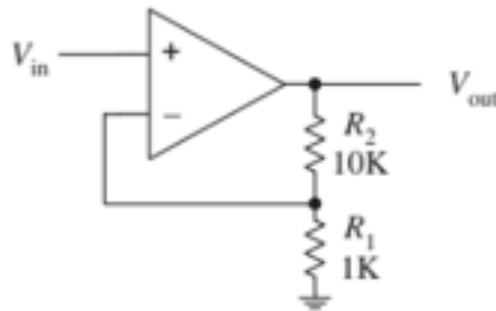


Figure 2.24: Non-inverting amplifier circuit

An operation amplifier take an input signal or voltage and amplifies it by a factor proportional to the resistors chosen. The total increase the input signal gains is proportional to $\frac{R_2}{R_1}$ times the input signal itself. It is also important to note that the maximum amount the signal can be amplified by is equal to the amount the operational amplifier requires for power. An average op-amp uses a positive and a negative 15 volts to power the integrated circuit. Since the desire voltage for the electric plates is much higher, an average op-amp will not be sufficient to amplify the signal. The op-amp would be overwhelmed and burn out from the high voltage and heat. However, high voltage op-amps can be purchased on most circuit component websites, including Amazon. It was important to consider the operational frequency that the components can handle. From the initial calculations, the frequency that the input voltage needs to run at was in the MHz range, which is well beyond the capabil-

ities of a normal op-amp. The required op-amp needed to be able to handle both a high voltage and a high frequency. Finding this specific component was challenging because it is a specialized part that only a few companies supply. Not to mention, the price for this type of op-amp is quite expensive. After looking at the possible options, there were only a couple that could actually handle a sufficiently high voltage and frequency. However, the highest voltage that would be attainable with this component was 200V, which is a little lower than desired. The higher voltage provides more flexibility for the distance between the plates while mounting them in the chamber. This would also increase the strength of the electric field, hence increasing the overall kinetic energy.

The next possible solution was using a complex circuit called an H-Bridge. An H-bridge is commonly used for controlling the direction of current flow in motors, but it can also be adapted for other applications where polarity reversal is required. In an H-bridge configuration, you have four switches (usually transistors or MOSFETs) arranged in a square with the load (in this case, the capacitor) connected in the center. By controlling the state of these switches, you can effectively reverse the polarity across the load. H-bridges are capable of switching states very quickly, allowing for rapid changes in polarity and you can precisely control the timing and duration of polarity reversal with an H-bridge, which may be beneficial depending on your application requirements. H-bridges typically have lower voltage drop compared to other configurations, which can be advantageous for maintaining higher efficiency. However, keep in mind that using an H-bridge also introduces complexities such as managing switching transients, ensuring proper isolation, and providing adequate drive signals to the switches. This circuit would be an ideal system to switch the voltage quickly, but is very complex to build. The complexity of building and customizing the circuit to specifically handle the electrical plates is difficult and will be a challenging task. Due to the complexity and time limitation, the H-bridge circuit is not the best option for this project. However, given more time and assistance, this would be a promising addition to the system in the future.

The next possible circuit that could be useful to the project is a HVHF circuit. This circuit is capable of handling very voltages at very frequencies. This circuit can be seen in figure 2.25. This circuit operates in a similar fashion to the H-bridge circuit in the sense that there are gates that only let a particular voltage through at certain times. When the transistors are supplied with the proper current, the gate opens and lets the signal through. However, this circuit has some added complexity because it requires a current sink to draw all the high current levels always from the plates. The circuit is essentially a mirror across the horizontal plane. Each half is responsible for amplifying a particular range of voltages. One would amplify the voltage above zero and the other below zero.

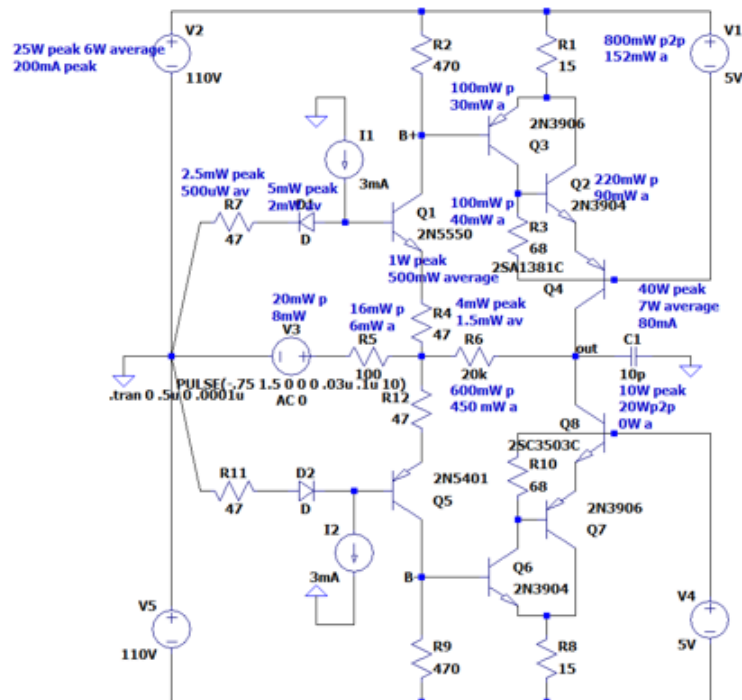


Figure 2.25: The HVHF circuit

All the components for this circuit were ordered and the circuit was actually assembled. Since the system is so complex, it was very easy to flip a diode or transistor. The circuit didn't work upon the first attempt, so it was double checked and built again. When the second attempt didn't work, the lower half of mirror plane was completely removed to only concentrate on the upper half. After checking the whole circuit numerous times, it was

declared that the breadboard didn't work correctly. The circuit should be built on another board to test its capabilities and frequency response time.

While working on the HVHF circuit, a difference amplifier circuit was also constructed. The difference amplifier uses a number of transistor and resistors to flip the signal from positive to negative. Difference amplifiers, also known as differential amplifiers, are electronic circuits designed to amplify the voltage difference between two input signals while rejecting any signals that are common to both inputs. They are widely used in instrumentation and signal processing applications where it's necessary to amplify only the signal of interest. Together a simple square wave and a external voltage source of 200V are able to output a high voltage fast frequency square wave. The output is sent directly to the plates, which is shown as a capacitor in figure 2.26. This was a promising design and would be easily made with many parts already purchased, except for the transistors. After building the circuit, the first test of the system using a 10MHz signal and a 50V input signal failed due to a bad breadboard. Upon building the circuit on a new breadboard and testing the same system, the circuit was successfully able to amplify the signal at fast frequencies. However, the frequency of which the signal will be running is much faster than that of the circuit was able to successfully switch without clipping the edges. The time it takes for the signal to rise was longer than what the frequency requires, so the output wave is not a perfect square wave. Since all the possible circuits that could possibly be used will take a long time to perfect the system, the plan shifted to dictate the frequency and voltage based on the equipment available. The maximum high voltage frequency that could be provided by an accessible amplifier was 100V 1MHz, so the cyclotron frequency was adjusted accordingly. The magnetic field was set to a value that would produce a cyclotron frequency of 1MHz and the distance between the electric plates was adjusted to account for the drop in voltage. Using equipment that was already accessible sped up the time frame of testing the system and reduced the complexity of the task, but it does limit the system as a whole.

As a side effect of the plates acting like a conductor, it is important to think about the

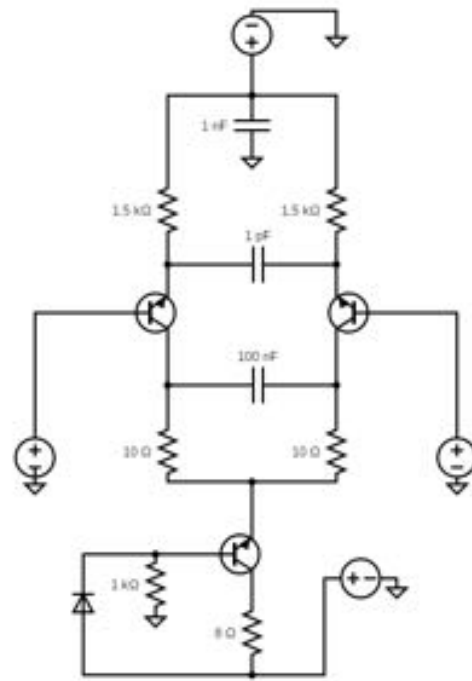


Figure 2.26: Difference amplifier circuit

distance between the plates and the ability for an electric discharge to occur. The voltage will flow between the plates at small distances, it will start to spark or arc across the plate gap. This is important because the ionization process will require hydrogen to flow into the chamber and a spark could ignite the hydrogen gas, causing an explosion. The explosion is not only dangerous for me while working, but it could also destroy the vacuum chamber. While the vacuum is actively at a negative pressure, the chamber will be void of any oxygen, which inhibits the hydrogen's ability to ignite. Hydrogen only becomes volatile when it interacts with oxygen which means that there is little chance the voltage jumping between the plates will be able to ignite the hydrogen gas. A relationship can be seen between the magnitude of the voltage and the distance between the plates. As the distance increases the minimum voltage required to arc also increases. As a general rule of thumb, it takes approximately $30,000V$ to jump $1cm$ [27]. The voltage will arc differently under vacuum conditions, so it is necessary to look at the Paschen curves¹⁰ for different gases under vacuum.

¹⁰Paschen's curves gives the breakdown voltage. The voltage necessary to start a discharge or electric arc,

Depending on the gas medium, the voltage will breakdown at a different minimum voltage. The setup should not encounter any issues with electrical discharge because the pressure will be well below the minimum pressure to discharge at the expected gap distance.

2.3 The Chamber and Generating a Vacuum

2.3.1 Chamber Design

When designing the vacuum chamber, it was important to think about the chamber material and size. The chamber needed to fit between the electromagnets and into the steel frame. The chamber roughly needed to be less than 9 cm in height including space for bolts and some space to easily remove the chamber without damaging the magnetic poles.

The most important aspects of the chamber are the material and the ability to maintain a stable vacuum pressure. Since the magnets are outside the chamber and need to penetrate the chamber walls, the material must allow the magnetic forces to go through it. Materials like copper, brass and aluminum are all good choices because they have very little to no affect on the magnetic field. Materials like steel and iron are not a good option because they shield magnetic fields. Copper and brass are rather quite difficult to cut and shape, not to mention they are more expensive. Aluminum is a strong, malleable, and a relatively cheap material, which makes it a ideal candidate for the chamber. To further show this, the magnetization M of each material was calculated to see how different materials affect the magnetic field. Magnetization is a vector quantity that measures the density of permanent or induced dipole moment in a given magnetic material using equation 2.6. For the moment, this equation purely looks at the magnitude of the magnetization, not the direction.

$$M = \chi_m \cdot \frac{B}{\mu_0 \cdot (1 + \chi_m)} \quad (2.6)$$

between two electrodes in a gas as a function of pressure and gap length

B is the magnetic field the material is exposed to, χ_m is the magnetic susceptibility of the material¹¹, and μ_0 is the vacuum magnetic permeability constant¹². The magnetization for different materials under a constant magnetic field was calculated and compared to determine the effects of various material affects on the magnetic field. For iron (Fe), χ_m is 150 and aluminum (Al) is $2.2 \cdot 10^{-5}$. χ_m is a unit-less value. Iron has a much higher susceptibility than aluminum which means that it amplifies and disrupts the magnetic field much more. Using equation 2.6 and a constant field of $0.2T$, $M_{Fe} = 158101A/m$ and $M_{Al} = 3.50133A/m$. Iron has a much greater affect on the field by nearly a factor of 50,000. Clearly showing that aluminum is a better choice of material to construct the chamber. The next hurdle to tackle for the chamber was the physical design and size of the chamber. The chamber needed to be strong enough to handle a vacuum pressure of $1 \times 10^{-3}torr$ and small enough to fit between the electromagnets. The maximum distance between the electromagnets is approximately $9cm$ and the approximate radius of the coils is $40cm$. Using these dimensional constraints, a simple model was created in Fusion360 with the intention of sending the design to a chamber manufacturing company for a price estimate. The initial design was crude and doesn't show any bolts or any perpendicular ports out of the chamber.



Figure 2.27: Concept design of aluminum vacuum chamber

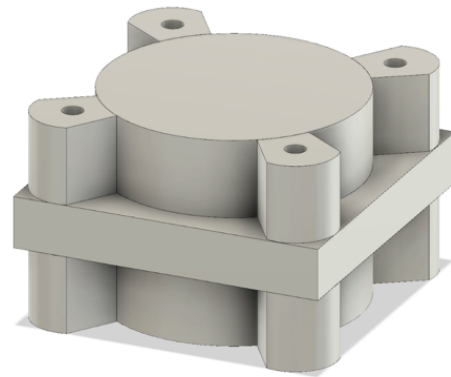


Figure 2.28: Original vacuum chamber

¹¹ χ_m , the magnetic susceptibility of a material is equal to the ratio of the magnetization M within the material to the applied magnetic field strength H . Also a unitless value.

¹² μ_0 , the magnetic permeability of vacuum, permeability of free space or magnetic constant.

After sending the initial design out to Kurt J. Lesker Company¹³ for an cost estimate, the original chamber used with the electromagnets from many years ago was found. The chamber seemed to be in good shape, but it needed to be tested and fitted into the system. The vacuum chamber design was very simple but clever because it primarily uses the negative forces of the vacuum to maintain a clean seal. The assembled chamber is below in figure 2.28. After removing the four long bolts holding the chamber together, one in each corner of the block, the chamber interior was exposed. Even though the old gaskets seemed to be in decent shape, a new set was installed to create a better vacuum pressure. The center aluminum block sandwiched between the magnetic pole faces has seven port connects that can be plugged with thread-less bolts. Each plug has a small groove that holds a rubber gaskets to create a sealed connection. The chambers negative pressure pulling inward keeps the plug in place and maintains the pressure using the gaskets. If the pressure were to be positive, also known as a high pressure system, the plug would want to be pushed outwards away from the chamber. However, this does make it challenging to have other port connections like external wire connections or hydrogen gas lines that need to run into the chamber. A number of plugs were missing from the chamber when found, so replacements were require. Designing plug connections in Fusion360 with the intention to eventually carve them out of aluminum or brass on the CNC machine was a great candidate for replacing the missing parts. Using a material like aluminum or brass provides strength, but won't interfere with the magnetic field. After some research, it was discovered that some 3D filament plastics like PLA¹⁴ and ABS¹⁵ are strong enough to withstand low level vacuum pressure, so printing the parts was a viable option. The two parts in figure 2.29 were designed in Fusion360 using the original plugs as references. The threaded gasket plug goes through the chamber and attaches to a mount in the center, which was used to hold sample material. In previous experiments, the mount was used to hold Alpha and Beta ray emitting materials. Each

¹³A company that specializes in manufacturing vacuum chambers, parts, and pumps.

¹⁴PLA, Polylactic Acid. Made from renewable resources such as corn starch or sugar cane.

¹⁵ABS, Acrylonitrile Butadiene Styrene. ABS is a thermoplastic material commonly used for injection molding.

plug has a gasket placed in the groove towards the top end of the bolt. The smaller gasket plug, only acts as a seal to create a vacuum, while the large threaded plug holds material in the center. Designing the plugs in Fusion360 provided the ability to change the design for any situation that needed, easily customizing parts quickly and effectively. The quality of the PLA printed parts was impressive but there were concerns about the overall structural strength of the plug under high strain. The Princeton Plasma Physics Laboratory (PPPL) conducted experiments towards the viability of using PLA printed parts in vacuum chamber systems at a variety of pressures, reaching as low as $1 \times 10^{-6} \text{ torr}$. Their experiments revealed, 3D printed parts are able to withstand the low pressure environment[40]. The next concern of using the printed parts was off-gassing, which means the parts may release any residual gas built-up within the plastic from the printing process or even expelling plastic particles into the chamber. This would make achieving a low pressure difficult or even impossible. The PPPL concluded that there was no detectable change in the RGA spectra¹⁶ caused by off-gassing[40].



Figure 2.29: Threaded gasket plug and gasket plug

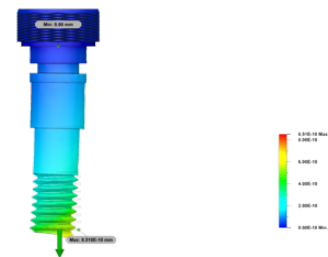


Figure 2.30: Simulated pressure displacement test on PLA filament at 0.0133 MPa.

To think about the strength of the 3D printed bolts further, a simulation of the potential stress experienced in a low pressure environment was conducted on the bolts. Using Fusion360 simulated environments, figure 2.30 shows the bolt slightly warped under the pressure. The simulation required a fixed point on the bolt and an area that experiences

¹⁶Residual Gas Analyzers (RGA) evaluate all the gases present within a space over time.

the pressure. The fixed point on the bolt was selected to be the surface area that makes contact with the exterior walls of the vacuum chamber. The rest of the bolt on the inside of the chamber was selected to experience the force. Figure 2.30 shows the displacement of the bolt after experiencing the pressure. The colorbar to the right determines how much the bolt had shifted; blue represents no displacement and red is the maximum effects of warping. The top of the bolt, where the fixed point was located experienced almost no shifting or warping, but the bottom end experienced quite a lot. The part of the bolt that would be farthest in the chamber experienced the most warping at around $8.510^{-10}mm$. Relatively speaking this was very little warping, but it was not practical to print a new bolt after each test to ensure the security of the chamber. With all this information in mind, it does make printing parts for the chamber a viable option, but there are still concerns about the strength and reliability of each plug. The variation while printing could make achieving a low pressure difficult. Two printers were used to print prototypes of each plug, the first being an Ender Series 3 Printer and the second was a Bambu Pro Printer. The Ender 3 was my personal printer that has good print quality and the Bambu Pro was the newest printer added to the department. The Bambu Pro has the ability to print with stronger materials like carbon fiber, which could be used to print chamber parts in the future.

The first attempt printing set the gasket plug with a 15% in-fill¹⁷ in a cross pattern. A cross pattern was selected because it is frequently recommended in user manuals as the beginner fill pattern when printing small parts that require high strength. To test the strength of the part, the parts were put under a number of weights with the intention to snap and break the components along potential weak points. The top of textured part of the plug was also pulled aggressively because this section would take most of the force from the vacuum. Since this part of the plug sits outside the chamber, it keeps the plug from being completely pulled into the chamber under the intense pressure. The top of the plug separated from the bottom, which means that the in-fill needed to be much higher. The in-fill of the next

¹⁷The in-fill is the relative percentage of the internal volume of the print that is filled with material. So the inside of the plug was filled with that percentage of material in the set pattern.

iteration was increased to 50%. This print iteration was noticeably heavier and feels much stronger, remaining together after testing the same way as the first iteration.

The next step was to print the threaded plug and test its strength. The in-fill was set to 50% to ensure a strong reliable print. The threaded plug held together and didn't appear to be crack under any pressure exerted upon it. However, this was only a visual analysis of the damage to the plug, a more conclusive stress test would be continuing the weight exerted on the plug until it tears apart. There was much concern about the plug breaking or cracking while at a low pressure, which would potentially damage the pump and the other delicate components within the chamber. Risking the chamber getting damaged if the bolt warps and breaks the vacuum seal could be catastrophic for the experiment. If the vacuum seal breaks, the rapid rush of air into the chamber may damage the internal components. To overcome this potential failure, it was decided to convert all the connections to a half an inch aluminum KF16 port fitting. Figure 2.31 depicts the KF16 fitting adaptor and its specifications.



Figure 2.31: KF16 1/2" NPT adaptor[30]



Figure 2.32: Compact precision extreme-pressure steel threaded pipe fittings[22]

Five KF16 adaptors were ordered through Amazon and order four half an inch steel hex plugs from McMASTER-CARR. The initial designed apparatus only needed four KF16 port connects and are as follows: a vacuum connect for the pump, a input line for the hydrogen gas, a connection for the electrical wires, and a connection for our detector. So the remaining holes were filled with the simple plugs from figure 2.32 until KF16 attachment ports are needed. Using the KF16 adaptors would allow for any connection flange or fitting that was

needed in the future without making major changes to the chamber structure. When the vacuum chamber was found, there were seven holes already drilled into the perimeter of the chamber. Only one of the seven holes was threaded with a tapered drill bit¹⁸, which ensures a tighter fitting bolt connection. The next step is to thread the remaining six holes and test the KF16 adaptor fittings. To tap the holes, the interior diameter was increased to allow the tapered tap to create a perfect set of threads. A reference was used to verify the new threaded holes were the same size as the original threaded hole in the chamber. The chamber came with a quick release valve that screws into the chamber port that was already threaded, so this was used as a test fitting until the adaptors arrive. Using a scrap piece of aluminum from the supply room and a series of drill bits, test holes were drilled. The largest drill bit was a 37/64, which was just slightly larger than the half an inch adaptor connection because the required tapered tap requires a little extra space to cleanly thread the hole. Once the hole was cleaned and the burr removed, the tap was twisted through the hole to create threads. It is important to use a lubricant throughout the process because it makes the threads cleaner and much easier to cut material away. Cutting threads into the holds was a much more tedious and exhausting process than original predicted. The drill press¹⁹ could have been used to create nice clean threads in the metal, but the tap requires a low speed that the press can't provide. To properly tap the holes, it was also important to use a sequence to cut away material and remove it. The tap should be rotated two full turns clockwise to cut material and then one full turn counterclockwise to remove the cut material from the hole. The drill press would not easily allow for this process, so it must be done by hand. The four test holes were successfully tapped and fitted with the quick release fitting, which means that the chamber holes were ready to be tapped. Placing the chamber into a vice sandwiched between two pieces of wood creates a solid support while using the tap. The wood ensured that the soft aluminum chamber was not bent or damaged in the process. After tapping the first hole, the quick release fitting was tested to make sure that

¹⁸The tool that creates the internal threads to hold bolts or screws.

¹⁹A standing drill that is lowered to the material to create a straight and uniform hole.

nothing went wrong in the process. This process was repeated for the remaining holes out of an abundance of caution. All six of the untapped holes were successfully tapped without damaging the chamber. A 3D render of the chamber after threading can be seen in figure 2.33.

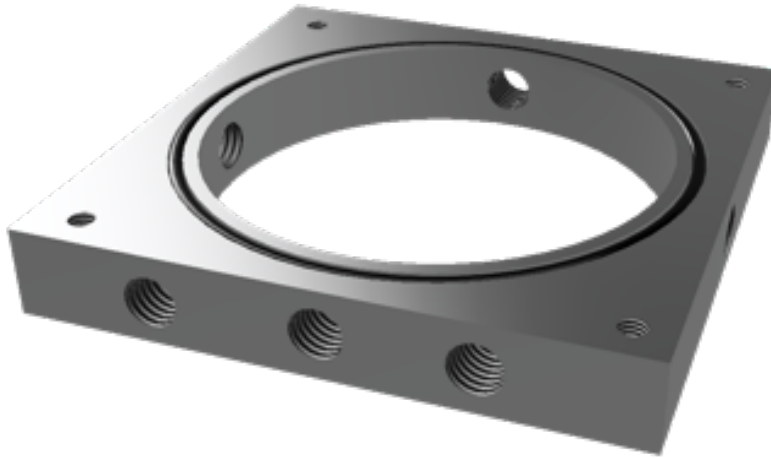


Figure 2.33: The chamber render after threading the holes

The four plugs arrived from McMASTER-CARR without issue, but the KF16 adaptors was another story. Only one connection was ordered instead of five, so the remaining four connection came in a couple weeks. Now that the plugs and a singular fitting had arrived, they were tested in the chamber to make sure they were the right parts to create a vacuum. Luckily all the fittings were fastened perfectly in the threaded holes.

The vacuum chamber must now be reassembled to eventually test the capabilities of the chamber and pump. It was important to assemble the chamber soon to test if it was even still possible to create a low pressure vacuum environment since modifying the structure. If this can not be achieved, then an alternative vacuum system will be required for this experiment. To reassemble the system, the pole faces were removed from the magnetic field system. For instruction on their removal, consult section 2.1. After the pole faces are removed, one can be placed facing up with four of the eight corner attachment blocks in each corner of the pole. Then the aluminum chamber is placed on top of the pole face, aligning the bolt holes with

the four corner blocks. The other pole face is then placed on top of the chamber covering the rubber gasket and then the four remaining corner blocks are placed on the edges with the holes aligned as seen in figure 2.28. Each corner block has a small extruding lip to hold the pole faces to the chamber and ensure everything stays together. Then tighten the bolts through the top corner block down to the bottom corner blocks and tighten thoroughly. The next step in the project is to pull vacuum in the chamber, so all the ports need to be filled with either a steel plug or a KF16 adaptor. So the ports should all be filled before placing the chamber into the magnetic frame. As 4/5 of the KF16 adaptors will be arriving soon, most of the ports will be filled using the steel plugs. This left only one port connection with a KF16 adaptor and one unfilled hole. To fill this last hole is difficult because the department doesn't have anymore plugs or KF16 adaptors, so a substitute plug was required. The only possible part that could do this is a old high pressure gauge using a half an inch NPT adaptor fitting. This gauge won't tell us anything about the pressure and serve no other function but to plug the hole. Having the gauge in the system does increase the chance of a leak, resulting in more difficulty achieving a stable vacuum pressure. Before inserting the plugs, KF16 adaptors, and the high pressure gauge, all the threaded parts need to be wrapped in Teflon tape.

2.3.2 Generating a Low Pressure Vacuum

Now that the chamber was assembled, a low vacuum environment could be tested. The vacuum pump used to remove air from the chamber was the Agilent IDP-3 Dry Scroll Vacuum Pump 60Hz, as shown in figure 2.34.

The pump already had a KF16 adaptor attachment at the top to connect to the chamber, which was another benefit of switching from the original brass plug to the KF16 adaptors. To connect the system, a High-Vacuum Exhaust Hose was ordered with Quick-Clamp Fittings from McMASTER-CARR as seen in figure 2.36. This allowed for the pump to be connected to the chamber easily and gave the option to add connection between the pump and chamber.



Figure 2.34: Agilent IDP-3 vacuum pump[2]



Figure 2.35: The Adixen vacuum pump[1]

The hose had a maximum pressure of $1 \times 10^{-8} \text{ torr}$, which was well beyond the desired pressure[23]. To measure the pressure inside the chamber, a low pressure gauge capable of withstanding pressures of $1 \times 10^{-3} \text{ torr}$ was required. The original intention was to connect the pressure gauge directly into the chamber using one of the ports, but most commercial gauges for low pressure environments have internal components that generate a strong magnetic field.



Figure 2.36: Vacuum hose[23] and tee connectors[24]

Having the gauge connected to the chamber would interfere with the uniform magnetic

fields of the coils, so the gauge needed to be connected somewhere else in the system between the pump and the chamber. The next best location for the gauge is connected directly to the pump using a Tee Connectors Tube, as seen in figure 2.36. The difficulty with adding another connection was it creates more opportunities for a possible leak in the system and therefore more difficult to achieve a low pressure environment. To help ensure no leaks occur, the KF16 connections have a small rubber gasket sandwiched between the flange faces. Then a clamp was pushed onto the two connections and tightened to push the flanges together. The only task that must be completed before testing was finding a pressure gauge to accurately measure the pressure inside the chamber. The department has a number of high pressure gauges and only a couple of low pressure gauges, but it was a challenge to find the low pressure gauges. A very large electronic pressure gauge that could work was found, but the cables and control system were missing. The lab technician was able to find another gauge, the Pfeiffer Vacuum electronic gauge as shown in figure 2.37. The electronic gauge was connected into the system and then connected to an external control box. The control box supplies power to the gauge and displays the pressure measurements. The sensor configuration can be seen in figure 2.38.



Figure 2.37: Pfeiffer vacuum electronic gauge PCR 280[29]



Figure 2.38: Current vacuum connection

After connecting the gauge to the tee and the control box, the changing pressure can be measured as the air is removed the chamber. The first test was able to pull a vacuum pressure of 17torr , which was well below room pressure. Normal atmospheric pressure is 760torr , so the first test was much lower and heading in the right direction. However, the pressure didn't continue to lower with time because there was a large leak present in the system. To achieve a lower pressure, the fittings were inspected and new Teflon tape was applied to all components. The rubber gaskets of the chamber was also replaced to hopefully improve the pressure. Another factor that could be affecting the pressurization is the internal walls of the chamber may not be clean after the drilling process. The residual dirt and grime could make it difficult to pull a lower vacuum pressure. Taking the whole system apart to clean everything, and replace all Teflon tape improved the vacuum quality. The other major concern about the system thus far is the ultimate pressure²⁰ that the Agilent Vacuum system could achieve. The data sheet states that the ultimate pressure of the Agilent IDP-3 is $2.5 \times 10^{-1}\text{torr}$ [2]. A supplemental pump was needed to lower the pressure further to create the best environment for the protons while accelerating.

After searching the many closets of Hegeman²¹, a new vacuum pump was found that could have the potential to achieve the low pressure desired. The new pump found is not necessarily a vacuum pump, but a gas leak detector for vacuum systems. Inherently, the equipment has a vacuum pump to remove all the air from a chamber and detect the levels of a specified gas. The Pfeiffer Adixen ASM 182 TD+ Standard Helium Leak Detector has the capability to reach pressure well beyond $10 \times 10^{-4}\text{torr}$ and can determine the approximate levels of hydrogen within the chamber. This was useful during the H_2 ionization process to ensure that the chamber was not flooded with H_2 gas. Instead of using the Agilent IDP-3, the Adixen provided a low stable pressure suitable for the experiment. Removing the Agilent IDP-3 and replacing it with the Adixen did prove to be a valuable decision because it dropped the pressure by a whole order of magnitude.

²⁰The ultimate pressure is the lowest possible pressure within a realistic evacuation pressure

²¹The beloved Bard Physics Building! :)

Date	Pump	Pressure(<i>torr</i>)
12/22/23	Agilent	17.62
02/06/24	Agilent	3.32
02/07/24	Agilent	6.72×10^{-1}
02/08/24	Agilent	7.28×10^{-1}
02/08/24	Agilent	4.17×10^{-1}
02/012/24	Agilent	3.14×10^{-1}
02/23/24	Adixen	4.44×10^{-2}
03/04/24	Adixen	5.13×10^{-2}
03/04/24	Adixen	1.39×10^{-2}
03/10/24	Adixen	1.97×10^{-2}
04/14/24	Adixen	6.23×10^{-2}
04/24/24	Adixen	2.78×10^{-2}

Table 2.3: Pressure measurements

Table 2.3 shows the change in pressure as the system was revised and modified. Throughout the process, a variety of techniques were used to improve the vacuum pressure, including cleaning the entire surface with isopropanol. The change in pressure is very clear when the new pump was integrated into the system. The pressure went from 6.72×10^{-1} to 1.97×10^{-2} , which is a significant pressure decrease. However, after months of testing and working with the Adixen system, it was concluded that a new vacuum system was required. While the pump does provide a lower pressure than the Agilent, it was quite unreliable and had the tendency to randomly release air back into the chamber during testing. This is a problem because it could damage the internal components of the chamber, particularly the heating filament. When the heating filament is exposed to oxygen it becomes oxidized and no longer functions properly. Until a new pump was acquired, the Adixen and the Agilent pumps were connected using a tee connector to hopefully improve the pressure. The two pumps working in unison lower the pressure slightly, but not into the desired range.

2.3.3 Supplying Voltage into the Chamber

To maintain the vacuum pressure and supply the internal components with the required voltages/current, a special electrical port connection was needed. The electrical feedthrough port connects directly to the KF16 adaptors installed in the chamber previously. This specialized part allowed for a voltage/current to safely travel into the system without compromising the

vacuum. Due to the high voltage requirement of the electric plates and the high current requirements of the heating filament, a particular feedthrough was needed. One capable of maintaining its structural integrity when a high frequency AC source is applied without causing any noise in the signal. The connector must also be capable of withstanding high heat generation due to current running through the prongs.

An electrical feedthrough with four conductive prongs was ordered from Kurt J. Lesker. The first component that arrived did not match the specifications of the one that was order from online. The part sent was in fact the wrong part, so the part was sent back to the manufacture and the correct component was shipped shortly after. Upon receiving the next feedthrough, it was tested and determined to be proper fitting component. Figure 2.39 shows a size schematic and the placement of the four conductive prongs on the component[5].

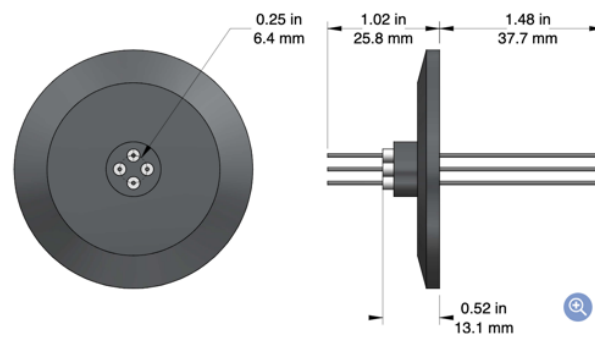


Figure 2.39: The electrical feedthrough

The specifications of the part of listed below in figure 2.4[5]:

Voltage(VDC):	2000
Current(A):	10
# of Conductors:	4
Conductor Material:	Nickel
Conductor Diameter(mm):	0.032
Insulator Material:	Alumina
Flange Mounting:	KF40 (2.16 in OD)

Table 2.4: Electrical feedthrough specifications

After receiving the part, it was fitted in the chamber and test to ensure it was compatible with the system thus far. The system was able to achieve a pressure that compared to that

of before installing the new part. The lowest pressure achieved so far with this new part was $2.6 \times 10^{-2} \text{ torr}$, but the pressure was reduced further later. To check for leaks, isopropyl was applied to all the ports in small quantities, but specifically to the port containing the new electrical fitting. If a leak was present, the pressure would decrease slightly and then spike upwards, acting as a signal for a specific location where a leak is present. A port opposite from the electrical fitting indicated a leak was present, so the entire port fitting was removed and a new layer of Teflon tape was applied. The adaptor was reinstalled and the leak test was conducted again. No noticeable leak was detected upon reinstalling the adaptor, so theoretically the pressure should continue to drop. However, this was not the case, the pressure remains roughly the same as before the adaptor was removed. More work is required to reduce the pressure, but the port fitting containing the feedthrough was secure and has no detectable leaks.

The pins are much longer than the space alluded within the chamber, so they were cut down significantly. Ideally, the pins would be cut down to reach through the chamber walls and just reach the interior cavity of the chamber.

From the beginning of the project, the pins have had specific purposes allocated to them. The initial thought process was to have two pins supplying a voltage to the electric plates and two to supply current to the heating filament. After progressing through the project, it was realized that an additional pin would be required to pull out the signal from the detector. Instead of ordering a new feedthrough with more pins, a simple alteration to the plan could be done. All the power requirements have a ground and all technically require their own pin to connect to the ground. Alternatively, the ground of all power supplies can be connected on a single pin because the ground will be connected somewhere in the building anyways. The power supplies all pull from the same source in the building and the ground pins on the cable to the outlet should hypothetically connect to the same ground. Even with combining all the possible grounds, the feedthrough would still be short a pin, so a second one was ordered.

2.4 Ionizing Hydrogen

2.4.1 Providing Hydrogen

The first step in ionizing hydrogen gas was procuring a hydrogen bottle and regulator. Since hydrogen is a combustible and flammable gas, it was important to protect the bottle. Hydrogen becomes flammable when it interacts with air, specifically with oxygen, so the hydrogen inside the vacuum chamber will be safe. However, the bottle and gas lines flowing to the chamber are dangerous and require a lot of thought. For safety, it is best to get a smaller bottle of hydrogen. While the Chemistry department has a large bottle from the 1970's, but it is far too large for my purposes. Having a large bottle requires a more secure and open environment, while the small bottle can be placed into a cabinet for protection. A 40CC bottle of pure hydrogen and a hydrogen regulator were ordered from Airgas. The hydrogen bottle needs to be connected to the chamber system using a plastic tube to run from the hydrogen bottle regulator to a needle valve. The needle valve as seen in figure 2.40[6] has a fine dial that can control the flow rate of the gas. This will allow for better control over the gas flowing into the chamber. Providing much more control than the regulator on the hydrogen bottle.



Figure 2.40: Gas needle valve



Figure 2.41: Gas quick-connect coupling

The needle valve has an intake and outtake KF16 port connection. The intake connection was connected directly to the hydrogen bottle using a plastic tube and the output was

connected to a gas quick-connect coupling KF16 fitting seen in figure 2.41[7]. A plastic tube is ideal because it is very hard to break or cut on accident, which is much safer than a metal or rubber tube. The quick-connect fitting allows the plastic tube to be put through the port and held in place using a swagelok²². The outtake of the needle valve was connected to a larger stainless steel tube which was fixed into place using a swagelok to snugly fit the tube to the connector. The steel tube was then fed into a quick-connect coupling KF16 fitting as seen in 2.41[7]. The fitting had a rubber gasket inside to wrap around the tube, making a airtight seal. The larger steel tube was then fed through the coupling far enough that it will just reach through the KF16 fitting coupling on the chamber. Then a thinner stainless-steel tube was inserted into the larger tube. This tube make the hydrogen flow easier to direct to a particular area of the chamber because it was easier to bend and pinch the smaller tube. This also allows for the end of the tube to be pinched creating a larger spread of hydrogen, which increases the probability of interactions with the electrons from the heating filament. The two tubes are connected using vacuum epoxy on the inside of the chamber. The thinner tube is directed under the electric field plates and bent upward to spray the hydrogen gas up between the gap of the electric field plates. The hydrogen gas line schematic can be seen in figure 2.42.

The thin metal tube must be directed in a specific orientation that will allow for easy access to a port connection that does not have close proximity to any electrical feedthrough. This is to prevent the ignition of the gas due to a spark between electrode. Under normal vacuum conditions, the H_2 won't ignite in vacuum, but could easily ignite if the chamber is flooded with air. The vacuum pump used has issues maintaining a steady pressure and frequently releases oxygen back into the chamber during the gas leak detection protocol.

²²The swagelok embeds itself into the tubing to create a clean and smooth seal. This connection allows for easy access to the tube and provides the ability to remove the tube for maintenance quite easily.

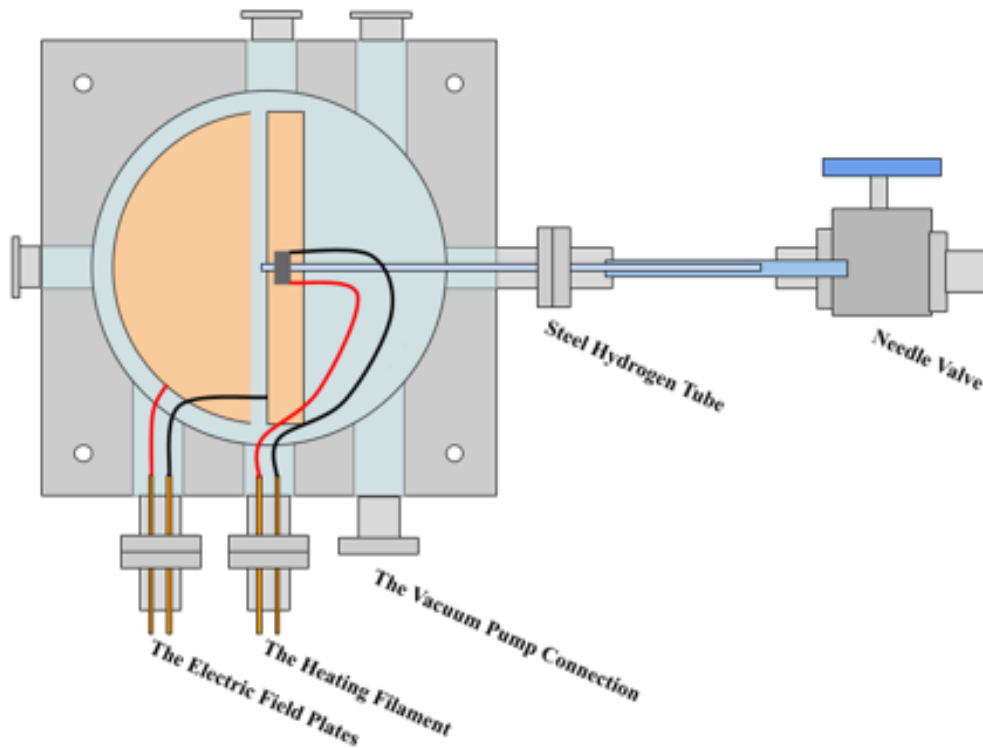


Figure 2.42: Schematic of the hydrogen lines

The supply tube also must be out of the way of the estimated proton trajectory to prevent premature collision. The tube must travel parallel to the plates as low as possible until outer edge of the mounting harness. The tubes should also be out of the way as much as possible because stainless steel is a shield against magnetic fields, so it may have small affect on the uniformity of the magnetic field. Generally the system should still operate within acceptable parameters, but the protons may not have a perfect spiral trajectory due to the inconsistency in field strength. To limit this affect, the tubes should be run as far way from the acceleration zone in the center of the chamber. Ideally, the tubes should run along the circular edge of the chamber walls until it reaches the port. This will minimize the shielding affects and concentrate the inconsistencies towards the outer edge of the protons circular orbit.

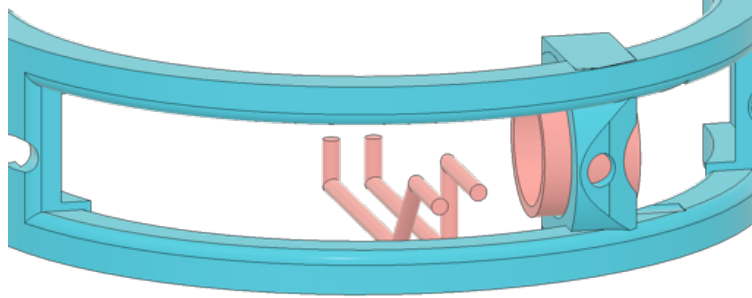


Figure 2.43: Potential configurations for the gas line tube

Figure 2.43 shows two potential designs that should minimize the shielding affects of the tube and prevent premature collisions. The overall affects of the shielding are basically negligible due the high strength of the electromagnets. However, if the magnetic field strength was lowered significantly, the shielding affects may play a more significant role. One configuration shown in figure 2.43 has a 90° angle close to the mounting harness, while the other has a 45° angle. The 90° angle is much easier to make, but slightly interferes with the proton trajectory because it is almost directly in front of the detector. A 45° angle is more difficult to make, but doesn't present as an obstacle for the protons and has is much easier to ensure the tube was not pinched during the bending process. The best choice between the two configurations is the 45° angle tube because of its lack of conflict with the proton trajectory. The gas line must run in this particular half of the chamber because of the limited space and inability to access any port on the other half. The specific design of the half-moon plates creates a challenge when trying to access any port near the plate. The port connected to the pump should be located on this side of the chamber because it frees up a valuable port on the other side.

2.4.2 Safely Handling Hydrogen

Hydrogen is a very combustible gas and requires special precautions when working with it. Not only supplying hydrogen into the chamber dangerous, but simply having the hydrogen

bottle can be hazardous. To prevent serious damages and injury, a few extra steps were taken. The bottle was stored in an empty metal cabinet to prevent a leak from the bottle or regulator from filling the room. This method of containment has its own dangers, if the cabinet fills with gas and ignites, the explosion would have much bigger force and cause more damage because the gas is concentrated. To help prevent damages in the case of leak, a well ventilated room is vital to the safety of myself and others. The ventilation system in Rose 107 was excellent and will be invaluable in the case of a leak. The other benefit of being in Rose 107 is the size of the room because the room was large, the overall volume of the room would not completely fill with hydrogen even if the bottle release all the gas. If a leak occurs, the windows should be opened immediately and all the air in the room needs to be cycled out quickly.

To determine if a leak was present without experiencing an explosion, small H_2 detectors were installed. Commercial H_2 detectors are expensive and also detect a vast variety of other gases which have the potential for setting off the alarm. In this particular case, the H_2 gas was the only one of importance. To isolate H_2 and stay within a budget, a couple of MQ-8 gas detectors were purchased from DigiKey as seen in figure 2.44[10].

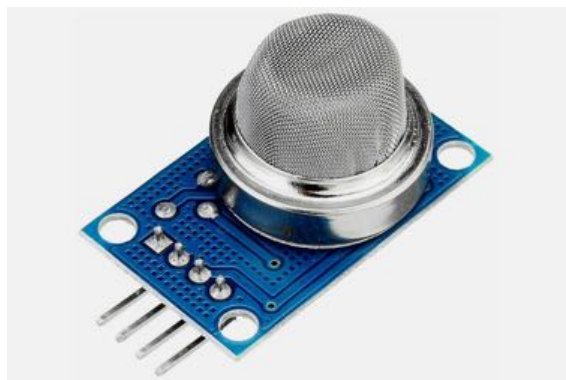


Figure 2.44: The MQ-8 sensor mounted on a PCB



Figure 2.45: The sensor in the protective box

For general operation, there will be two hydrogen detectors running continuously, one in the bottle storage cabinet and one on the ceiling. To mount the sensors in a reusable way, a small box was designed in Fusion360 and printed in PLA. The detectors are quite

inexpensive, but keeping all components for future experiments is important. So instead of gluing the detectors into place, a box container was constructed and then glued. The simple requirements of the box were to securely hold the sensor, allow access ports for cables, and a clear area for the sensor probe to collect measurements. Not to mention the boxes should protect the sensors internal components from falling or unforeseen external forces. Figure 2.45 shows the sensor mounted in the protective box with a the required wires connected to the pins. These detectors are to be connected with an Arduino board and programmed to detect a specific gas. If the gas is detected at high levels, the circuit notifies the user with an LED light and an alarm buzzer. The Arduino board that was purchased was the Arduinio UNO R4, which has the capability to connect to the Arduino cloud through WIFI and can be checked from any computer anywhere. This would be invaluable because a notification could be sent when a high level leak is detected, preventing any injuries and damages to the space. The UNO R4 can be powered by a 9V battery and can simultaneously collect data from multiple gas detectors. One detector was placed in the storage cabinet and the other was mounted on the ceiling above the accelerator. When hydrogen gas is exposed to air, the H_2 gas rises, so having a detector on the ceiling would be an optimal place for detecting a leak.

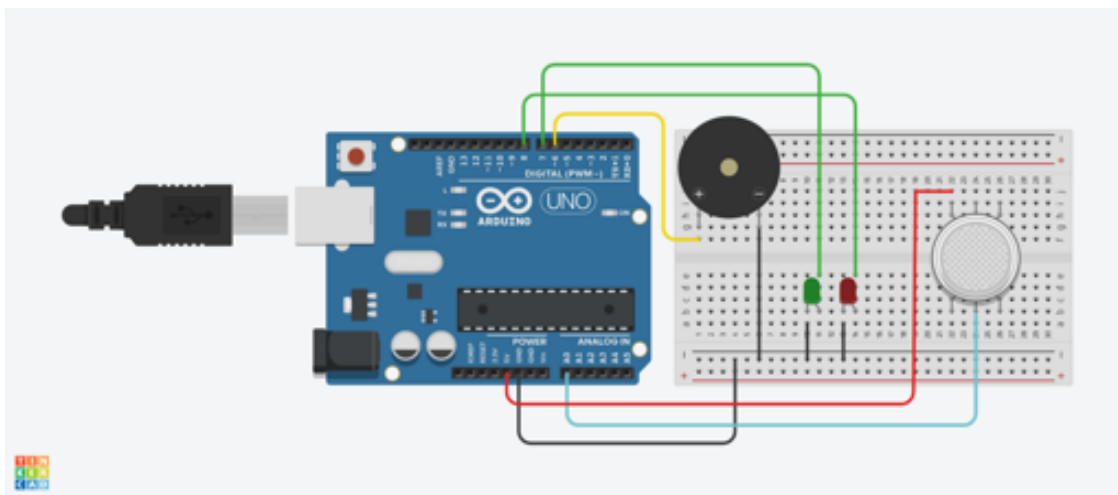


Figure 2.46: A simple version of the H_2 detector circuit

A simple version of the circuit with only one detector is shown in figure 2.46. This circuit

uses a piezo buzzer²³ to make a noise to indicate when a high level leak is detected. When the H_2 readings for the room are within allowable limits, the green LED light is on, but the red LED turns on when the H_2 level increase in the sensors proximity. At the moment, the average measurement of the room's H_2 levels fall with in $20 - 50ppm$ /²⁴ range and the high level threshold is set to $200ppm$. If there was a gas leak from the bottle, the hydrogen level will be much higher so, the threshold is set low but not too low that the surrounding equipment emission will trigger the sensor. Specifically the vacuum pump will be pumping out low levels of hydrogen from the vacuum chamber. All the excess hydrogen that was not successfully converted into protons, will be vented from the chamber to keep the vacuum pressure low. It is very possible that the amount of hydrogen expelled by the pump may exceed the limit, so the threshold may need to be adjusted accordingly.

Throughout the first test, a number of hydrogen detectors will be running in different areas of the experiment, primarily in location where there is a high chance of a leak. The code that determines what is an acceptable level and a high level of hydrogen was adapted from a code provided by SandBoxElectronics[32]. The code is quite simple, it requires a calibration measurement in a normal room not exposed to H_2 and used this a base line measurement. The base line is used to calculate the exact ppm of H_2 in the air at that moment. The code also takes into account the set resistance sensitivity level on the back of the sensor. By adjusting the trimmer pot²⁵ the sensitivity changes on the sensor, so this needs to be accounted for in the calibration check. For calibration sensitivity check, the code also requires a few set aspects of the sensor which are provided by the datasheet. Specifically the sensitivity ratios for different gases and vapors the sensor can detect as seen in figure 2.47.

To monitor the levels of hydrogen in the air, the Arduino was connected to a computer to print the measurements in the serial monitor. The Arduino IDE also has the capability

²³A type of electronic device that's used to produce a tone, alarm or sound.

²⁴ppm, parts per million. The total number of a specific molecules of a space of one million molecules.

²⁵An adjustable resistor that has a wide range. Allows the user to change the resistance in the circuit without replacing a resistor.

to track the H_2 level over time and plot them to show the fluctuations more concretely. To further expand the detection system, a small LED crystal screen could be connected to the board to display the gas concentrations without using an external computer. The Arduino IDE doesn't have the ability to save data directly from the user interface, but the serial monitor could also be opened from the terminal to save data.

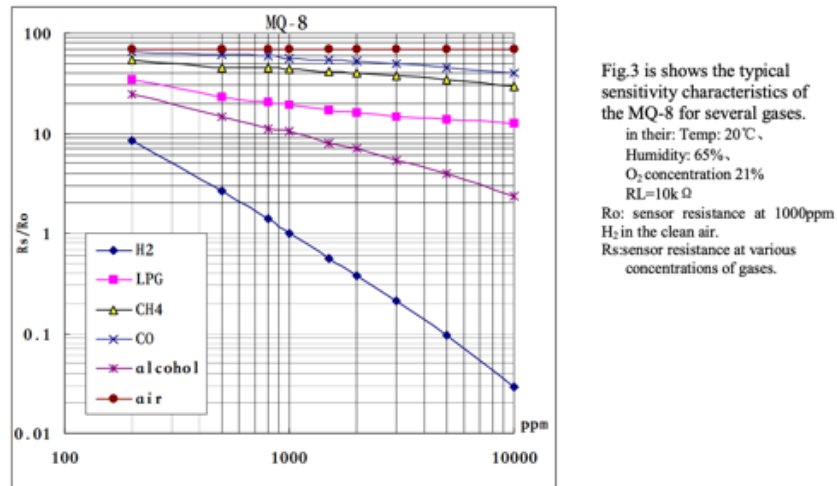


Figure 2.47: The MQ-8 sensitivity plot for different deductibles

2.4.3 Testing the Heating Filament

Now that the hydrogen was supplied into the chamber, its time to think about providing a steady flow of electrons. The electrons will be generated using thermionic emission, which is discussed further in Chapter 1. To generate electrons, a heating filament was required. The heating source was a small thin wire that has a high current passed through it. The high current builds up heat, thus giving off electrons to interact with the hydrogen gas. The heating filament selected was a tungsten coil from Kurt J. Lesker. This particular heating coil is frequently used to supply electrons in Scanning Electron Microscopes, however, there is no data sheet supplied by the company. The temperature generated at different currents should also be monitored throughout testing to determine the ideal configuration. Connecting a single heating filament to a voltage source that was capable of supplying 24A should be

sufficient for this, but it is important to figure out the minimum current required to make the filament glow. The first day of testing yielded little to no promising results, setting the current to 1A, 2A, 5A, and 8A. The maximum temperature reached was just barely 43°C . After some research into similar filaments of a different brand, the next day of testing was more fruitful. Setting the current to 24A, the temperature reached over 1000°C .

Voltage(V)	Current(A)	Temperature(C)
1.00	1.00	27.00
1.00	2.00	27.00
1.00	5.00	28.00
1.00	8.00	43.00
3.00	24.00	1000.00
3.0	20.00	900.00
3.0	15.00	850.00

Table 2.5: Change in temperature by increasing current

A thermal camera was used to monitor the temperature because it has the ability to visually show the temperature change compared to an object's surroundings. However, the temperature camera had a limited temperature range of roughly 150°C , so a thermal probe was used to measure the higher temperatures exceeding 150°C . Figure 2.48 shows the increase in the internal temperatures of the filament as the surrounding temperature remains constant.

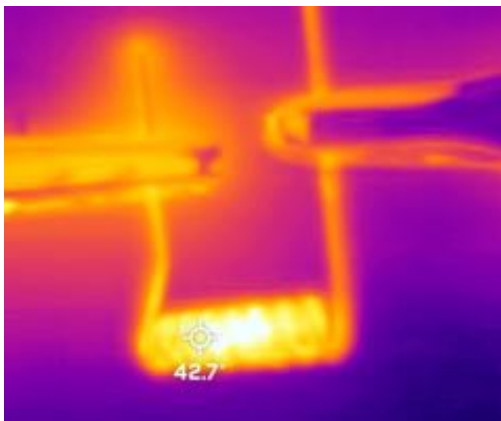


Figure 2.48: Image from thermal camera



Figure 2.49: The glow of the filament at 24A

At the lower temperature range of 25°C , no visual glow could be seen with the naked eye, but at higher temperature, a glow was visible as seen in figure 2.49

On the first day of testing, the current was increased slowly from 1-8A, while the second day, the current was set immediately to 24A. This method was poor planning because it affected the temperature measurement of the 20A and 15A trials. At 24A, the temperature reached over 1000°C , this high temperature might require a long period of time to fully cool. By going to a lower current after, there still may be some residual heat affecting the accuracy of the other measurements. Another factor that may affect this process was the amount of time the coil was allowed to heat before measuring the temperature. There should have been a consistent amount of time before taking the measurement. This uncertainty could be further reduced by recording the temperature as a function of time and averaging the results. The last factor that should be considered was the oxidation of the tungsten coil. At high temperatures, the tungsten coil oxidizes at a very fast rate, the oxidation process happens between 700°C to 1000°C [34]. After only one test at 24A, there was a visible layer of yellow oxidation on the coil. The rapid oxidation of the metal coil could affect the temperature probes ability to accurately record the temperature. Figure 2.50 shows the rapid oxidation of the heating filament only after one use.

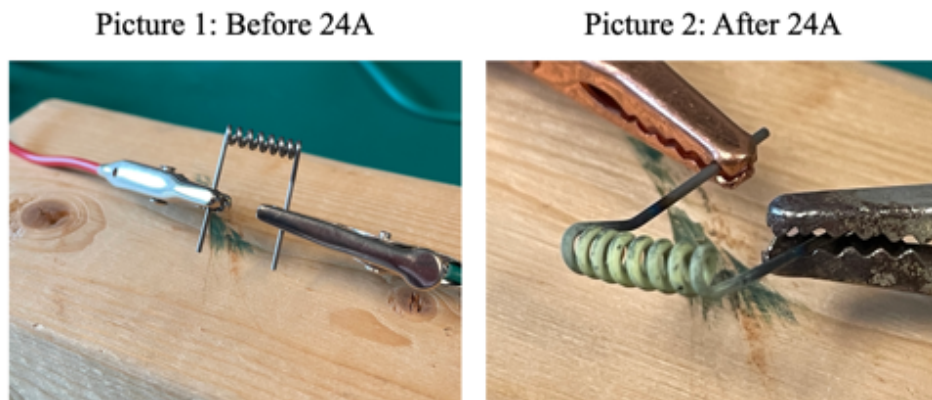


Figure 2.50: The oxidation of the filament before and after 24A

The oxidation won't affect the experiment because the filament will be inside a vacuum environment with little to no oxygen. The tungsten should not built up a layer of oxidation while inside the chamber or at the very least it shouldn't be at a rapid rate.

To increase the probability of attaining a proton, a strong and steady source of electrons is needed. The higher number of electrons bumped out of the filament, the higher the probability that an electron will interact with the hydrogen gas. It is important to calculate to how many electrons are being generated at certain temperatures and the current requirement for each temperature. Equation 2.3 can be used to calculation the heat generated at different currents. The resistance of the tungsten filament is roughly 0.1Ohm or lower and the time was set to be a constant 30 seconds. In reality, the data recorded was allowed to heat for different amounts of time. The heat generated can be convert to a temperature using the specific heat equation 2.7.

$$Q = m \cdot c \cdot \Delta T \quad (2.7)$$

By rearranging the equation and the final temperature of the system can be found. Changing the current, a reasonable estimate for the temperature can be determine with the hopes of creating ideal conditions for this experiment. The data from table 2.5 can be compared to the calculations to determine viability of our estimation method.

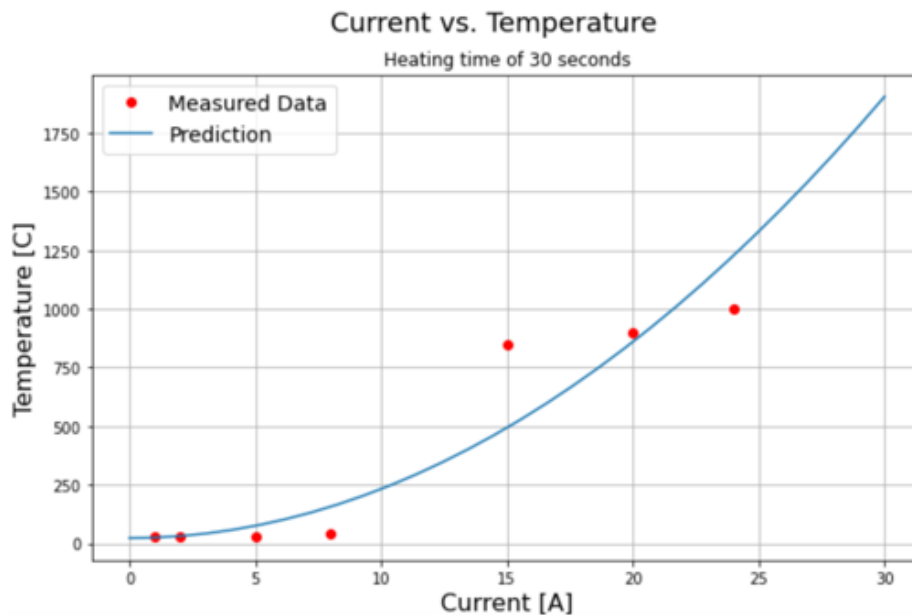


Figure 2.51: Temperature as a function of current

Figure 2.51 shows the estimate of the temperature as a function of current. It also shows the data recorded while testing the filament, there are a number of points that line up exactly with the prediction. However, there are also a number of points that are shifted quite a lot. Overall, this is a good estimate of the temperature and should be used to find the best current for our purposes. Using equation 2.8, the number of electrons generated by the filament can be estimated.

$$J = AT^2 e^{\frac{-W}{kT}} \quad (2.8)$$

This equation provides the emission current density J , which is the current over an area. This was then converted to a number of electrons by converting from A to e/s , which is the number of electrons per second.

$$n = J \cdot 6.241509 \times 10^{18} e/s \quad (2.9)$$

This predicts the number of electrons per second over an area. By varying the input temperature during the emission current density was deduced. Calculating the number of electrons generated at different temperatures. At lower temperatures, the number of electrons generated is less than one electron, so any result less than one was disregarded and only looked at viable temperatures that resulted in a higher number of electrons. To make this plot more intuitive, the functional data can be applied directly to the particular surface area of the filament used. By multiplying each data point by the approximate surface area of the filament, it determined the number of electrons per second generated for the specific geometry.

This plot, shows the minimum temperature needed to generate any electrons is roughly $500^\circ C$. The temperature of the filament should be as high as possible to generate a sufficient supply of electrons to increase the probability of interactions of the electrons and hydrogen gas. However, there are other internal components that may not be able to withstand the higher temperatures. The surface of the filament will be the hottest point in the vacuum

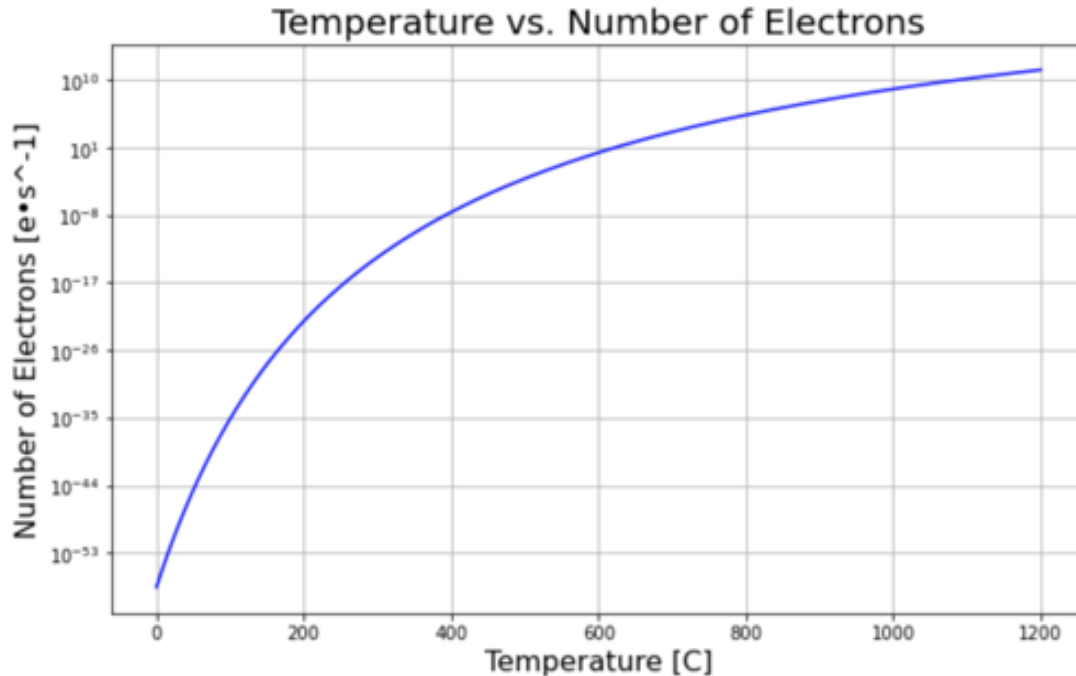


Figure 2.52: Number of Electrons as a function of temperature

chamber, but thermal radiation will increase the temperature of the surrounding components. To reduce damages or even melting, the temperature should be regulated to the minimum temperature that still facilitates a steady electron stream. In principle, the temperature should be in the range of 600°C to 900°C . The other concern about the heating filament inside the chamber is the residual magnetic field generated by running a high current through the coiled filament. Calculating the magnetic field surrounding the filament while running 20A through the coil (the maximum temperature range) estimates a magnetic field of about 0.0158T. Although this is very small compared to the strength of our uniform magnetic field, it still may affect the trajectory of the protons in the center of the chamber.

2.4.4 Securing the Filament and Gas Line

As seen in figure 2.42, the heating filament was mounted close to the center of the chamber. Ideally the filament should be mounted directly in the center and between the gap in the plate. The hydrogen supply line was feed directly under the filament to produce the highest

number of protons. To secure the heating filament and the hydrogen gas line and ensure that they don't shift at any point in the process a clip was design in Fusion360. This clip slides onto the rectangular plate and hold the filament on the top. On the bottom, the gas tube was feed through the clip and directed upwards. Figure 2.53 shows the 3D model of the clip on the rectangular plate. This image specifically shows the second version of the clip as the first version required more room for the wires to slide through the holding tubes on the top.

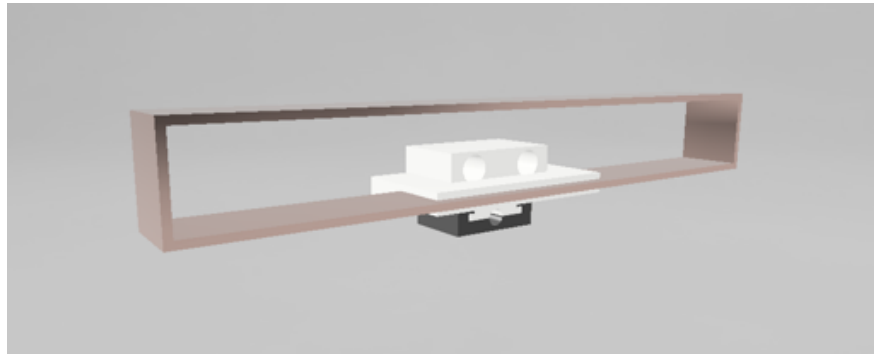


Figure 2.53: Clip to secure the heating filament and gas line

The upper half of the clip is shown in white and can be seen to have two tubes towards the top. These two tubes are used to hold the positive and ground wires for the heating filament. The tubes were adjusted to allow for a larger gauge wire to accommodate the high current. The bottom half of the clip is seen in black and has the ability slide over the tube to secure it. After the final designs were set in stone, the stainless steel tube was pinched and bent into place, so it can't easily slide in and out of a hole. This sliding mechanism provides the ability to easily take out and put the tube back into place without destroying the clip. The joint slides over the tube and pinches it to the upper half of the clip, creating a very snug fit. The clip should be strong and slight flexible to easily slide over the plate without fracturing. However, the clip must remain small to maximize the potential space the protons will have to circulate the chamber without possible collisions. A simple method of making the clip is printing it in PLA using the Bambu X1-Carbon. The first iteration has minor warping on the sections that stretch over the copper plate, but the warping doesn't affect the

overall performance. This first prototype served as a test for the sliding mechanism because there were some worries about the correct tolerance for the sliding mechanism. The joint worked perfectly as expected, provided a snug and secure fit, while easily removable. The tolerance level for the print was set $0.5mm$, which means that the space between all surface touching in the sliding has a $0.5mm$ clearance. The infill ration of the second iteration was set to 25%, while the first was set to 15%. This will provide a greater amount of strength and hopefully reduce the warping. After printing the second iteration, the overall quality of the clip was improved and appeared to be much sturdier than the first.

To test the overall capabilities of the clip, wires were fed into the clip to a heating filament. This test is primarily to inquire about the heat resistance or tolerance of the clip. However, this does provide another opportunity to test the temperature as a function of current. This new data would confirm the original results in figure 2.51 and perhaps match the theoretical data better. Nevertheless this test will provide more understanding and confidence in the required current for the desire temperature. To carry out this test, the filament was mounted to the clip, using two high gauge wires feed through the wire harnesses and soldered to the tungsten filament. The tungsten filament was particularly hard to create a solid bond to the wires using a lead zinc based solder, but upon further research a silver based solder acts as a better bonding agent[28]. For this initial test, the lead based solder should be sufficient, but in the future a silver solder should be acquired. The filament was soldered to the two wires and pulled tightly into the harnesses. The filament is positioned just over the edge of the rectangular plate. Since this test is destroying a filament and potentially a clip, it would be valuable to simulate the actual system as close to possible. So the first iteration of the rectangular electric field plate and the plate mount were used to secure the system. This also determined if there was any warping of the plates or mounting system due to the radiant heat of the filament. From the first test of current vs. temperature, the temperature started to show any noticeable change after the current passed 8A. For this test, the current started at 8A and increase by increments of 1A.

Trial	Voltage(V)	Current(A)	Temperature(C)
A	0.18	8.00	90.00
	0.21	9.00	120.00
	0.25	10.00	160.00
	0.28	11.00	200.00
	0.36	12.00	260.00
	0.43	13.00	330.00
	0.52	14.00	420.00
	0.59	15.00	460.00
	0.67	16.00	520.00
	0.76	17.00	570.00
	0.84	18.00	580.00
	0.97	19.00	660.00
	1.10	20.00	720.00
	1.21	21.00	760.00
1.38	22.00	800.00	
B	0.25	10.00	125.00
	0.28	11.00	156.00
	0.34	12.00	190.00
	0.40	13.00	236.00
	0.46	14.00	295.00
	0.57	15.00	338.00
	0.65	16.00	417.00
	0.76	17.00	480.00
	0.86	18.00	550.00
	1.01	19.00	620.00
	1.13	20.00	680.00
	1.21	21.00	710.00
	1.39	22.00	786.00

Table 2.6: Second stage of testing the change in temperature by increasing current

Table 2.6 has the second and third rounds of testing the filament. The data shows the temperature in trial three is close to that in trial two but was consistency just slightly below throughout the test. Since it was consistently lower, it indicates a trend in the data caused most likely by the increased oxidation from trial one. The oxidation of the tungsten at high temperatures is the most logical cause for the persistent variation in temperature between trial two and three. The data was plotted and compared to trail one and the theory in figure 2.54. The new data in figure 2.54 shows general consistency with the theory and fills in the missing sections of data for trial one. The data from trial two and three are slightly lower than that of the theory, but overall follow the same trend line. So it is safe to say that the filament was behaving as expected and the method of predicting the temperature as a function of current was accurate. At least in atmospheric conditions that is, the filament

will behave slightly differently in vacuum and should require less current to produce high temperatures.

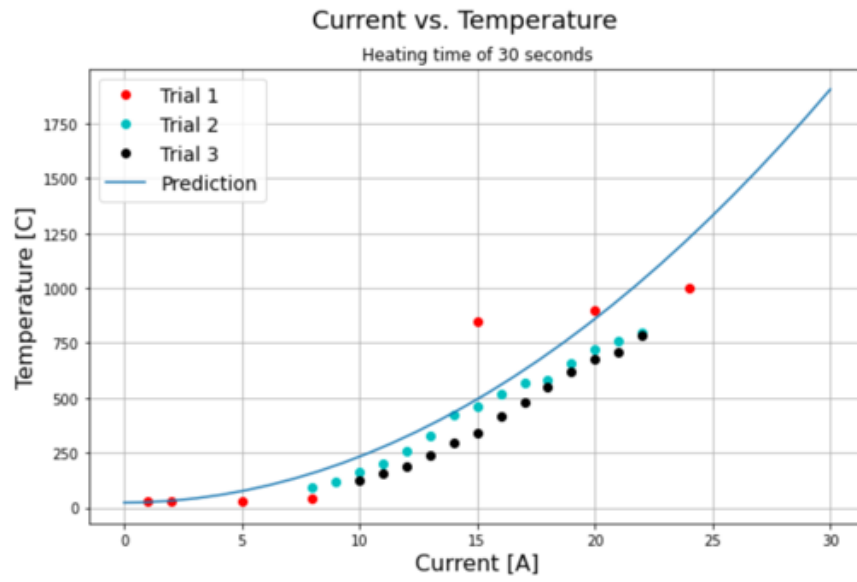


Figure 2.54: Temperature as a function of current(second round of testing)

The clip survived the test with very minimal damages and warping. The only place the clip experienced any form of warping was the section of wire harness that made contact with the bare leads. To prevent any warping and melting, the leads should be insulated using electrical tape or heat shrink to create a protective layer between the plastic and the hot leads. The clip showed no signs of visual warping or melting until reaching the higher temperatures at high currents. The first sign of melting was seen at around 19A and only got worse when more current was applied. The filament and the wires are fed through the clip while the clip is attached to the rectangular plates in the mounting harness as shown in figure 2.55. Figure 2.56 shows the damage to the clip following both trials. The damage is isolated to that section of the clip because of the lack of heat on the wire leads.

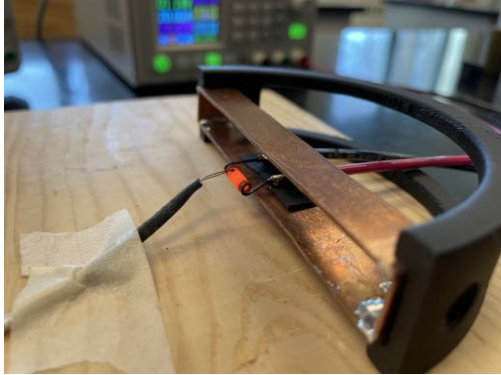


Figure 2.55: The testing setup with the thermocouple probe

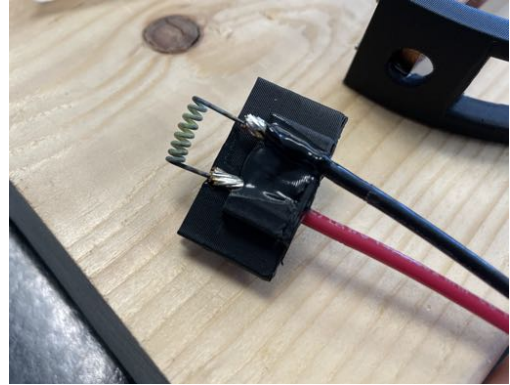


Figure 2.56: Damage to the clip after testing

2.5 The Particle Detector

2.5.1 Making the FC

Due to the lack of kinetic energy from charged particles upon impact with the detector, a normal common measurement tool would not be beneficial. Instead, using the Faraday Cup (FC) is the best option for catching particles with low kinetic energy. The FC will return a current source in the approximate range of $\mu A - nA$, so additional work is required to make the signal even readable and eventually usable[3]. Commercial FC can be ordered from a number of retail options, but few will fit within the vacuum chamber and most are quite expensive. Instead of ordering a custom part, the FC can simply be made in-house using a cylinder of brass and the lathe²⁶. Upon the initial design, the FC must fit within the chamber and be placed along the outer most edge of the system. By placing the FC on the outer edge, this provides the charged particles more time to accelerate and reach their maximum velocity. The FC should be large enough to catch all the charged particle within the acceleration range, so the diameter of the cup should be roughly the same as the height of the electric field plates. While the thickness of the cup is not the most important factor, it is still important to make the cup deep to ensure no charge particle escape the detector.

²⁶A lathe is a machine tool used to shape wooden or metallic products by rotating it about an axis while a stationary cutting tool keeps removing unwanted material

The FC was manufactured using a lathe to slowly and methodically remove metal from the inside and outside of the brass cylinder. First, the inside needs to be hollowed out using a drill bit attachment to the lathe. The approximate desired diameter of the inside should match the drill bit used. For this concept design, the thickness of the walls was suggested to be $2mm$ because it will still thin and provides the largest possible area of detection while ensuring strength. To hollow the center of the cup out, a very small drill bit must be used first, this method is called a pilot hole. This prevents the larger drill bits from jamming/catching the surface and ensure a clean first cut. The drill bits should then be increased in size once the desired interior height has been reached. The starting drill bit was a $4mm$ and incremented by $2mm$ up to the largest drill bit, a $12mm$. Figure 2.57 shows the process of hollowing out the center of the FC before moving to the exterior walls.

Figure 2.57: The Process of Hollowing Out the Center of the FC



It is also important to use a similar method when tapping holed for threads, the drill bit should cut away a little material and then pull the bit out to remove all the material from the work area. Without removing the cut material, the drill bit won't cut the metal as

effectively. A tapping oil lubricant should be used to reduce the heat generation throughout the cutting process and this also improves the quality of the cut. After the inside of the cup has been hollowed out and filed down to create a smooth surface, the outside can be shaved away. A simple lathe attachment can be used to slowly and symmetrically remove metal without compromising the integrity of the walls. The first area that should be shaved away is the front of the cup, this is called facing the component. It provides a smoother finish and more consistency in the part. Then the external walls can then be slowly shaved down with a diamond tipped cutting bit. The FC is shaved away in layers of 0.5mm at a time to prevent too much force on the part. If too much force is applied, the whole system may break and result in parts shattering into the air. From a safety perspective, it is vital to take the process slow and steady to keep everyone safe and produce the best possible part. After the external walls have been shaved down to the desired diameter, the next step is to cut the back end of the cup to separate it from the remaining round stock brass block. In this process, it is important to go slow because the cutting tool will maintain a constant 90° angle with the round stock. Cutting material this way is difficult and could result in serious injury if something breaks away. The cup should not be fully cut off the round stock using the lathe because there is an increased chance of the part flying into the air after it is fully separated. Instead, the cup should be cut down to roughly an eighth of an inch and cut the remaining by hand using a hacksaw²⁷. The handsaw method worked quite well to cleanly separate the two pieces, but sandpaper was used after to create a better smooth finish. In the long run, using sandpaper on the surface will make the FC look nicer, but it will be much harder to solder a lead to the external wall for detection. The finished product can be seen in figure 2.58.

After the first test of the electron emission from the heating filament, a couple of alterations were made to the initial design of the FC. To better collect the electrons and ensure that none bounce out of the cup, the filament should be mounted inside the cup during the

²⁷A fine-toothed saw, originally and mainly made for cutting metal.

Figure 2.58: A Finished Version of the Faraday Cup



testing. This will ensure that all charged particle are collected with minimal loss to collisions with the particles in the air. To mount the filament inside the cup, the interior walls must be expanded by approximately $2mm$, to allow for some wiggle room. A little wiggle room is necessary because the FC and the special ammeter are connected to the same ground, so there is a chance to sort the circuit if the parts are bumped. The other change that would be beneficial in the future for proton detection is reducing the exterior walls as much as possible. A reduction in the exterior walls reduces the chance of premature collisions between the accelerating protons and the detector. The process used to make the first cup was also used to manufacture this second batch of cups. Additional sanding of the cup interior was done to make a more smooth surface for the electrons to collide with. This batch includes two cups, one has a larger interior height, so the filament could go farther into the cup. Hopefully this will increase the probability of catching more efficiently because of the increase in surface area to catch incoming and ricocheting charges particles. The second cup has a shorter interior height to reduce the surface area that may be in the projected path of the charged particles while accelerating. The particles would induce its charge on the detector in the same way as if it hit the detector directly, but it would be premature hitting the sensor without achieving its maximal kinetic energy. Figure 2.59 shows the two cups made in this

second batch.

Figure 2.59: Comparison of First and Second batch of Faraday Cups



The cup on the right is from the original batch and the other two are from the second batch. The first cup is much larger and thicker than the two newest ones. The wall thickness was reduced by half and the weight difference is noticeable when holding the old and new cups. Although soldering a wire to the back of the cup is efficient and quick, a more secure method of connecting a wire is adding a connection bolt to the back. A small hole can be drilled and tapped in the back of the cup to add a small brass bolt. The wire to the ammeter can then wrap around the bolt and tighten to the surface to secure the wire. The first FC has a wire soldered directly to the surface, but the second batch will have the connecting bolt.

2.5.2 Current to Voltage Conversion and Detection

When the charged particles hit the FC, the overall charge of the cup can be measured using an ammeter. However, the levels of current flowing out of the cup are incredible small and will be impossible to detect with the average store bought multimeter. Measuring the current using a simple multimeter is not the most efficient or accurate method because the

multimeter doesn't have the sensitivity to capture any small changes in the current. Instead, the current can be converted to voltage and amplified to display the signal on an oscilloscope to track the output as a function of time. This method will provide a more accurate and dynamic response time with the capability to ascertain as fluctuation in the signal. A normal multimeter averages a few data points of a second, so the tool won't be able to determine any fluctuations in the output signal. To convert and amplify the signal, a simple op amp circuit can be built to do the task simultaneously. The circuit is called the transimpedance amplifier (TIA) and works on the same basic principle as the inverting amplifier discussed in 2.2. A simple and common TIA can be seen in figure 2.60.

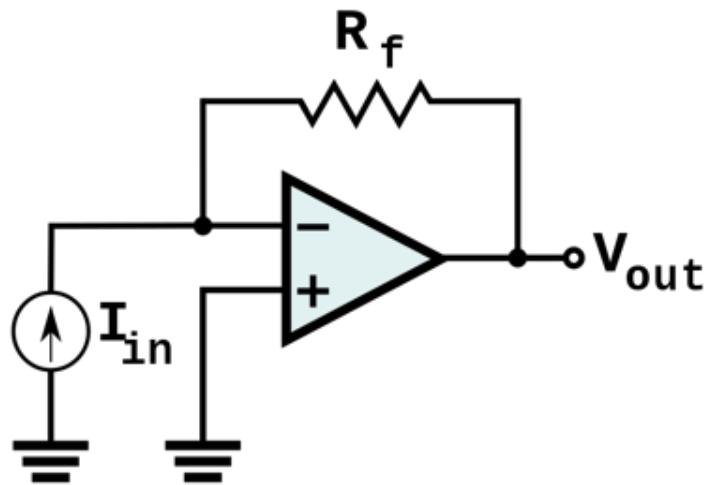


Figure 2.60: A Common Version of the Transimpedance Amplifier

However, the complexity of this problem stems from the small levels of input current. A common op amp, may not have the capability/sensitivity to be able to convert to a voltage signal. The way the amplifier works is based off the principle of ohms law, $V = IR$. Where the voltage is equivalent to the current times the resistance of the system. So the current input can be converted to voltage using a resistor to indicate to the op amp the required voltage to sustain that particular current value. This also allows voltage to be amplified coming out of the circuit based on the resistor chosen. If the current didn't need to be amplified, then a resistance of 1ohm could be used to simply get the same voltage out at the current in. To amplify the voltage a resistor can be chosen to amplify the output voltage

based on the input current draw. So to amplify by a factor of 100, a 100ohm resistor should be used. While the TIA is a good option for amplifying the output signal, a simpler option is using a high sensitivity ammeter to detect the low levels. The Kethley 2000 multimeter is borrowed from Professor Cadden-zimansky and has a high sensitivity for current in the range of nanoamps. Using this multimeter should provide a base line measurement while the transimpedance amplifier is being constructed. Using the ammeter means that the circuit doesn't need to be built now and the testing can proceed. However, if the signal is lower than nA then the ammeter may not be able to detect the output current, so the TIA will then be necessary.

2.5.3 Mounting the Detector

To mount the detector, a few modifications can be made to the mounting harness for the electric plates. This is also useful because it allows for a relative size comparison to be made in Fusion360. The first necessary piece is to determine the exact placement of the detector in the chamber. The FC should be placed at the edge of the expected trajectory of the charged particle and at the farthest possible distance from the center of the chamber. The FC must be placed at an angle to allow for FC to "catch" the charged particles, if the cup is not at an angle then the particles may not successfully stay within the detector and transfer the charge upon impact.

A simple ring can be added to the existing mounting support system for the electric plates. The ring needs to be large enough to securely hold the FC without any indication of shifting or falling while in the chamber. However, the edge closest to the center of the chamber needs to be modified further to remove any possible chance of a collision before reaching the FC. If the ring remains on that edge, the protons could potentially collide with the support structure and not continue their journey. A straight wedge of the ring can be removed to allow for the FC to be exposed along that particular side. This also give the ability to detect any protons that may have just missed the entrance of the detector and still

induce their charge on the side wall. It is also important to remove any other section of the ring that clips the edges of the chamber walls.

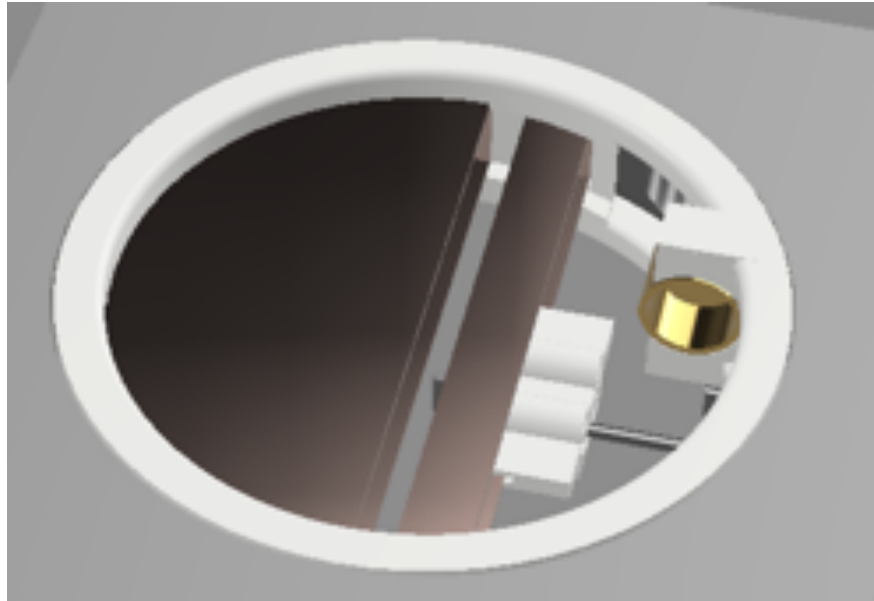


Figure 2.61: A Schematic of the Interior of the Chamber

Figure 2.61 depicts the FC in its angled position along the outer wall as well as all other components that will be housed inside the chamber. The interior of the chamber is quite compact, so it is important to minimize all unnecessary components and optimize the existing components to peak space efficiency.

2.5.4 Testing the Faraday Cup

While waiting on other parts, a general test of the FC can be done using the heating filament to detect an output current from an electron source. The principle method of for detecting protons and electrons is the same, so this is a valuable test to determine if the FC actually works as desired.

By placing the FC directly in front of the filament and running a current through the filament, the detector should measure the current as a function of time. To improve the chances of catching more electrons in the cup, a small positive voltage can be applied over the cup to attract the electrons and the filament can be place inside the cup. This will

maximize the potential current output and ensure a steady signal.

The first test conducted will be used an old testing filament that was used for the clip harness test. Using this in the first test will provide some baseline information about the system and its capabilities. However, an important caveat, the filament was originally tested in air, which produced a thick layer of oxidation on the external coils. This layer of oxidation affects the number of electrons produced greatly, so the results may not show any tangible data. Another important note is the test will also be conducted in room atmosphere in air because placing the old filament in the chamber may cause contamination of the chamber itself. Contaminating the chamber with oxidized material or ash residue from melted plastics would permanently have an affect on the overall pressure of the system. The Filament is placed in another 3D printed harness clip to secure the input current wires. Due to the high amount of current flowing through the wires and low resistance, they tend to generate a substantial amount of heat. This heat will most likely destroy the clip again, but also has the potential to partially melt the mounting harness for the plates. The clip should then be mounted on the spare rectangular electric plate to simulate real conditions that will be taking place inside the chamber in the near future. Any opportunity to test as many components as possible will provide further insight into possible points of failure. The plates were mounted in the harness and taped to the workbench to keep the harness in place. The wires connecting the filament and the power supply were run through the clip. For this test, a new mounting harness was designed and printed in PTEG with the specific idea of holding the FC in the middle of the chamber. By placing the FC in the middle of the chamber, directly in front of the filament, the probability of catching more electrons increases significantly. The new FC harness is shown in figure 2.62. The other new element to this test was the creation of a larger FC with a connecting screw threaded onto the back. This larger FC will more comfortably house and collect the bombardment of electrons without any chance of shorting the circuit when all components are connected to the same ground in the future. The larger FC has the same design as the previous iterations, but the interior radius is increased again

by 2mm. The larger FC can be seen in figure 2.62.

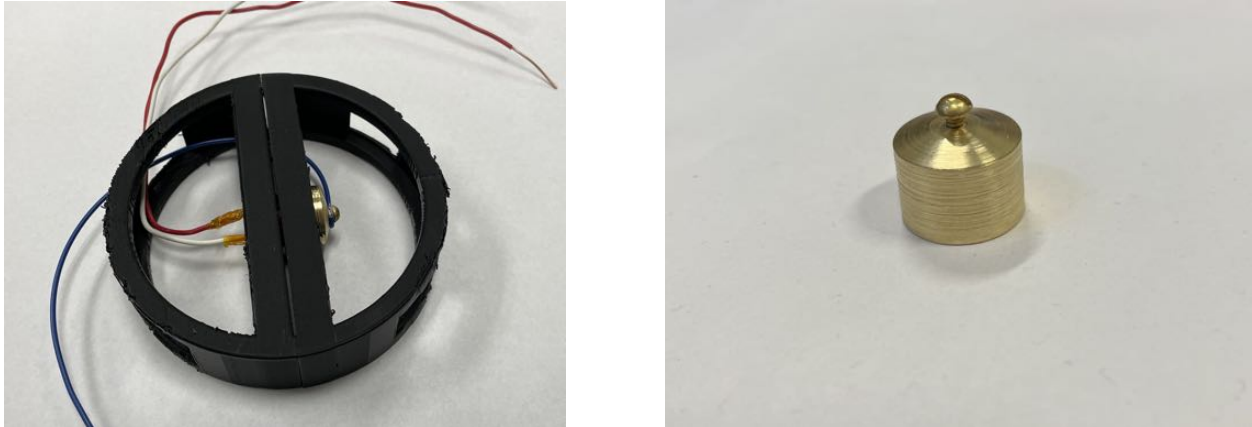


Figure 2.62: FC harness and the large FC

A wire was then run from the connecting screw on the back of the FC to a high sensitivity multimeter. The multimeter is connected in series with the voltage supply and the FC. The positive voltage lead is connected to the ammeter while the negative is set directly to ground. A positive voltage applied over the FC will attract and hopefully trap the electrons, allowing for the induced charge to be measured. Due to the high sensitivity of the Kethley system, it is very important to extreme caution when increasing the current supplied to the filament when the two system are connected to the same ground. While they are connected, it creates a common flow point, which can damage the multimeter if a circuit short occurs. A short may only occur when the FC and the filament touch, so it was important to ensure the two components don't touch. A complete schematic and a photo of the test can be seen in figure 2.63. After connecting all the wires and ensuring the settings are set, the system was turned on. Unfortunately, there was no detectable change in current while the filament was supposedly generating electrons.

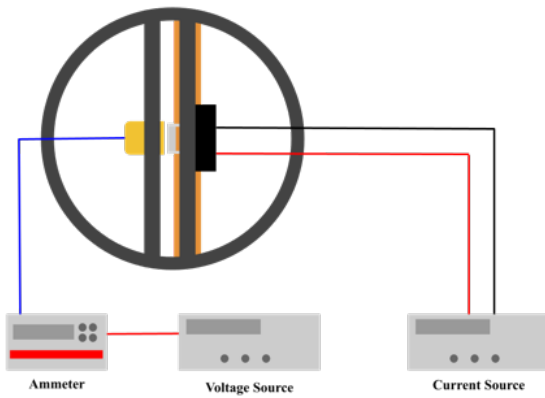


Figure 2.63: Schematic and an image of the testing setup

There are a number of possible explanations for not detecting a change in current. It is possible the filament is not producing enough electrons for the ammeter to determine a noticeable change, perhaps well beyond the sensitivity range. It is also possible the circuit for the FC is incorrect and requires more components. The last possible reason conceived was the electrons are colliding with the particles in air instead of the detector. To test this theory, the filament and FC can be placed in the vacuum chamber. With the lack of air, the electrons should only hit the detector and register a current. The filament will also not oxidize in the chamber because the lack of oxygen. Another benefit of placing the system under vacuum is the fact that the filament should require less current to generate a sufficient heat source.

The second test was conducted under vacuum, but failed due to the limitations of the wires used. Of course, the FC didn't read any current before the test completely failed. This suggests that there is another issue with the system. To solve this issue, the system needs to be broken down into sections and test each individually. The first being the filament heating under vacuum without excessive current. A bright glow can be observed while running current through the filament, but the chamber currently doesn't have the ability to see directly into the sealed system. A glass view port could be ordered, but they are a very expensive part. So a simple but effective version was designed and constructed in

house using the metal shop. Using a common KF16 flat face flange, poly-carbonate plastic, vacuum epoxy, and the metal gasket sealing ring, a cheap glass window port can be made. A flat flange was placed in the drill press and punched a drill through the center using a number of different drill bits. The flange is stainless steel, so it is important to lubricate the drill bit prior to drilling and to push the drill down slowly. The poly-carbonate round plate can be cut using a hole saw drill bit to cut a perfect circle. Vacuum epoxy is then applied to the inside surface of the flange and the plastic circle, and metal gasket are placed onto the epoxy. A smooth seal must be created on the inside and outside edge of the plastic sheet to ensure the vacuum pressure is not lost. A simple diagram of view port can be seen in figure 2.64. Approximately 10 hours after mixing the two part epoxy can the new component be tested in the chamber under full vacuum. After removing the FC, the filament can be placed directly in the line of sight of the viewing port. If the filament is working properly, the glow will be visible from the port.

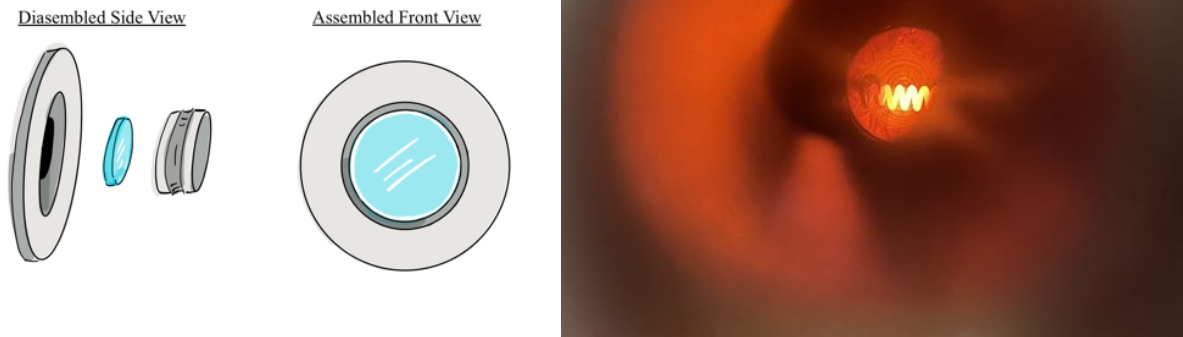


Figure 2.64: Viewing port and image of internal view

The vacuum was engaged first to determine if the part is strong and a low pressure was achievable with the new component integrated into the system. The pressure held at $2.15 \times 10^{-2} \text{ torr}$ and then the other current generator was activated at a low current. Starting from 5A moving up to 20A, the filament started to glow as seen in figure 2.64. At approximately 16A, the current really started to glow and was visible through the port.

However, shortly after moving to 20A, the filament glow was no longer visible and the vacuum pump was having trouble maintaining the pressure. The pressure kept rapidly increasing and then decrease again. The filament was no longer visible and would have no affect when the current was changed, it was believed that the wires had melted and were off gassing. The off gassing would be a logical explanation for the rapid changes in pressure. Upon opening the chamber, the smell of melted plastic was very strong. The wires inside the chamber has completely melted from the high current levels causing the rapid pressure changes. They didn't catch fire because of the lack of oxygen, but they produced fumes and vapors that would increase the system pressure. Figure 2.65 shows the internal system before and after the test.

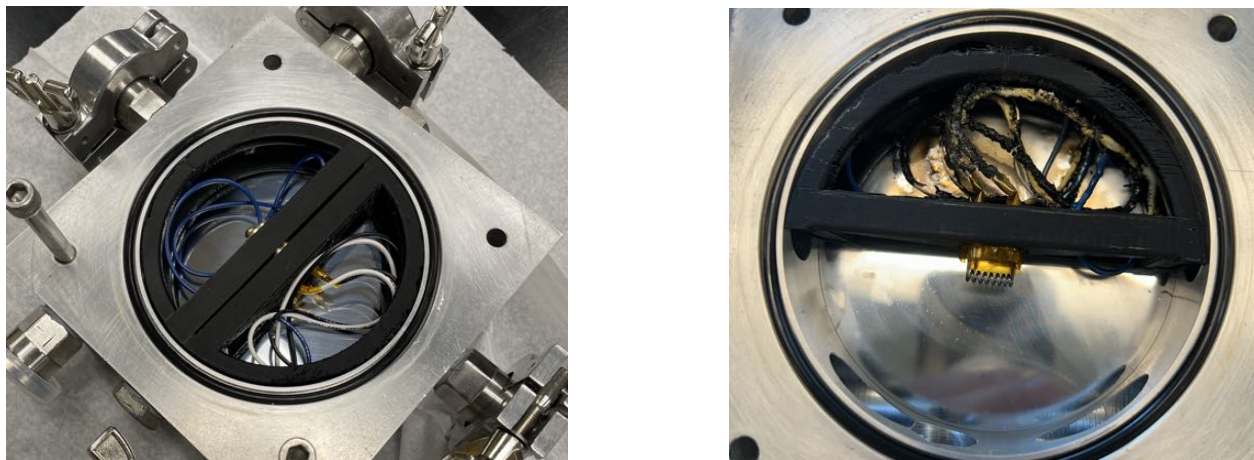


Figure 2.65: Internal system before and after testing

The next phase of testing involves increasing the gauge of wire used to provide current inside the chamber. Using a high gauge wire means that the wire is much harder to maneuver and fit in the chamber. The large gauge take more space, but has a high temperature capacity. From the results of the second test, the filament can be heated inside the chamber successfully, so the FC can be added back into the system to test the current output. Upon further research of the system, the voltage applied across the FC must be significantly increased. Throughout test one and two, the voltage was held constant at 10V, but this third test will increase the voltage to 100 – 300V. The high voltage would make the electron

trapping process much easier and would hopefully reduce the current levels required by the filament to produce electrons. A resistor should also be added into the circuit to act as a current limit and essentially a fuse for the whole system.

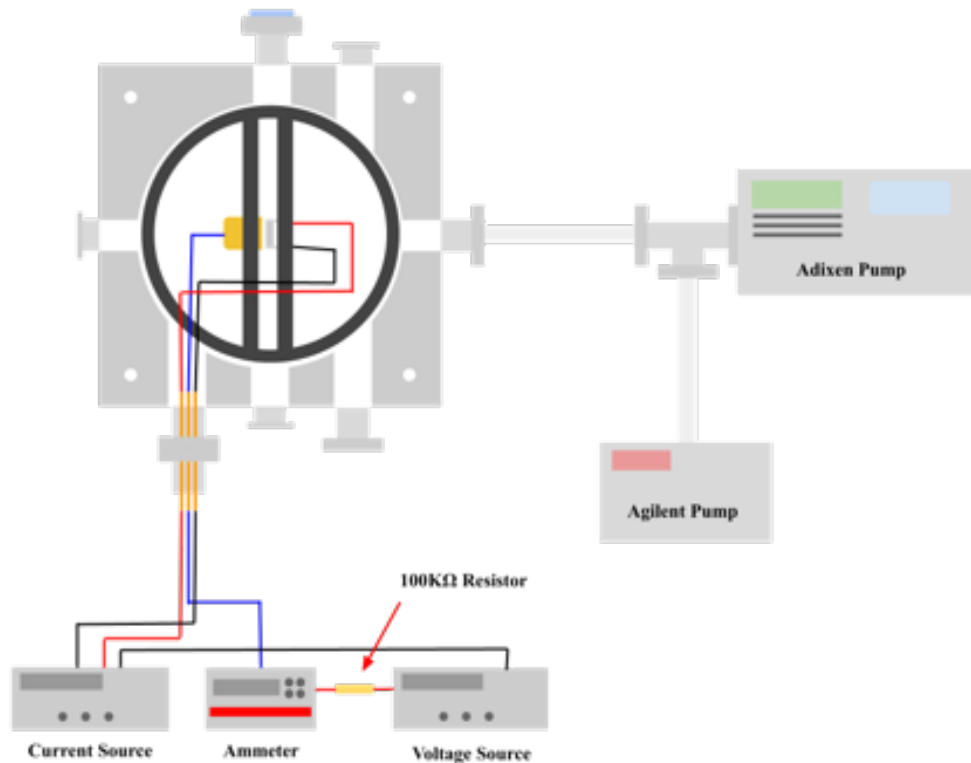


Figure 2.66: Electron test #3 setup

Using the setup shown in figure 2.66, the FC was able to successfully detect electrons. The voltage was changed throughout the process to determine the ideal minimum voltage required to effectively collect electrons. When the voltage is high, the chance of an electrical breakdown arc is increased significantly. Similarly to the behavior of the high voltage applied to the electric field plates, the possible arcing must be carefully considered. When the voltage was pushed too high, a short in the circuit was caused by the FC arcing with something connected to ground. Most likely the FC connected with the ground of the filament and shorted the whole system. Luckily, the current flowing through the Faraday Cup is very small, so no damage was done to the ammeter. The current flowing through the

filament was set to a constant 17A because it appeared to be the minimum current required to register any change in current on the ammeter. Theoretically the current could be set higher to increase the output current signal, but the level of heat the wire would emit would greatly increase. Even at 17A, the wires started to melt in areas where the wires would cross. After some time of collecting data, the current would spike from roughly $1\mu A$ to dozens of mA , which indicates a short is occurring. Upon opening the chamber, the current supply wires were fused together completely, resulting in a short in the circuit. Inherently, current will follow the path of least resistance, so the current was just jumping from wire to wire and not even reaching the filament. The resistor started to smoke because the current was completely pumped into the resistor, which ensures the ammeter doesn't take the full load. Due to this increase in current in the resistor, a relatively larger amount of current was able to reach the ammeter.

Voltage(VDC)	Current Output(μA)	Filament Input(A)
100	0.003	17
200	1.0	17
200	0.6	16
250	0.7	16
300	1.3	17
160	1600	17

Table 2.7: Electron current output measurements

Table 2.7 shows the change in current output based on different voltages and filaments input currents. The last measurement has a set voltage at 160V because a spike in the output current was detected moments before. As a result of 160V, the output current was $1600\mu A$. This was caused the wires melting inside the chamber, causing a electrical short. The wires should be insulated better with electrical tape and the test should be done again. Nevertheless, the test was successful and proves that the Faraday Cup made is functional.

Instead of using the large heating filaments from Lesker, smaller filaments can be obtained from a common light bulb. The issue with the large filaments is the amount of current required to generate electrons, but the tungsten coil in a light bulb is much smaller, so it will require far less current. Using the light bulb filament would reduce the current requirement

and the total amount of heat generated. The ammeter detected current from electrons generated by a common 12V, 0.6A light bulb filament. Since the light bulb filament worked so well, the plan shifted away from the large high end tungsten wire to relying on the light bulb filament to generate electrons in the chamber. The test showed that the filament produced an adequate amount of current and should be a good source for the hydrogen ionization process.

Chapter 3

Simulations Of the Protons Trajectory

3.1 Trajectory

Along with physically building the cyclotron, simulations were made to predict the behavior of the protons throughout the acceleration process. Using Python, a simulation was devised to map the trajectory and calculate different values. The simulation was important because it provided valuable insight into the capabilities of the designed setup. The maximum radius of travel for the proton was changes systematically and determined how it affects the trajectory. The simulation can also used identify the optimal characteristic for different aspects of the project like voltage and the distance between the electric field plates. The simulation uses a while-loop¹ to calculate all the desired/required numerical values and uses them in the next step of the simulations. To clarify, at each position each numerical values is calculated and applied to the next position. The position is also determined numerically because all aspects of the simulation affect the trajectory and hence the position. This method ensures an accurate projection of the charged particles behavior. One value that is calculated each step is the kinetic energy because of its importance in a number of other calculations. Most commercial particle detectors will fail to acknowledge a signal because of the lack of kinetic

¹A looping operation that repeats a process for an infinite amount of iterations until a ending condition has been met.

energy. So kinetic energy will not be measured in the physical setup, but it will still be calculated numerically for use in other calculations.

Due to the electric field \vec{E} and the magnetic field \vec{B} , the trajectory of the proton should take the shape of a outward spiral. The proton will start in the center and experience the initial force of the magnetic field, causing it to start a circular orbit. If the electric field wasn't present then the proton would continuously move in a circular pattern while the magnetic field is active. However since there is an electric field present, the proton gains energy every time it moves through the \vec{E} . When the proton gains energy, the velocity increase as a result, so the radius of the proton's orbit is continuously increasing with every revolution. The proton will continue on its spiral path until it hit the edges of the vacuum chamber or reaches the detector. The path of travel looks like similar to the spiral trajectory shown in figure 3.1.

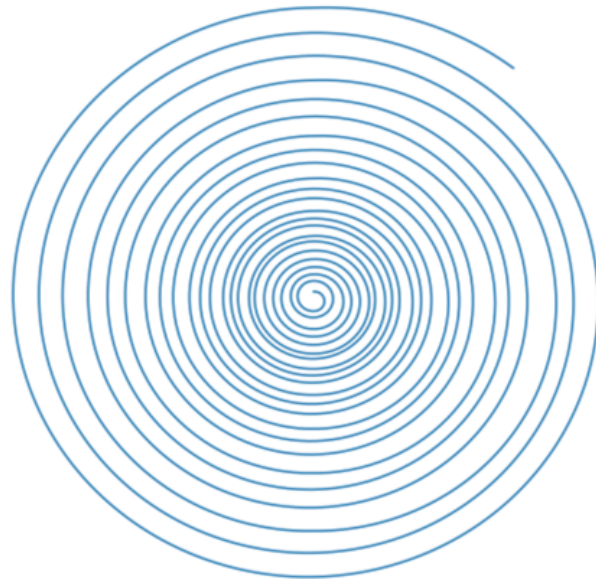


Figure 3.1: The trajectory spiral pattern of a proton in the cyclotron

This figure in particular has a high magnetic field and a relatively low electric field which caused a large number of revolutions. With a large electric field, the energy gain upon each orbit is greater, so the particles require fewer revolutions to reach the maximal radius. The total number of times a single charged particle will enter the electric field to gain energy is

represented by N_{kick} . N_{kick} is calculated using the kinetic energy and the voltage across the plates as seen in equation 3.1.

$$N_{Kick} = \frac{KE}{2 \cdot V} \quad (3.1)$$

N_{kick} primarily determines the number of spiral turns, but it can also be used to estimate the total distance the proton travels on its journey as seen in equation 3.2. Knowing the total distance of travel is valuable because it provide insight into the spot where the proton gets stuck in a fixed radial orbit.

$$d = N_{kick} \cdot 2\pi \cdot R \quad (3.2)$$

In the equation, R is the maximum radius of the chamber and thus the maximum radius the proton can travel. The simulation will also be able to provide the final velocity by recalculating it after each iteration of the while-loop. The final velocity can be used to determine the kinetic energy upon impact with the detector. The velocity can also be used to calculate the total time for the protons to collide with the outer wall or the detector. A valuable check for simulation's accuracy is the sum of all time steps because the sum of every single jump in time, should be equivalent to the total calculated time. If these two values are not equivalent than something in the simulation is going wrong.

The most important factor of the simulation is to be sure that the proton has a smooth trajectory as seen in figure 3.1. This is dependant on the magnetic field strength, voltage of the plates, distance of the plates, hydrogen flow rate and many other factors. However the simulation can provide a huge amount insight into the correct distance between the place based on the voltage over the plates. This concept is discussed further in 2.2.

To check the simulations capability and reliability, results from other experiments and theory should be confirmed. A few test cases were selected, the first being the from a paper regarding proton acceleration in a cyclotron. After confirming the results of the first test,

other test cases of my design can be tested. The following table shows the input data and output measurements from the simulation for a number of test cases.

	Case 1	Case 2	Case 3	Case 4	Case 5	Case 6
$\vec{B}(T)$	2.7	0.3	0.701	0.701	0.701	0.06558
Voltage(V)	50	50	50	500	1000	100
R(cm)	8	8	4	4	4	4
Plate dist(m)	0.03175	0.03175	0.000254	0.0011	0.0011	0.002
KE(KeV)	2232	28	56	49	53	0.466
V(Km/s)	20695	2299	3290	3056	3184	299
f(MHz)	41	5	11	11	11	1

Table 3.1: Test case data

For test case 1, a comparison can be done with a paper that actually built a similar setup and simulation. The paper predicts a final kinetic energy of $2MeV$ and frequency of $41MHz$, which roughly matches the simulation[9]. The paper perhaps rounded their results throughout the calculation which could be responsible for the difference. Overall the simulation matches the results of the paper which builds more confidence in the expected results of the other tests. Figure 3.2 shows the trajectory plots for the six test cases from table 3.1. Each spiral is slightly different and has its own characteristics. The end point on all the spirals is the same but the number of turn is different for each configuration. Case one is from the paper and is a similarity check. Case two is based off the highest magnetic field achieved without placing the vacuum chamber into the system. The distance between the pole face is much larger which resulted in a weaker magnetic field. Case three is the full strength of the magnetic field when the vacuum chamber is place into the system. The distance between the plates went from $9cm$ to $4.5cm$. Case four has the same magnetic field strength, but the voltage and the distance between the plates has been increased. Case five have the same magnetic field strength, and distance between the plates, but the voltage creating the electric field has been increased. Case six is the latest iteration of the system and has a dramatic decrease in many variables. Due the limitations of the equipment accessible, the frequency and amplitude of the square wave supplied to the electric field plate must be heavily reduce. The fastest frequency generator/ amplifier available at Bard can only

reach 100V at 1MHz. So to accommodate this change and produce a nice trajectory for the protons, the magnetic field strength must be reduced. Normally, the \vec{B} determines the cyclotron frequency, but in this particular case it is opposite. Due to the decrease in voltage, the distance between the plates is increased which makes mounting them easier and more precise. This case theoretically should work to produce a uniform beam with a sufficiently strong energy to stick to the FC upon impact.

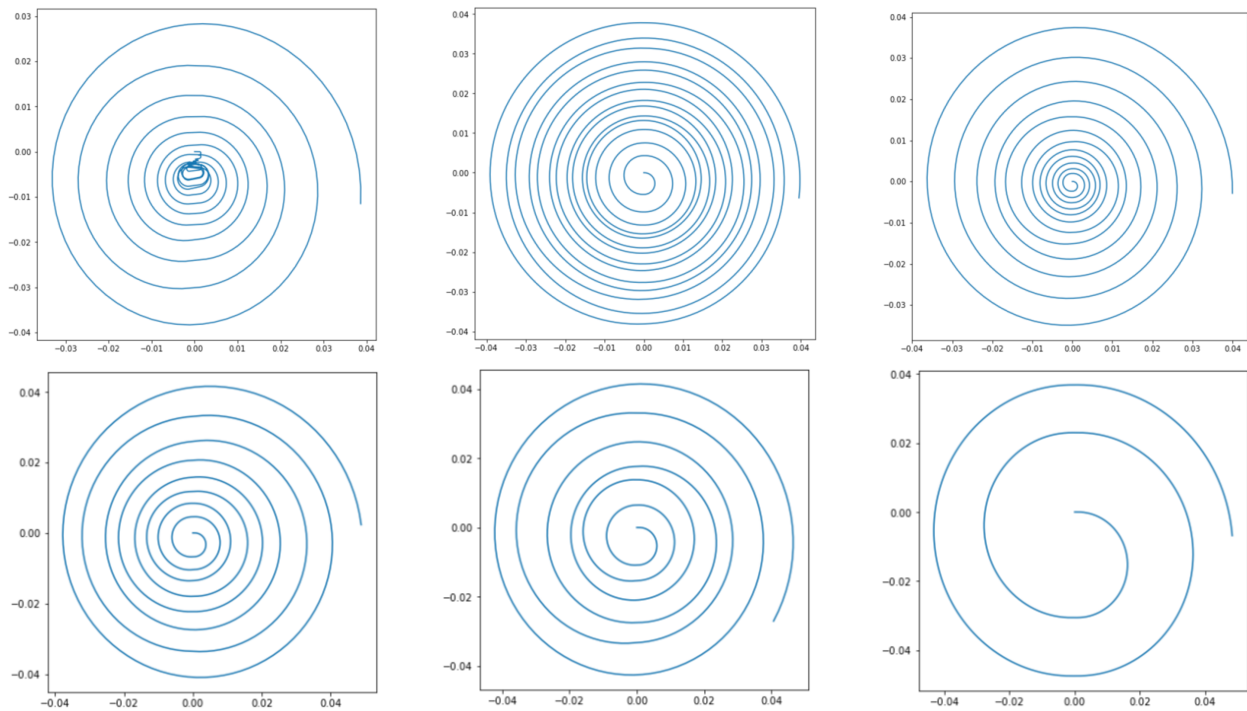


Figure 3.2: Trajectory plots for figure 3.2: left first row-case 1, middle first row-case 2, right first row-case 3, left second row-case 4, middle second row-case 5, right second row-case 6,

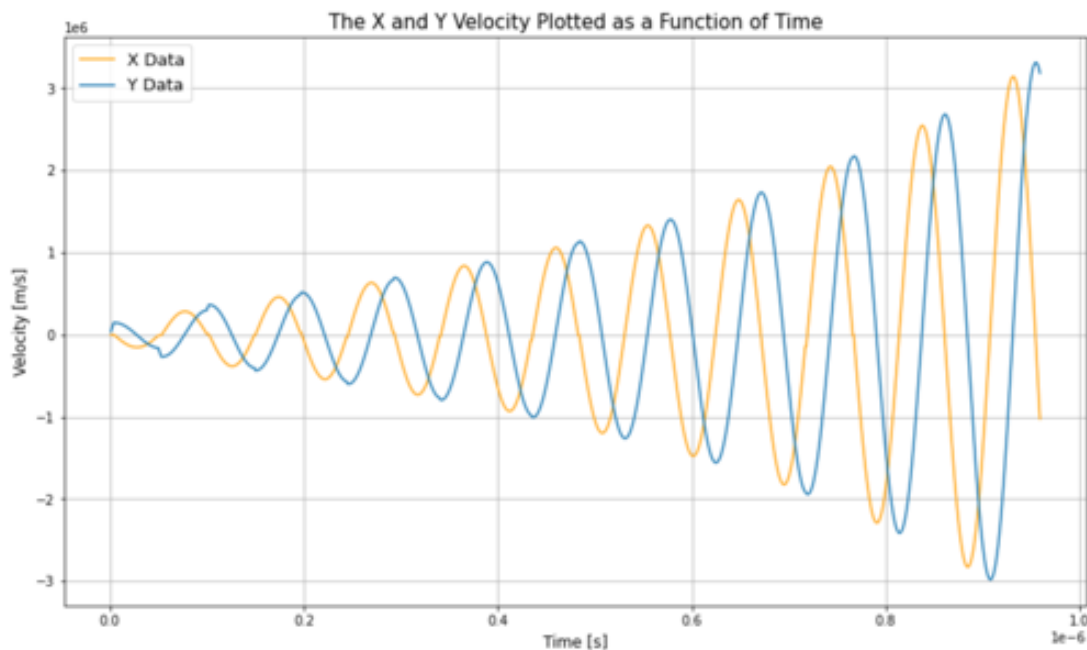
The simulated trajectory plots help characterize the most optimal elements of the system help visualize the process. It is one thing to merely describe the process inside the chamber, but to physically see a representation helped developer a better intuition for the proton behavior. This simulation considers an ideal case of the proton trajectory, which means that the proton only travels along a single plane. However, realistically the proton will travel in all 3 dimensions because the magnetic field will have some variability along the ideal plane of travel. To make a more accurate representation of the protons path a 3D plot should be constructed with a slightly variable \vec{B} . This could easily be done by creating a matrix of the

field strength in all three directions at different positions within the chamber bounds.

3.2 Velocity Plots

Before building the internal components of the cyclotron, the distance between the electric field plates is calculated and set. The distance between the plates not only affects the capacitance of the system, but also the uniformity of the spiral. If the plates are set in the most optimized position possible, the spiral should be completely uniform. A uniform spiral indicates that the proton is accelerating at a constant rate, so a linear line. Throughout the simulation proton, the velocity can be tracked and plotted to see a linear growth. To show this, the velocity can be plotted as a function of time. Figure 3.3 shows the velocity in both the x and y direction as a function of time.

Figure 3.3: A Plot of the Velocity Over Time



Accounting for directional of travel, the plot should look like a a sinusoidal wave with a linear increase in the perfect scenario. However, figure 3.3 expresses a exponential growth instead of a linear acceleration. This is most likely caused by the electric field plates being

just slightly off the most optimized position. To make the charged particle have the most kinetic energy possible, the plates can be adjusted until the spiral is perfectly uniform, hence a constant acceleration. From this plot, the rate of increase of the velocity or the acceleration can be extracted by fitting a 3rd order polynomial to the peaks of each directional velocity. It doesn't matter if the peak above or below the x-axis are used for the fit, theoretically they should return the same acceleration function. The fit of the peaks for the x velocity should match the fit of the peaks for the y direction because it should have a relatively constant acceleration outwards. So it accelerates equally in the y and x direction at any given point, but the total acceleration may vary at different points. The peaks of the plot are isolated and then fit with a 3rd order polynomial which can be compared to the total magnitude of the change in velocity. The magnitude can be calculated with equation 3.3 and the function should match the fits of the peaks.

$$|V| = \sqrt{(v_x)^2 + (v_y)^2} \quad (3.3)$$

To determine how perfect a spiral trajectory is, a line of best-fit can be applied to the peaks and compared to the 3rd order polynomial fit. If the line of best-fit matches polynomial then the percent difference should be equal to zero. This would mean that the acceleration is constant and the spiral is progressing outwards evenly.

Figure 3.4 shows the 3rd order polynomial fit of the peaks for both the x and y velocity. Figure 3.5 shows the line of best-fit for the peaks data and the 3rd order polynomial fit. For this particular data set, the line of best-fit and the 3rd order polynomial fit are similar, but not quite a perfect fit. Towards the beginning of the process, the lines are similar and has a lot overlap. However, the lines diverge in the middle and continue to vary for the rest of the process. To optimize the distance between the plates, a while-loop structure can be utilized to cycle through different distances and compare the fits until a minimal percent difference is achieved.

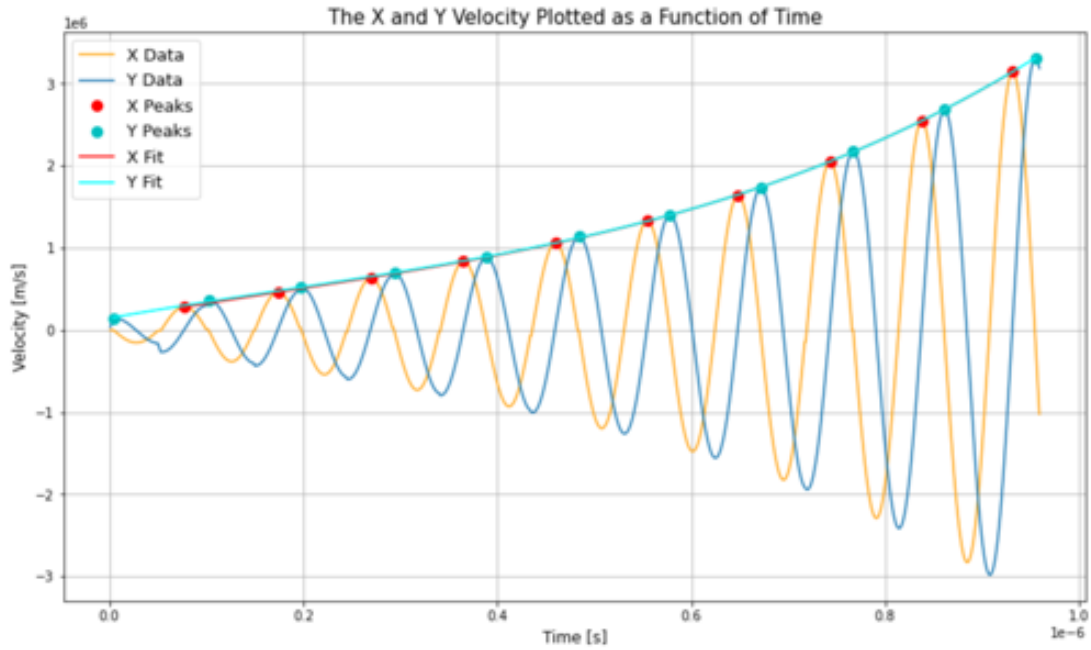


Figure 3.4: Fitting the Peaks With a 3rd Order Polynomial

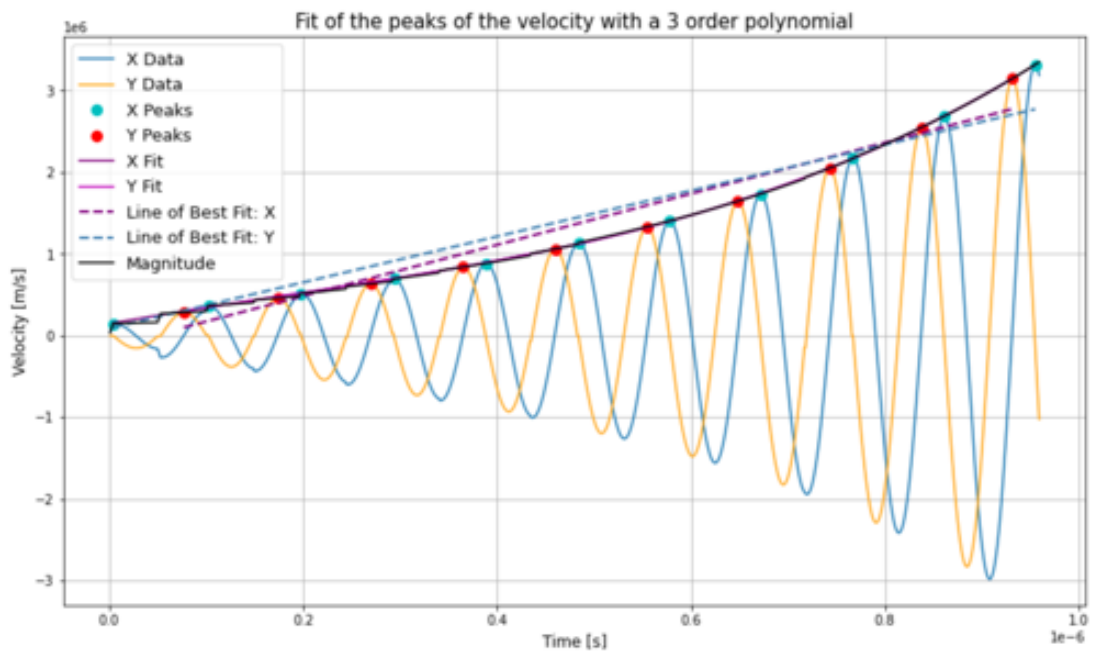


Figure 3.5: Fitting a Line of Best to the Peaks Data

Chapter 4

Operating the Cyclotron

4.1 Operational Manual

Now that all the components have been built and tested individually, it is time to assemble everything and test the full system. The system as a whole has not been tested, but the process would have been tested using the following instructions. This section serves as a full assembly and operation manual for the complete system. The internal components must be connected first, specifically the electric plates must be placed into their respective mounts. Then the filament and gas line are secured into the attachment clip which slides over the rectangular plate. A Faraday Cup should also be secured into its mount at this time. After all these components are in place, the electrical connections for all parts should be connected to the external feedthrough port. Specifically, the positive line for the plates, the positive line the filament, the Faraday Cup output line, and the ground for all these systems to one pin. After connecting the electrical components, the internal mechanisms are fully connected and ready to be sealed within the vacuum chamber. Now that the chamber is sealed, the vacuum hose should be connected to the chamber and the vacuum pump. Depending on the vacuum pump configuration, it may be two pumps connected in parallel or it may only be one pump. A pressure sensor needs to be placed either at the base of the pumps using a

tee connector or attached directly to the chamber. The chamber should then be placed into the electromagnet frame and the bolts should be secured with great caution. The chamber is very heavy, so having a second person for this phase is useful but not necessary. Once the chamber is secured, the power supplies for all internal components should be connect to the feedthrough and insulated using electrical tape. At high voltages, there is a chance of electrical discharge between the connecting leads outside the chamber, so the electrical tape is a secondary precaution from shorting the circuit. All power supplies should be set to the required voltages and current, but it is important NOT to turn them on right after connecting them. A precise order must be followed to ensure all components are not damages and the best possible results are achieved. Lastly, the hydrogen gas line should be connected from the bottle to the chamber port. The hydrogen valve should not be opened until much later into the process. All hydrogen leak detectors should be in place and turned on to detect excess levels of hydrogen in the air.

Now that all components are connected, we are ready to start turning on individual instruments. A low pressure vacuum is the first step of the equation, so the pump should be turned on and the pressure needs to be closely monitored. The pressure should ideally be below $2 \times 10^{-3} \text{ torr}$, but the setup should be tested as the lowest possible pressure achieved.. Once a stable low pressure is achieved, the voltage supplied to the Faraday Cup should be turned on as well as the ammeter measuring the output current. This ensures that all possible charged particles can be caught once the system is running. The electric plates and electromagnets should be engaged in unison. When the charged particles are generated, the electric and magnetic fields will be able to accelerate them into a high speed orbit until reaching the Faraday Cup. Ionizing the hydrogen gas is the last piece of the puzzle, so the electron generating filament should be supplied the necessary current and the hydrogen gas valve can be opened slowly. The current and voltage draw from the filament needs to be watched closely to catch any potential shorts as soon as possible. The filament can also be monitored visually using the glass port window. Introducing the hydrogen gas to the

vacuum environment will slightly increase the chamber pressure, so don't panic if the pressure increases. If the pressure increases drastically, the amount of hydrogen being pumped into chamber is far too much and should be lowered immediately. If the system is working properly, the output current from the Faraday cup should be slowly increasing in the range of μA . A simple check to verify the current output is actually the proton collisions and not pulling current from an alternate source is disconnecting the voltage supply to the Faraday Cup. The output current should be disconnected from the circuit and the current should drop to zero. If the wire is reconnected into the circuit and the current source comes back, the current is most likely from accelerated protons.

If a current output is achieved and verified, congratulations you have successfully accelerated protons!

4.2 Common Problems

Throughout the process, there have been many learning moments that have shared valuable insight into the construction and operation of a cyclotron. The best method to build an intuition for failures when building something is to learn from any and all mistakes. Don't treat every mistake as a complete waste of time, use it as a moment to learn and better your skills. This section serves to help solve simple problems that may be experienced when operating the cyclotron based on my many learning experiences.

1. Low vacuum pressure:

If a low pressure is achieved after connecting the chamber to the pump, there are a number of potential problems. The first being a large leak is present in the chamber, most likely one of the KF16 fittings is not properly secured. Check all the fittings using isopropanol because the pressure will increase slightly if the isopropanol penetrates the chamber. The isopropanol evaporates almost immediately in air, so the vapor will increase the pressure if a leak is present. If all fittings have been tested and ruled out,

check the KF16 adaptor connecting to the chamber. Each fitting is wrapped in Teflon tape and should theoretically be air tight; it took many attempts to isolate all leaks when they were installed. If all fittings and adaptors are ruled out, then the chamber may just be unclean and require a full cleaning with isopropanol. If all these methods are unsuccessful, then look to replacing the rubber gaskets.

2. Output current irregularities:

While testing the output current from the Faraday Cup, the current may fluctuate slightly within a $50\mu A$ range. However, if the current jumps by a factor of mA then there is definitely a problem in the system. Most likely the filament has burnt out from excess use or high levels or heat. To test if the filament is still intact, use the continuity setting of a multimeter. If the filament is broken, there is no longer a continuous circuit. It is also possible that the high levels of heat has warped the filament causing it to touch another component. All electrical components are connected to the same ground, so it is possible that the circuit is shorting because the filament is touching the electric field plates. An easy test to do without opening the chamber is testing the continuity of the filament to the electric field plates. If all these test fail, then the chamber must be opened and the internal components must be inspected. First check the electrical connections, specifically the electrical feedthrough port. The wire may have been simply disconnected and can easily be reconnected.

3. The pressure plummets mid-test:

If a low pressure was secured prior to testing and it plummets mid-test, there is a failure occurring in the internal system. There are two possible explanations to this problem, the first is simple, while the second is much more complex. The first possible situation is that a simple leak was created by a flange fitting coming loose. Throughout my testing, the glass view port had come loose and pulled the glass pane into the chamber. This resulted in air flooding the chamber and a complete loss of pressure. All fittings should

be inspected to ensure a sealed system. The second possible issue is a complete failure of internal components due to high levels of heat. Throughout testing, there were a number of failures due to numerous components melting because of high current levels in wires and heat generated by the filament. Many of the internal parts are solely made of plastic, so high levels of heat will melt them and they will release plastic particle/gas into the system. While the parts are melting, they will fill the chamber and cause the pressure to return to normal because the pump is not capable of keeping up with the influx of high particular matter in the system. After a few seconds, the pressure is returned to a low vacuum environment, but having high plastic matter in the system is not safe in the long term. The current levels through the filament should be lowered or higher strength wires should be used.

4. **Ammeter not registering a signal:**

If the ammeter is not registering a proper signal or is registering noticeably incorrect data, then the system is connected wrong. Check the connection in and out of the ammeter as well as the connections to the voltage supply. If the connections aren't secure or are in the wrong spot, the data output may be odd. It is also possible that the connection line to the Faraday Cup is not secure anymore and has slipped the screw inside the chamber. In this case, the chamber needs to be opened and the screw must be secured.

5. **Lack of output current signal:**

If there is no signal present and everything is supposedly connected correctly, it is most likely a faulty connection. The connections should all be reinspected and the instruction check list from the previous section should be consulted. It is also possible that the hydrogen flow rate is incorrect and the levels are too low. The hydrogen flow rate should be double checked using the needle valve. A simple test that can be done is flooding the chamber with hydrogen gas to increase the pressure. When the gas floods

the chamber, the pumps can't keep up with the fast influx of gas entering the chamber so the pressure rapidly increases for a moment. The gas should only be flooded for a second and the gas valve should not fully be opened. It is important to have many windows open during this test because all the hydrogen in the system will be pumped out into the room. If all the hydrogen is pumped into the room, there is a chance the hydrogen gas could ignite.

Chapter 5

Conclusions

5.1 Findings

Each individual components was constructed and the full system was assembled. After combining the the components, an initial test was attempted. However, there was a leak in the hydrogen regulator that could not be isolated. When the H_2 line is connected to the system, the chamber wasn't able to maintain a pressure below 1 torr . Since the pressure was not within the acceptable range, the ionization process and the acceleration process would not have worked. Along with the leak in the system, the voltage source for the electric field plates was not correctly tuned. The amplification process corrupted the output signal slightly, which caused the signal to have a slow rise time. As a result of these two circumstances, the system was not able to be tested fully.

The full setup assembled is shown in figure 5.1. Not all the wire connections are shown in the figure, nor the water cooling setup, but all the port fittings are shown accurately. With more time, the system could be fully implemented and tested. Knowing all the components work individual provides hope that all the components will work in unison when connected together. More likely, the system will need to be refined and tested extensively to get promising results.

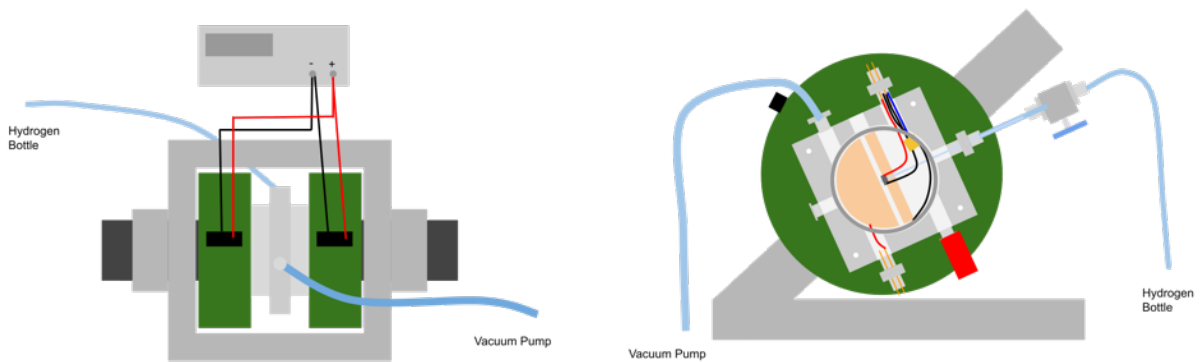


Figure 5.1: The final setup

5.2 Future Plans

This project has been full of failures and successes, but the experience of this project was invaluable. In the end, the system was not fully tested and results were not gathered, but the system has been fully prepared for testing soon and for future seniors. In addition to testing the protons, the system could be modified to allow for the acceleration of other materials, like positrons and and potentially electrons. This project would use the basic setup built over the last year, but would require numerous changes and additions. Another interesting road to follow would be developing a second cyclotron to potentially collide the accelerated material from both cyclotrons. Or possibly create a holding ring to maintain the kinetic energy of the first accelerated material until the second is ready for the collision. I am proud and excited to pass this project to the rising seniors and look forward to see what inspiring ideas they devise for this cyclotron.

Bibliography

- [1] A and J Vacuum System. Pfeiffer adixen asm 182 td+ standard helium leak detector, 2024.
- [2] Agilent. Agilent IDP-3 Dry Scroll Vacuum Pump 60Hz with Power Cord, 2024.
- [3] E. D. Cantero. Design of a Compact Faraday Cup for Low Energy, Low Intensity Ion Beams. *Nuclear Instruments and Methods in Physics Research A*, November 2015.
- [4] LibreText Chemistry. Ionization Energies of Diatomic Molecule, April 2024.
- [5] Kurt J. Lesker Company. Electrical Feedthrough, 2024.
- [6] Kurt J. Lesker Company. Gas Needle Valve, 2024.
- [7] Kurt J. Lesker Company. Gas Quick-Connect Fitting, 2024.
- [8] C. Davisson and L. H. Germer. The Thermionic Work Function of Tungsten. *American Physical Society*, 20, October 1922.
- [9] Leslie Dewan. Design and Construction of a Cyclotron Capable of Accelerating Protons to 2 mev. *MIT*, pages 1–123, June 2007.
- [10] DigiKey. Mq-8 sensor, 2024.
- [11] Science Direct. Dielectric breakdown, 2024.
- [12] Chemistry LibreTexts Editors. Chemistry LibreTexts, November 2021.

- [13] Quantum Electronics. *B2 Electromagnet Operation Manual*. Quantum Electronics Corporation, 1st edition.
- [14] Center for Scientific Education. *Radio Waves*, 2024.
- [15] David Griffiths. *Introduction to Electrodynamics*. Cambridge University Press, 4th edition, 2017.
- [16] David Griffiths. *Introduction to Quantum Mechanics*. Cambridge University Press, 3rd edition, 2018.
- [17] Edwin H. Hall. Thermionic Emission and the "Universal Constant" A. *National Academy of Sciences*, (<https://www.jstor.org/stable/84655>), May 1927.
- [18] David Halliday. *Fundamentals of Physics*. John Wiley and Sons, 10th edition, 2014.
- [19] Environmental Health and Safety Department. *Electromagnetic Fields Factsheet*. Iowa State University, pages 1–3, 2022.
- [20] Ernest Lawrence. The Evolution of The Cyclotron. *The Nobel Prize*, pages 1–14, December 1951.
- [21] Oxford Languages. The meaning of 'cyclo-' and '-tron', 2024.
- [22] McMaster. Compact Precision Extreme-Pressure Steel Threaded Pipe Fittings, 2024.
- [23] McMaster. High-Vacuum Exhaust Hose with Quick-Clamp Fittings, 2024.
- [24] McMaster. Tee Connections, 2024.
- [25] Wayne B. Nottingham. *Thermionic Emission*. RESEARCH LABORATORY OF ELECTRONICS MASSACHUSETTS INSTITUTE OF TECHNOLOGY, 1st edition, December 1956.
- [26] OnlineMetals. Melting Temperature, 2024.

- [27] John Papiewski. Spark Gap, March 2018.
- [28] I.E. Petrunin. Interaction of tungsten with copper, manganese, silver, and tin. *Met Sci Heat Treat*, 11(<https://doi.org/10.1007/BF00655167>):24–26, 1969.
- [29] Pfeiffer. Pfeiffer Vacuum Activeline Gauge PCR 280, 2024.
- [30] QMINOX. Ss304 KF16 NPT Male Adaptor Thread 1/2" nw16 kf male coupling iso-kf16 x npt 1/2", 2024.
- [31] Arnold L Reimann. *Thermionic Emission*. London Chapman Hal, 1st edition, 1935.
- [32] SandBoxElectronics. Arduino code for hydrogen detection, 2024.
- [33] Paul Scherz. *Practical Electronics for Inventors*. Mc Graw Hill Education, 4th edition, 2016.
- [34] W. Watt Webb. Oxidation of Tungsten. *The Electrochemical Society*, 103(10.1149/1.2430238), August 1956.
- [35] Wikipedia. Mean Free Path, 2023.
- [36] Wikipedia. Cyclotron Resonance Frequency, 2024.
- [37] Wikipedia. Faraday Cup, 2024.
- [38] Wikipedia. Thermionic Emission, 2024.
- [39] Wikipedia. Work Functions, 2024.
- [40] A. Bloom Zwicker. The Suitability of 3D Printed Plastic Parts for Labritory Use. *Offics of Scientific and Technical Information*, 1(PPPL-5057):1–12, August 2014.

Appendix A

Arduino Codes

A.1 Arduino Code for A Single Detector

```
/******Demo for MQ-8 Gas Sensor Module V1.0*****
```

```
Contact: support[at]sandboxelectronics.com
```

```
Lisence: Attribution-NonCommercial-ShareAlike 3.0
```

```
Unported (CC BY-NC-SA 3.0)
```

```
Note: This piece of source code is supposed to be  
used as a demonstration ONLY. More  
sophisticated calibration is required  
for industrial field application.
```

```
Sandbox Electronics 2014-02-03
```

```
Luke Ingraham
```

```
Version 1
```

Modifaction to code: April 17, 2023

```
*****/

/*****Hardware Related Macros*****/

#define MQ_PIN (0)//analog input channel you are going to use
#define RL_VALUE (10)//load resistance on the board, in kilo ohms
#define RO_CLEAN_AIR_FACTOR (9.21)
//RO_CLEAR_AIR_FACTOR=(Sensor resistance in clean air)/RO,
//which is derived from the chart in datasheet

#define LED_PIN1 (7) //output LED pin 1
#define LED_PIN2 (8) //output LED pin 2
#define BUZZER (10) //output pint for buzzer

/****Software Related Macros*****/

#define CALIBARAION_SAMPLE_TIMES (50)
//define how many samples you are going to take in the calibration
// phase
#define CALIBRATION_SAMPLE_INTERVAL (500)
//define the time interal(in milisecond) between each samples in the
//cablibration phase
#define READ_SAMPLE_INTERVAL (50)
//define how many samples you are going to take in normal operation
#define READ_SAMPLE_TIMES (5)
//define the time interal(in milisecond) between each samples in
//normal operation
```



```
Serial.print("kohm");
Serial.print("\n");

}

void loop()
{
  Serial.print("H2:");
  int sensorValue = MQGetGasPercentage(MQRead(MQ_PIN)/Ro,GAS_H2);
  Serial.print(sensorValue);
  Serial.print( "ppm" );
  Serial.print("\n");
  delay(200);
  if(sensorValue>175){
    digitalWrite(LED_PIN2, HIGH);
    digitalWrite(LED_PIN1, LOW);
    tone(BUZZER, 1000); // Send 1KHz sound signal...
    delay(1000);      // ...for 1 sec
    noTone(BUZZER);   // Stop sound...
    delay(1000);      // ...for 1sec
  }
  else {
    digitalWrite(LED_PIN1, HIGH);
    digitalWrite(LED_PIN2, LOW);
    // digitalWrite(LED_PIN3, LOW);
  }
}
```

```

/**** MQResistanceCalculation ****
Input:  raw_adc - raw value read from adc,
        which represents the voltage
Output:  the calculated sensor resistance
Remarks: The sensor and the load resistor forms a
        voltage divider.
        Given the voltage across the load resistor and
        its resistance, the resistance of the sensor could
        be derived.

*****/
float MQResistanceCalculation(int raw_adc)
{
    return ( ((float)RL_VALUE*(1023-raw_adc)/raw_adc));
}

/**** MQCalibration ****
Input:  mq_pin - analog channel
Output:  Ro of the sensor
Remarks: This function assumes that the sensor is in clean air.
        It use MQResistanceCalculation to calculates the
        sensorresistance in clean air and then divides it
        with RO_CLEAN_AIR_FACTOR. RO_CLEAN_AIR_FACTOR is about 10,
        which differs slightly between different sensors.

*****/
float MQCalibration(int mq_pin)
{

```

```
int i;
float val=0;

for (i=0;i<CALIBARAION_SAMPLE_TIMES;i++) {
    //take multiple samples
    val += MQResistanceCalculation(analogRead(mq_pin));
    delay(CALIBRATION_SAMPLE_INTERVAL);
}
val = val/CALIBARAION_SAMPLE_TIMES;
    //calculate the average value

val = val/RO_CLEAN_AIR_FACTOR;
    //divided by RO_CLEAN_AIR_FACTOR yields the Ro
    //according to the chart in the datasheet

return val;
}

/**** MQRead *****/
Input:  mq_pin - analog channel
Output: Rs of the sensor
Remarks: This function use MQResistanceCalculation to caculate
the sensor resistenc (Rs).

The Rs changes as the sensor is in the different
concentration of the target gas. The sample times
and the time interval between samples could be
configured by changing the definition of the macros.

*****/
```

```
float MQRead(int mq_pin)
{
    int i;
    float rs=0;
    for (i=0;i<READ_SAMPLE_TIMES;i++) {
        rs += MQResistanceCalculation(analogRead(mq_pin));
        delay(READ_SAMPLE_INTERVAL);
    }
    rs = rs/READ_SAMPLE_TIMES;
    return rs;
}

/**** MQGetGasPercentage ****
Input:  rs_ro_ratio - Rs divided by Ro
        gas_id      - target gas type
Output: ppm of the target gas
Remarks: This function passes different curves to the
          MQGetPercentage function which calculates the
          ppm (parts per million) of the target gas.
*****/
int MQGetGasPercentage(float rs_ro_ratio, int gas_id)
{
    if ( gas_id == GAS_H2) {
        return MQGetPercentage(rs_ro_ratio,H2Curve);
    }
    return 0;
}

/***** MQGetPercentage *****/
```

Input: `rs_ro_ratio` - R_s divided by R_o
`pcurve` - pointer to the curve of the target gas

Output: ppm of the target gas

Remarks: By using the slope and a point of the line.

The x(logarithmic value of ppm) of the line
could be derived if y(`rs_ro_ratio`) is provided.

As it is a logarithmic coordinate, power of 10
is used to convert the result to
non-logarithmic value.

*****/

```
int MQGetPercentage(float rs_ro_ratio, float *pcurve)
{
    return (pow(10, ( ((log(rs_ro_ratio)-pcurve[1])/pcurve[2])
        + pcurve[0])));
}
```


Appendix B

Python Codes

In addition to the code listed below, all codes used in this project can be found on Github using the following link.

<https://github.com/LukeIngraham/Senior-Thesis-Project-Cyclotron.git>

B.1 Trajectory Calculation and Simulation

```
import numpy as np
import sympy as sp
import matplotlib.pyplot as plt
import pandas as pd
from scipy.signal import find_peaks
from matplotlib import pyplot
import csv
from scipy.optimize import curve_fit
import scipy.optimize as opt;

def kinetic(V_max, m):
    T = (m*(V_max**2))/2
```

```
    return T

def max_kinetic(q, B, r, m):
    KE_m = ((q**2)*(B**2)*(r**2))/(2*m)
    return KE_m

def V_max(T, m):
    V_max = np.sqrt((2*T)/m)
    return V_max

def V_max2(q, B, R, m):
    V_max2 = (q*B*R)/m
    return V_max2

def B_field(V_max , m, q, R):
    B = ((V_max*m)/(R*q))
    return B

def eV_to_J(T):
    ke = T*(1.6*(10**-19))
    return ke

def J_to_eV(T):
    ke = T/(1.6*(10**-19))
    return ke

def cyclo_freq(q, B, m):
```

```
w = (q*B)/m
return w

def freq(q, B, m):
    f = (q*B)/(2*np.pi*m)
    return f

def expected_radius(v, b, q, m):
    expected_radius = v / ( b * (q/m) )
    return expected_radius

def expected_period(b, q, m):
    expected_period = 2.0*np.pi/( b * (q/m) )
    return expected_period

def expected_time(m, q, b):
    expected_time = ((m*np.pi)/(q*b))
    return expected_time

def percent_diff(x1, x2):
    pd = np.abs((x2 - x1)/x1)*100
    return pd

def in_to_m(inch):
    unit = inch/39.37
    return unit
```

```
def m_to_in(m):
    unit = m*39.37
    return unit

def check_structure():
    if w == Cyclotron_frequency:
        print("---->w matches")
        print(w, " rad/s vs.", Cyclotron_frequency, "rad/s")
        print("Pd: ", percent_diff(w, Cyclotron_frequency), "%")
    else:
        print("---->w doesn't match")
        print(w, " rad/s vs.", Cyclotron_frequency, "rad/s")
        print("Pd: ", percent_diff(w, Cyclotron_frequency), "%")

    if np.linalg.norm(particlev) == V_maximum:
        print("---->V matches")
        print(np.linalg.norm(particlev), "m/s vs.", V_maximum, "m/s")
        print("Pd: ", percent_diff(np.linalg.norm(particlev), V_maximum), "%")
    else:
        print("---->V doesn't match")
        print(np.linalg.norm(particlev), "m/s vs.", V_maximum, "m/s")
        print("Pd: ", percent_diff(np.linalg.norm(particlev), V_maximum), "%")

    if round(J_to_eV(KE)) == T_kinetic:
        print("---->KE matches")
        print(J_to_eV(KE), "eV vs.", T_kinetic, "eV")
        print("Pd: ", percent_diff(J_to_eV(KE), T_kinetic), "%")
```

```
else:
    print("--->KE doesn't match")
    print(J_to_eV(KE), "eV vs.", T_kinetic, "eV")
    print("Pd: ", percent_diff(J_to_eV(KE), T_kinetic), "%")

if t == time:
    print("--->t matches")
    print(t, "s vs.", time, "s")
    print("Pd: ",percent_diff(t, time), "%")
else:
    print("--->t doesn't match")
    print(t, "s vs.", time, "s")
    print("Pd: ", percent_diff(t, time), "%")

def model_f(x,a,b,c):
    return a*(x-b)**2+c

def Gauss(x, A, B):
    y = A*np.exp(-1*B*x**2)
    return y

def fitter(V, Alpha, Beta, Gamma, Delta, C1, C2, C3):
    fit=Alpha-np.exp(-Gamma*V)*Beta*
        (np.cos((2*np.sqrt(2)*np.pi*
                (C1*V+(C2*V)**2+(C3*V)**3))/Lambda + Delta))
    return fit

#Luke Ingraham
```

```
def vel_plot(X, Y, title, color):
    peaks, _ = find_peaks(X, height=0)

    # calculate polynomial
    z = np.polyfit(X[peaks],Y[peaks], 3)
    f = np.poly1d(z)

    # calculate new x's and y's
    x_new = np.linspace((Y[peaks])[0], (Y[peaks])[-1], 50)
    y_new = f(x_new)

    plt.figure(figsize=(14,8))
    plt.title("Fit of the peaks of the" + str(title) +
              "with a 3 order polynomial", size=15)
    plt.xlabel("Time [s]", size=12)
    plt.ylabel("Velocity [m/s]", size=12)
    plt.plot(X, Y, color , label = 'Curve')
    plt.plot(X[peaks],Y[peaks], 'ko', markersize = 8, label = 'peaks')
    plt.plot( x_new, y_new, 'r',label = 'Fit_order 3')
    plt.legend(fontsize=10)
    plt.show()
    print("Acceleration" + str(title) + "= ")
    print(f)

def distance_traveled(KE, V, R):
    d = (KE *np.pi*R)/V
```

```
    return d

def Tesla_to_Gauss(B):
    return B*1e4

def Gauss_to_Tesla(B):
    return B/1e4

# Function gathered data
m_proton = (1.67*(10**-27))
q_proton = (1.6 *(10**-19))
b = 0.701
R = 0.04875

Max_kinetic = max_kinetic(q_proton, b, R, m_proton)

V_maximum = V_max(Max_kinetic, m_proton)
print("V_max = ", V_maximum, " m/s (", (round(V_maximum/1000)), "km/s)")

V_Maximum2 = V_max2(q_proton, b, R, m_proton)
print("V_max2 = ", V_Maximum2, "m/s (", (round(V_Maximum2/1000)), "km/s)")

Kinetic = kinetic(V_Maximum2, m_proton)
print("Kinetic = ", J_to_eV(Kinetic), "eV (",
      (round(J_to_eV(Kinetic)/1000)), "KeV )" )
```

```
print("Max Kinetic Energy = ", J_to_eV(Max_kinetic), "eV (",

Mag_field = B_field(V_maximum, m_proton, q_proton, R)
print("B = ", Mag_field, " T (or kg/s•C)")

Cyclotron_frequency = cyclo_freq(q_proton, Mag_field, m_proton)
print("w = ", Cyclotron_frequency, " rad/s")

frequency = freq(q_proton, Mag_field, m_proton)
print("f = ", frequency, " Hz (", (round(frequency/1e6)), "MHz)")

time = expected_time(m_proton, q_proton, Mag_field)
print("time = ", time)

distance = distance_traveled(round(J_to_eV(Kinetic)), 50, R)
print("d_expected = ", distance, "m (", round(distance), "m)")

T_kinetic = J_to_eV(Kinetic)

# Simulation Data
particlepos = np.array([0.0,0.0,0.0])
particlev = np.array([0.0,0.0,0.0]) #Set the initial particle speed to 0

#create an array for the x position of the particle
particleposx = [particlepos[0]]
#create an array for the y position of the particle
particleposy = [particlepos[1]]
```



```
q = 1.6e-19 #Set the charge of the particle to the charge of a proton
m = 1.67e-27 #Set mass of the particle to the mass of a proton

V = 50 #Set voltage between the plates to 50V
d = in_to_m(0.01) #Separation between the plates to 90 micrometers
#Electric field based on voltage between the D's and separation
E_0 = V/(d)

#Set magnetic field to 0.3T in the +Z direction
B = np.array([0.0,0.0,0.701])
r_cyclotron = 0.04875 #set the radius of the D's to 8cm
w = q*np.linalg.norm(B)/m #define the cyclotron frequency
f = q*np.linalg.norm(B)/(2*np.pi*m)

t = 0 #initialize time to 0
dt = 10**-9 #Set timestep to 5 picoseconds

Vx = []
Vy = []
T = []
d_magnitude = []

#loop while the magnitude of the proton's position
while (np.linalg.norm(particlepos) < r_cyclotron):
    #remains within the cyclotron radius

    #create a vector for the net force on the particle.
```

```

Fnet = np.array([0.0,0.0,0.0])

    #if the particle is between the two D's calculate the electric force
if np.absolute(particlepos[0]) < d/2:
    Fnet[0] = q*E_0*np.cos(w*t)
#if the particle is not, calculate the magnetic force
else:
    Fnet = q*np.cross(particlev,B)

particlev = particlev + Fnet*dt/m #Update the velocity of the particle
    #Use velocity to update the position of the particle
particlepos = particlepos + particlev*dt
    #append the x position to the x-position list
particleposx = np.append(particleposx, particlepos[0])
    #append the y position to the y-position list
particleposy = np.append(particleposy, particlepos[1])

t = t + dt #update the timestep
Vx = np.append(Vx,particlev[0])
Vy = np.append(Vy,particlev[1])
T = np.append(T, t)
d_magnitude = np.append(d_magnitude,
    np.sqrt((particlepos[0]**2)(particlepos[1]**2)))

print("Cyclotron Frequency is", w, "rad/s (or ", f, " Hz,", round(f/1e6), "MHz)")
print("The final speed of the particle is", np.linalg.norm(particlev), "m/s, ",
    round(np.linalg.norm(particlev/1000)), "km/s")

```

```
KE = kinetic(np.linalg.norm(particlev), m)
print("Kinetic Energy is", KE, "J (", J_to_eV(KE) ,"eV",
      round( J_to_eV(KE)/1000),"KeV")
print("Distance Traveled is",sum(d_magnitude), "m")

# Change in Velocity plot
plt.figure(figsize=(8,8))
plt.plot(T, Vx, label="X")
plt.plot(T, Vy, label="Y")
plt.title("Velocity vs. Time")
plt.xlabel("Time[10e-9 s]")
plt.ylabel("Velocity[m/s]")
plt.legend()

tot = np.sqrt((Vx**2)+ (Vy**2))
plt.plot(T, tot)

#Trajectory Plot
txt = ("β = " + str(B[2]) + "T",
      "V = " + str(V) + "volts",
      "d = " + str(round(d,6)) + "m",
      "r = " + str(r_cyclotron) + "m"
      )

plt.figure(1, figsize=(8,8)) #create the figure
plt.plot(particleposx, particleposy) #create the plot
plt.title("Case3: Modified Theory data from paper")
#plt.savefig("Test2_β2-7_V50_d1.25_r8cm_2.jpeg")
```

```
plt.show()
print(txt)

check_structure()

peaks_x, _ = find_peaks(Vx, height=0)
# calculate polynomial
z = np.polyfit(T[peaks_x],Vx[peaks_x], 3)
f = np.poly1d(z)

# calculate new x's and y's
x_new = np.linspace((T[peaks_x])[0], (T[peaks_x])[-1], 50)
y_new = f(x_new)

plt.figure(figsize=(14,8))
plt.title("Fit of the peaks of the X-velocity with a 3 order polynomial",
          size=15)
plt.xlabel("Time [s]", size=12)
plt.ylabel("Velocity [m/s]", size=12)
plt.plot(T, Vx, 'tab:blue',label = 'Curve')
plt.plot(T[peaks_x],Vx[peaks_x],'ko', markersize = 8, label = 'peaks')
plt.plot( x_new, y_new, 'r',label = 'Fit_order 3')
plt.legend(fontsize=10)
plt.show()
print("Acceleration X =")
print(f)
```

```
peaks_y, _ = find_peaks(Vy, height=0)

# calculate polynomial
zy = np.polyfit(T[peaks_y],Vy[peaks_y], 3)
fy = np.poly1d(zy)

# calculate new x's and y's
x_newy = np.linspace((T[peaks_y])[0], (T[peaks_y])[-1], 50)
y_newy = fy(x_newy)

plt.figure(figsize=(14,8))
plt.title("Fit of the peaks of the Y-velocity with a 3 order polynomial",
          size=15)
plt.xlabel("Time [s]", size=12)
plt.ylabel("Velocity [m/s]", size=12)
plt.plot(T, Vy, 'orange', label = 'Curve')
plt.plot(T[peaks_y],Vy[peaks_y],'ko', markersize = 8, label = 'peaks')
plt.plot( x_newy, y_newy, 'r',label = 'Fit_order 3')
plt.legend(fontsize=10)
plt.show()
print("Acceleration Y = ")
print(fy)
```

B.2 Plate Distance Estimate

```
import numpy as np
```

```
import sympy as sp
import matplotlib.pyplot as plt
import pandas as pd
from scipy.signal import find_peaks
from matplotlib import pyplot
import csv
from scipy.optimize import curve_fit
import scipy.optimize as opt;

def kinetic(V_max, m):
    T = (m*(V_max**2))/2
    return T

def max_kinetic(q, B, r, m):
    KE_m = ((q**2)*(B**2)*(r**2))/(2*m)
    return KE_m

def V_max(T, m):
    V_max = np.sqrt((2*T)/m)
    return V_max

def V_max2(q, B, R, m):
    V_max2 = (q*B*R)/m
    return V_max2

def B_field(V_max , m, q, R):
    B = ((V_max*m)/(R*q))
```

```
    return B

def eV_to_J(T):
    ke = T*(1.6*(10**-19))
    return ke

def J_to_eV(T):
    ke = T/(1.6*(10**-19))
    return ke

def cyclo_freq(q, B, m):
    w = (q*B)/m
    return w

def freq(q, B, m):
    f = (q*B)/(2*np.pi*m)
    return f

def expected_radius(v, b, q, m):
    expected_radius = v / ( b * (q/m) )
    return expected_radius

def expected_period(b, q, m):
    expected_period = 2.0*np.pi/( b * (q/m) )
    return expected_period

def expected_time(m, q, b):
```

```
    expected_time = ((m*np.pi)/(q*b))
    return expected_time

def percent_diff(x1, x2):
    pd = np.abs((x2 - x1)/x1)*100
    return pd

def in_to_m(inch):
    unit = inch/39.37
    return unit

def m_to_in(m):
    unit = m*39.37
    return unit

def check_structure():
    if w == Cyclotron_frequency:
        print("--->w matches")
        print(w, " rad/s vs.", Cyclotron_frequency, "rad/s")
        print("Pd: ", percent_diff(w, Cyclotron_frequency), "%")
    else:
        print("--->w doesn't match")
        print(w, " rad/s vs.", Cyclotron_frequency, "rad/s")
        print("Pd: ", percent_diff(w, Cyclotron_frequency), "%")

if np.linalg.norm(particlev) == V_maximum:
    print("--->V matches")
```



```
print(np.linalg.norm(particlev), "m/s vs.", V_maximum, "m/s")
print("Pd: ", percent_diff(np.linalg.norm(particlev), V_maximum), "%")
else:
    print("--->V doesn't match")
    print(np.linalg.norm(particlev), "m/s vs.", V_maximum, "m/s")
    print("Pd: ", percent_diff(np.linalg.norm(particlev), V_maximum), "%")

if round(J_to_eV(KE)) == T_kinetic:
    print("--->KE matches")
    print(J_to_eV(KE), "eV vs.", T_kinetic, "eV")
    print("Pd: ",percent_diff(J_to_eV(KE), T_kinetic), "%")
else:
    print("--->KE doesn't match")
    print(J_to_eV(KE), "eV vs.", T_kinetic, "eV")
    print("Pd: ", percent_diff(J_to_eV(KE), T_kinetic), "%")

if t == time:
    print("--->t matches")
    print(t, "s vs.", time, "s")
    print("Pd: ",percent_diff(t, time), "%")
else:
    print("--->t doesn't match")
    print(t, "s vs.", time, "s")
    print("Pd: ", percent_diff(t, time), "%")

def model_f(x,a,b,c):
    return a*(x-b)**2+c
```

```
def Gauss(x, A, B):
    y = A*np.exp(-1*B*x**2)
    return y

def fitter(V, Alpha, Beta, Gamma, Delta, C1, C2, C3):
    fit=Alpha-np.exp(-Gamma*V)*Beta*(np.cos((2*np.sqrt(2)*
        np.pi*(C1*V+(C2*V)**2+(C3*V)**3))/Lambda + Delta))
    return fit
    #Luke Ingraham

def vel_plot(X, Y, title, color):
    peaks, _ = find_peaks(X, height=0)

    # calculate polynomial
    z = np.polyfit(X[peaks],Y[peaks], 3)
    f = np.poly1d(z)

    # calculate new x's and y's
    x_new = np.linspace((Y[peaks])[0], (Y[peaks])[-1], 50)
    y_new = f(x_new)

    plt.figure(figsize=(14,8))
    plt.title("Fit of the peaks of the" + str(title) +
        "with a 3 order polynomial", size=15)
    plt.xlabel("Time [s]", size=12)
    plt.ylabel("Velocity [m/s]", size=12)
```

```
plt.plot(X, Y, color , label = 'Curve')
plt.plot(X[peaks_y],Y[peaks],'ko', markersize = 8, label = 'peaks')
plt.plot( x_new, y_new, 'r',label ='Fit_order 3')
plt.legend(fontsize=10)
plt.show()
print("Acceleration" + str(title) + "= ")
print(f)

def distance_traveled(KE, V, R):
    d = (KE *np.pi*R)/V
    return d

def Tesla_to_Gauss(B):
    return B*1e4

def Gauss_to_Tesla(B):
    return B/1e4

def microMeter_to_meter(unit):
    return unit/1e6

def meter_to_microMeter(unit):
    return unit*1e6

def capacitance(A, d):
    ep = 8.854*10**(-12) #F•m-1
    return (ep*A)/d
```

```
def cm_to_m(unit):
    return unit/100

def cm2_to_m2(unit):
    return unit/10000

def Area(base, width):
    return base*width

def mm_to_m(unit):
    return unit/1000

def calculate_R(f, C):
    return (1/f)/C

m_proton = (1.67*(10**-27))
q_proton = (1.6 *(10**-19))
b = 0.701 #T
R = 0.04875 #m

Max_kinetic = max_kinetic(q_proton, b, R, m_proton)

V_maximum = V_max(Max_kinetic, m_proton)
print("V_max = ", V_maximum, " m/s (", (round(V_maximum/1000)), "km/s)")

V_Maximum2 = V_max2(q_proton, b, R, m_proton)
```

```
print("V_max2 = ", V_Maximum2, "m/s (", (round(V_Maximum2/1000)), "km/s)")

Kinetic = kinetic(V_Maximum2, m_proton)
print("Kinetic = ", J_to_eV(Kinetic), "eV (",
      (round(J_to_eV(Kinetic)/1000)), "KeV )" )

print("Max Kinetic Energy = ", J_to_eV(Max_kinetic), "eV (",
      (round(J_to_eV(Max_kinetic)/1000)), "KeV )" )

Mag_field = B_field(V_maximum, m_proton, q_proton, R)
print("B = ", Mag_field, " T (or kg/s•C)")

Cyclotron_frequency = cyclo_freq(q_proton, Mag_field, m_proton)
print("w = ", Cyclotron_frequency, " rad/s")

frequency = freq(q_proton, Mag_field, m_proton)
print("f = ", frequency, " Hz (", (round(frequency/1e6)), "MHz)")

time = expected_time(m_proton, q_proton, Mag_field)
print("time = ", time)

distance = distance_traveled(round(J_to_eV(Kinetic)), 50, R)
print("d_expected = ", distance, "m (", round(distance), "m)")

T_kinetic = J_to_eV(Kinetic)

particlepos = np.array([0.0,0.0,0.0])
```

```
particlev = np.array([0.0,0.0,0.0]) #Set the initial particle speed to 0

    #create an array for the x position of the particle
particleposx = [particlepos[0]]

    #create an array for the y position of the particle
particleposy = [particlepos[1]]

q = 1.6e-19 #Set the charge of the particle to the charge of a proton
m = 1.67e-27 #Set mass of the particle to the mass of a proton

V = 50 #Set voltage between the plates to 50V
    #Set the separation between the plates to 90 micrometers
d = in_to_m(0.01)
    #define the electric field based on voltage between the D's and separation
E_0 = V/(d)

B = np.array([0.0,0.0,0.701]) #Set magnetic field to 0.3T in the +Z direction
r_cyclotron = 0.04875 #set the radius of the D's to 4.875cm

w = q*np.linalg.norm(B)/m #define the cyclotron frequency
f = q*np.linalg.norm(B)/(2*np.pi*m)

t = 0 #initialize time to 0
dt = 10**-9 #Set timestep to 5 picoseconds

Vx = []
Vy = []
```

```

T = []
d_magnitude = []
    #loop while the magnitude of the proton's position
while (np.linalg.norm(particlepos) < r_cyclotron):
    #remains within the cyclotron radius
        #create a vector for the net force on the particle.
Fnet = np.array([0.0,0.0,0.0])
        #if the particle is between the two D's calculate the electric force
if np.absolute(particlepos[0]) < d/2:
    Fnet[0] = q*E_0*np.cos(w*t)
else: #if the particle is not, calculate the magnetic force
    Fnet = q*np.cross(particlev,B)

particlev = particlev + Fnet*dt/m #Update the velocity of the particle
    #Use velocity to update the position of the particle
particlepos = particlepos + particlev*dt
        #append the x position to the x-position list
particleposx = np.append(particleposx, particlepos[0])
        #append the y position to the y-position list
particleposy = np.append(particleposy, particlepos[1])
t = t + dt #update the timestep
Vx = np.append(Vx,particlev[0])
Vy = np.append(Vy,particlev[1])
T = np.append(T, t)
d_magnitude = np.append(d_magnitude,
    np.sqrt((particlepos[0]**2)+ (particlepos[1]**2)))

```

```

print("Cyclotron Frequency is", w, "rad/s (or ",
      f, " Hz,", round(f/1e6), "MHz)")
print("The final speed of the particle is", np.linalg.norm(particlev), "m/s, ",
      round(np.linalg.norm(particlev/1000)), "km/s")
KE = kinetic(np.linalg.norm(particlev), m)
print("Kinetic Energy is", KE, "J (", J_to_eV(KE) ,"eV,",
      round( J_to_eV(KE)/1000),"KeV)")
print("Distance Traveled is",sum(d_magnitude), "m")

# Change in Velocity plot
plt.figure(figsize=(8,8))
plt.plot(T, Vx, label="X")
plt.plot(T, Vy, label="Y")
plt.title("Velocity vs. Time")
plt.xlabel("Time[10e-9 s]")
plt.ylabel("Velocity[m/s]")
plt.legend()

txt = ("β = " + str(B[2]) + "T",
      "V = " + str(V) + "volts",
      "d = " + str(round(d,6)) + "m",
      "r = " + str(r_cyclotron) + "m"
      )

plt.figure(1, figsize=(8,8)) #create the figure
plt.plot(particleposx, particleposy) #create the plot
plt.title("Case3: Modified Theory data from paper")

```



```
#plt.savefig("Test2_β2-7_V50_d1.25_r8cm_2.jpeg")
plt.show()
print(txt)

check_structure()

def plateGapDistance(iterations, step, start):
    acc_check = True
    vel_check = True
    for i in range(0, iterations):
        particlepos = np.array([0.0,0.0,0.0])
        particlev = np.array([0.0,0.0,0.0]) #Set the initial particle speed to 0
            #create an array for the x position of the particle
        particleposx = [particlepos[0]]
            #create an array for the y position of the particle
        particleposy = [particlepos[1]]

        q = 1.6e-19 #Set the charge of the particle to the charge of a proton
        m = 1.67e-27 #Set mass of the particle to the mass of a proton

        V = 100 #Set voltage between the plates to 50V
        d = start + i * step #m
            #Electric field based on voltage between the D's and separation
        E_0 = V/(d)
            #Set magnetic field to 0.3T in the +Z direction
        B = np.array([0.0,0.0,0.701])
        r_cyclotron = 0.04875 #set the radius of the D's to 4.875cm
```

```
w = q*np.linalg.norm(B)/m #define the cyclotron frequency
f = q*np.linalg.norm(B)/(2*np.pi*m)

t = 0 #initialize time to 0
dt = 10**-9 #Set timestep to 5 picoseconds

Vx = []
Vy = []
T = []
d_magnitude = []

    #loop while the magnitude of the proton's position
while (np.linalg.norm(particlepos) < r_cyclotron):
    #remains within the cyclotron radius
        #create a vector for the net force on the particle.
Fnet = np.array([0.0,0.0,0.0])
        #if the particle is between two D's calculate electric force
if np.absolute(particlepos[0]) < d/2:
            Fnet[0] = q*E_0*np.cos(w*t)
        #if the particle is not, calculate the magnetic force
else:
            Fnet = q*np.cross(particlev,B)

        #Update the velocity of the particle
particlev = particlev + Fnet*dt/m
        #Use velocity to update the position of the particle
```

```

particlepos = particlepos + particlev*dt
    #append the x position to the x-position list
particleposx = np.append(particleposx, particlepos[0])
    #append the y position to the y-position list
particleposy = np.append(particleposy, particlepos[1])
t = t + dt #update the timestep
Vx = np.append(Vx,particlev[0])
Vy = np.append(Vy,particlev[1])
T = np.append(T, t)
d_magnitude = np.append(d_magnitude,
    np.sqrt((particlepos[0]**2)+ (particlepos[1]**2)))

print("Cyclotron Frequency is", w, "rad/s (or ", f,
    " Hz,", round(f/1e6), "MHz)")
print("The final speed of the particle is", np.linalg.norm(particlev),
    "m/s, ", round(np.linalg.norm(particlev/1000)), "km/s")
KE = kinetic(np.linalg.norm(particlev), m)
print("Kinetic Energy is", KE, "J (", J_to_eV(KE) ,"eV,",
    round(J_to_eV(KE)/1000),"KeV)")
print("Distance Traveled is",sum(d_magnitude), "m")
area = (Area(mm_to_m(105.2), mm_to_m(12.7)))-(Area(mm_to_m(104.2),
    mm_to_m(11.7)))
print(area,"m")
print("Capacitance", capacitance(area, d), "F")
print("Resistor", calculate_R(f, capacitance(area, d)), "ohm")

# Change in Velocity plot

```

```

plt.figure(1)
plt.figure(figsize=(8,5))
plt.plot(T, Vx, label="X")
plt.plot(T, Vy, label="Y")
plt.title("Velocity vs. Time")
plt.xlabel("Time[10e-9 s]")
plt.ylabel("Velocity[m/s]")
plt.legend()

txt = ("β = " + str(B[2]) + "T",
      "V = " + str(V) + "volts",
      "d = " + str(round(d,6)) + "m",
      "r = " + str(r_cyclotron) + "m"
      )

plt.figure(2)
plt.figure(1, figsize=(6,6)) #create the figure
plt.plot(particleposx, particleposy) #create the plot
plt.title("Plate Position"+str(d)+"m")
plt.savefig("Test2_β2-7_V50_d1.25_r8cm_2.jpeg")
plt.show()
print(txt)

#check_structure()

#-----sprial check-----
if(acc_check):
    peaks_x, _ = find_peaks(Vx, height=0)

```

```
# calculate polynomial
z = np.polyfit(T[peaks_x],Vx[peaks_x], 3)
f = np.poly1d(z)

# calculate new x's and y's
x_new = np.linspace((T[peaks_x])[0], (T[peaks_x])[-1], 50)
y_new = f(x_new)

peaks_y, _ = find_peaks(Vy, height=0)

# calculate polynomial
zy = np.polyfit(T[peaks_y],Vy[peaks_y], 3)
fy = np.poly1d(zy)

# calculate new x's and y's
x_newy = np.linspace((T[peaks_y])[0], (T[peaks_y])[-1], 50)
y_newy = fy(x_newy)

plt.figure(figsize=(8,6))
plt.title("Fit of the peaks of the velocity with a 3 order polynomial"
          , size=15)
plt.xlabel("Time [s]", size=12)
plt.ylabel("Velocity [m/s]", size=12)
plt.plot(T, Vy, 'orange', label = 'Curve')
plt.plot(T[peaks_y],Vy[peaks_y],'ko', markersize = 8, label = 'peaks')
plt.plot( x_newy, y_newy, 'r',label = 'Fit_order 3')
```

```
plt.plot(T, Vx, 'tab:blue',label = 'Curve')
plt.plot(T[peaks_x],Vx[peaks_x],'ko', markersize = 8, label = 'peaks')
plt.plot( x_new, y_new, 'cyan',label ='Fit_order 3')

plt.legend(fontsize=10)
plt.show()

print("Acceleration X =")
print(f)
print("Acceleration Y = ")
print(fy)
f_diff = f-fy
f_avg = (f+fy)/2
f_div, f_remain = np.polydiv(f_diff, f_avg)
print("Percent Difference", f_div*100, "%")
print("Remainder", f_remain)

if(vel_check):
    pX = particleposx[1:,]
    peaks_x, _ = find_peaks(pX, height=0)

    # calculate polynomial
    z = np.polyfit(T[peaks_x],pX[peaks_x], 3)
    f = np.poly1d(z)

    # calculate new x's and y's
    x_new = np.linspace((T[peaks_x])[0], (T[peaks_x])[-1], 50)
```

```
y_new = f(x_new)

pY = particleposy[1:,]
peaks_y, _ = find_peaks(pY, height=0)

# calculate polynomial
zy = np.polyfit(T[peaks_y], pY[peaks_y], 3)
fy = np.poly1d(zy)

# calculate new x's and y's
x_newy = np.linspace((T[peaks_y])[0], (T[peaks_y])[-1], 50)
y_newy = fy(x_newy)

x_fit = np.polyfit(T[peaks_x], pX[peaks_x], 1)
fxD = np.poly1d(x_fit)
new_x_data = fxD(x_new)

y_fit = np.polyfit(T[peaks_y], pY[peaks_y], 1)
fyD = np.poly1d(y_fit)
new_y_data = fxD(x_newy)

plt.figure(figsize=(8,6))
plt.title("Fit of the peaks of the Y-velocity
          with a 3 order polynomial", size=15)
plt.xlabel("Time [s]", size=12)
plt.ylabel("Position [m]", size=12)
```

```
plt.plot(T, pY, 'orange')
plt.plot(T[peaks_y], pY[peaks_y], 'ko',
         markersize = 8, label = 'peaks')
plt.plot(x_newy, y_newy, 'r', label = 'Fit_order 3')
plt.plot(x_newy, new_y_data, color='purple',
         linestyle='--', linewidth=2)
plt.legend(fontsize=10)
plt.show()

plt.figure(figsize=(8,6))
plt.plot(T, pX, 'tab:blue')
plt.plot(T[peaks_x], pX[peaks_x], 'ko',
         markersize = 8, label = 'peaks')
plt.plot(x_new, y_new, 'cyan', label = 'Fit_order 3')
plt.plot(x_new, new_y_data, color='steelblue',
         linestyle='--', linewidth=2)

plt.legend(fontsize=10)
plt.show()

print("Position X =")
print(f)
f_diff_x = f-x_fit
print(f_diff_x)
f_avg_x = (f+x_fit)/2
print(f_avg_x)
```



```
f_div_x, f_remain_x = np.polydiv(f_diff_x, f_avg_x)
print(f_div_x)
print("Percent Difference", f_div_x*100, "%")
print("Remainder", f_remain_x)

print("Position Y = ")
print(fy)
f_diff_y = fy-y_fit
f_avg_y = (fy+y_fit)/2
f_div_y, f_remain_y = np.polydiv(f_diff_y, f_avg_y)
print("Percent Difference", f_div_y*100, "%")
print("Remainder", f_remain_y)

peaks_x, _ = find_peaks(Vx, height=0)

# calculate polynomial
z = np.polyfit(T[peaks_x], Vx[peaks_x], 3)
f = np.poly1d(z)

# calculate new x's and y's
x_new = np.linspace((T[peaks_x])[0], (T[peaks_x])[-1], 50)
y_new = f(x_new)

plt.figure(figsize=(14,8))
plt.title("Fit of the peaks of the X-velocity
          with a 3 order polynomial", size=15)
plt.xlabel("Time [s]", size=12)
```

```
plt.ylabel("Velocity [m/s]", size=12)
plt.plot(T, Vx, 'tab:blue',label = 'Curve')
plt.plot(T[peaks_x],Vx[peaks_x],'ko',
         markersize = 8, label = 'peaks')
plt.plot( x_new, y_new, 'r',label ='Fit_order 3')
plt.legend(fontsize=10)
plt.show()
print("Acceleration X =")
print(f)

peaks_y, _ = find_peaks(Vy, height=0)

# calculate polynomial
zy = np.polyfit(T[peaks_y],Vy[peaks_y], 3)
fy = np.poly1d(zy)

# calculate new x's and y's
x_newy = np.linspace((T[peaks_y])[0], (T[peaks_y])[-1], 50)
y_newy = f(x_newy)

plt.figure(figsize=(14,8))
plt.title("Fit of the peaks of the Y-velocity
         with a 3 order polynomial", size=15)
plt.xlabel("Time [s]", size=12)
plt.ylabel("Velocity [m/s]", size=12)
plt.plot(T, Vy, 'orange', label = 'Curve')
plt.plot(T[peaks_y],Vy[peaks_y],'ko',
```

```
        markersize = 8, label = 'peaks')
plt.plot( x_newy, y_newy, 'r',label = 'Fit_order 3')
plt.legend(fontsize=10)
plt.show()
print("Acceleration Y = ")
print(fy)
```

Luke Ingraham Senior Thesis